

THE MECHANICAL PROPERTIES OF SISAL FIBRE
REINFORCED COMPOSITES OF EPOXY RESIN
AND RICE HUSK ASH POZZOLANIC CEMENT

WYCLIFFE ODEGINGALA B.Sc. (Hons)

“A thesis submitted in partial fulfilment of the requirements for the award of the
degree of Master of Science in Engineering (Applied Mechanics) of the University of
Nairobi”

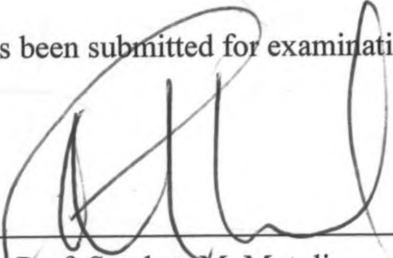
2001

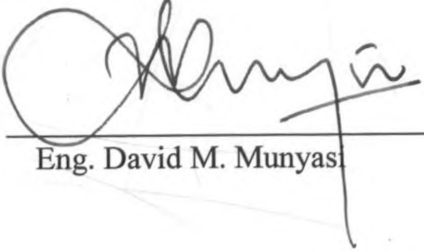
DECLARATION

I declare that this thesis is my own original work and has not been presented in this or any other university for examination, or any other purposes.

Signature  Date 2/5/2001
WYCLIFFE ODEGI NGALA

This thesis has been submitted for examination with our approval as university supervisors.

Signature  Date 29/5/2001
Prof. Stephen M. Mutuli (First supervisor)

Signature  Date 04/06/2001
Eng. David M. Munyasi (Second supervisor)

DEDICATION

To Mum Mary and Dad Philemon Mangla,
For the noble cause and foresight in providing for this valuable education.

ACKNOWLEDGEMENTS

I am greatly indebted to my supervisor Prof. Stephen M. Mutuli, Professor of mechanical engineering, who has been my constant source of inspiration through out the course of this study. His guidance, help and advice has been invaluable. His interest in my work through out the research programme gave me great encouragement. I would also like to express profound gratitude to my second supervisor Eng. David M. Munyasi for his guidance, criticisms and inspiration. This thesis is the ultimate result.

Sincere thanks to my sponsor Japan International Co-operation Agency (JICA) for their financial support. A word of thanks also goes to Mrs B. S. Waswa, Lecturer –HABRI and the entire staff of Housing and Building Research Institute (HABRI) -U.O.N for their friendliness and willingness in passing of information during the preliminary literature survey of this study. My sincere gratitude goes to the entire staff of the departments of mechanical engineering U.O.N and JKUAT, teaching and non-teaching for their contributions directly or indirectly to the completion of this work. Special thanks to you all. A few others however deserve a special mention. Mr. S. Ndulu (Senior technician – U.O.N) assisted in the mechanical testing of the composite materials. Mr. Okoth and Mr. G. Wanyoike assisted in the fabrication of the moulds. Mr. Muchina, technician of the concrete laboratory assisted in the fabrication of the sisal/cement composites.

I have not ceased to be amazed by the incredible patience and support of my wife Dorothy, Dad Philemon Mangla, Mum Mary Mangla, Brother Elly Ocholla (Jakonyango) and Sister Eva Anyango (Nyakona). They shared with me during these trying times and encouraged me a great deal. Lastly special thanks to dear brethren who supported me on their knees, crying to the LORD that it may come to pass. May I mention Brother Owande on behalf of those known and unknown to me. GOD knows you.

Except for GOD ALMIGHTY'S grace through our LORD and SAVIOUR JESUS CHRIST, nothing has been that is, Glory and honour be unto him forever more.

I...do not cease to give thanks for you, making mention of you in my prayers -Ephesians 1:16

ABSTRACT

Sisal is a vegetable fibre extracted from the leaves of *Agave Sisalana*. The fibre is long, bold and creamy white besides being exceptionally strong. It can be used for making agricultural and parcelling twines of various kinds as well as ropes, sacks, carpets and upholstery.

Some research has been done to investigate the effects of sisal fibre reinforcement on base materials such as ordinary portland cement paste, mortar and epoxy resin [1-3]. However their results on strengths of sisal fibre reinforced epoxy resin composites lacked certain features accompanying composite failure at high fibre volume fractions. Similarly rice husk ash pozzolanic cement (RHAC) is a relatively new product in the Kenyan market, and not much work has been done to investigate the strength aspects of its sisal fibre reinforced composite. The wide scale use of any material however, requires among other things a considerable understanding of its mechanical and physical characteristics. It is with this objective in mind that an experimental programme was carried out on sisal fibre reinforced RHAC mortar and epoxy resin. The results of this work were compared with theoretical predictions. Based on the results suitable choices of fibre incorporation techniques, critical fibre length, optimum and critical fibre volume fractions were identified. The results obtained from sisal/RHAC composites will be of considerable potential in such areas as housing construction in rice growing developing countries. Components made from epoxy resin may find extensive use in applications requiring high strength-to-weight ratio, artificial limbs, liquid containers, bodies of domestic appliances and low strength structural members.

The primary purpose of this research was to study and evaluate the use of sisal as a reinforcing fibre in the form of continuous longitudinally aligned and discontinuous randomly aligned arrangements in RHAC mortar and epoxy resin matrices. The casting process employed in composite production involved laying and curing. Principles of continuum mechanics were used in the analysis of various strength aspects of the resulting composites. The effects of fibre volume fractions, aspect ratios, reinforcing index and alignments on the tensile strength, flexural strength, flexural toughness and modulus of elasticity were investigated. In addition the fibre/matrix interfacial bond strength was evaluated. Finally the occurrence of multiple matrix fracture (MMF) and fibre pull-out phenomena were also studied. The mechanical properties of the resulting composites were examined in direct tension, three point and four point bending tests.

It was found that the tensile and flexural strength characteristics of sisal/epoxy composites improved with the increases in reinforcement volume fractions (V_f) from 0 to 45% V_f in continuous parallel aligned fibres. However no effective reinforcement was observed in chopped sisal/epoxy composites. Both chopped and continuous reinforcing fibres improved the strength and toughness in sisal/RHAC composites. Maximum ultimate strength values of 8.61 N/mm^2 at 9.5% V_f and 3.64 N/mm^2 at 9.0% V_f were obtained from flexural and direct tension tests respectively for continuous parallel-aligned fibre reinforced composites. On the other hand chopped fibre composites gave relatively lower strength values. In this category peak strengths values of 5.13 N/mm^2 at 7.3% V_f and 2.74 N/mm^2 at 8.4% V_f were realised for the Modulus of Rupture and tensile strengths respectively. The optimum fibre volume fractions in flexural loading occurred at 8.5% and 7.4% V_f in the case of continuous and chopped fibre reinforcements respectively. However the stiffness of the composites did not vary appreciably with increasing reinforcement levels.

Both the fibre/matrix interfacial bond strength and the average crack spacing decreased with fibre additions in the composites. The average fibre/matrix interfacial bond strength computed for 63 continuous parallel aligned sisal/RHAC specimens was found to be 0.139 N/mm^2 while that of discontinuous randomly aligned fibres was obtained as 0.121 N/mm^2 . Increasing the reinforcement volume fractions also increased the toughness and toughness indices. The study showed that only the higher toughness index I_{10} is sensitive to fibre contents, while the lower toughness index I_5 showed very little variation with the fibre volume fractions in the composite. Flexural toughness has an inverse relationship to the water/cement (W/C) ratio. However the proportional relationship between W/C and toughness index is not clear. The present results also showed that both the toughness and toughness indices increased with curing age. Finally it was also noted that fibre additions resulted in a decreased composite density and a corresponding increase in the amount of voids present in the composite.

Plain mortar specimens failed without any warning exhibiting a brittle failure, while the fibre reinforced specimens had a slow ductile failure. Multiple matrix cracking was observed with fibre pull-out taking place after large visible cracks had appeared. The composites were therefore able to maintain some residual strength even at large displacements and thus continued to absorb energy with increasing deformations even long after the matrix had cracked. Fibres consequently allowed the composites to retain some post-cracking strength hence withstanding deformations much greater than could be sustained by the matrix alone.

TABLE OF CONTENTS

	Page
Declaration.....	(ii)
Dedication.....	(iii)
Acknowledgements.....	(iv)
Abstract.....	(v)
List of figures.....	(xi)
List of tables.....	(xiv)
List of plates.....	(xv)
Abbreviations.....	(xv)
Nomenclature.....	(xvi)
1. Introduction.....	1
2 Literature review.....	5
2.1 Fibre reinforcement.....	5
2.1.1 Fibres.....	6
2.2 Sisal.....	7
2.2.1 Historical background.....	7
2.2.2 Morphology.....	8
2.3 Matrices.....	14
2.3.1 Rice husk ash pozzolanic cement.....	14
2.3.1.1 Background, availability and sources.....	14
2.3.1.2 Production.....	15
2.3.1.2.1 Raw material.....	15
2.3.1.2.2 The production process.....	15
2.3.1.3 Properties.....	16
2.3.2 Epoxy resin.....	17
2.4 Mechanical properties of fibre reinforced composites.....	21
2.4.1 Strength characteristics of fibre reinforced composites.....	21
2.4.1.1 Stress distribution in fibre reinforced composites...	21
2.4.1.2 Rule of mixtures.....	22
2.4.1.3 First crack strength under axial tension.....	24
2.4.1.4 Ultimate tensile strength.....	24
2.4.1.5 Ultimate flexural failure.....	24

2.4.2	Stress-strain curve.....	25
2.4.3	Post cracking ductile behaviour.....	27
2.4.4	Energy absorbing mechanisms.....	29
2.4.5	Fracturing energy.....	30
2.4.6	Interfacial bond strength.....	31
2.4.7	Efficiency factors.....	34
2.4.7.1	Fibre length efficiency factor.....	34
2.4.7.2	Fibre orientation efficiency factor.....	35
2.4.7.3	Fibre randomness efficiency factor.....	36
2.4.8	Critical fibre length.....	38
2.4.9	Critical fibre volume fraction.....	38
2.4.10	Flexural toughness.....	40
2.5	Objectives.....	42
3.	Experimental procedure.....	44
3.1	Moulds.....	44
3.2	Specimen preparation.....	44
3.2.1	Preparation of sisal fibres.....	44
3.2.2	Preparation of pure epoxy resin specimens.....	44
3.2.3	Sisal fibre reinforced epoxy resin specimens.....	48
3.2.3.1	Continuous parallel aligned fibre composites.....	48
3.2.3.2	Discontinuous randomly aligned fibre composites...	48
3.2.4	Unreinforced RHAC specimens.....	49
3.2.5	Sisal fibre reinforced RHAC mortar specimens.....	50
3.2.5.1	Continuous parallel aligned fibre composites.....	50
3.2.5.2	Discontinuous randomly aligned fibre composites...	50
3.3	Mechanical testing.....	51
3.3.1	Sisal fibre reinforced RHAC specimens.....	51
3.3.1.1	Tensile test.....	51
3.3.1.2	Interfacial bond strength.....	56
3.3.1.3	Flexure test.....	56
3.3.1.4	Flexural toughness.....	60
3.3.1.5	Composite density and void volume value.....	61

3.3.1	Sisal fibre reinforced epoxy resin specimens.....	61
3.3.1.1	Tensile test	61
3.3.1.2	Flexure test	64
3.4	Description of the equipments used.....	66
3.4.1	Vibration table.....	66
3.4.2	Torsee Senstar (Tokyo) type SC 10 CS Electronic Universal Testing Machine.....	66
4.	Results.....	67
4.1	Sisal fibre reinforced RHAC mortar composites.....	67
4.1.1	Flexural strength.....	67
4.1.1.1	Continuous parallel aligned fibre reinforced specimens.....	67
4.1.1.2	Discontinuous randomly aligned fibre reinforced specimens.....	70
4.1.2	Tensile strength and Modulus of Elasticity.....	75
4.1.2.1	Continuous parallel aligned fibre reinforced specimens.....	75
4.1.2.2	Discontinuous randomly aligned fibre reinforced specimens.....	82
4.1.3	Interfacial bond strength.....	87
4.1.4	Flexural toughness.....	89
4.1.4.1	Variation of flexural toughness with fibre volume fractions.....	89
4.1.4.2	Variation of flexural toughness with W/C ratios.....	93
4.1.4.3	Variation of flexural toughness with curing age.....	94
4.1.5	Workability of plain RHAC mortar and sisal/RHAC composites.....	95
4.1.6	Composite density and void volume fraction.....	95
4.2	Sisal fibre reinforced epoxy resin composites.....	97
4.2.1	Tensile strength.....	97
4.2.2	Flexural strength.....	102

5.	Discussion.....	106
5.1	Sisal fibre reinforced RHAC mortar composites.....	106
5.1.1	Flexural strength.....	106
5.1.2	Tensile strength and Modulus of Elasticity.....	111
5.1.3	Interfacial bond strength.....	116
5.1.4	Flexural toughness.....	119
5.1.5	Workability.....	122
5.1.6	Density and void volume fraction.....	122
5.2	Sisal fibre reinforced epoxy resin composites.....	124
6.	Conclusions.....	128
7.	Recommendations for further work.....	131
8.	References.....	134
9.	Appendix.....	140
9.1	Experimental data.....	140
9.1.1	Sisal/RHAC specimens, flexural strength results.....	140
9.1.2	Sisal/RHAC specimens, tensile strength results.....	143
9.1.3	Sisal/RHAC specimens, interfacial bond strength results.....	147
9.1.4	Sisal/RHAC specimens, flexural toughness results.....	150
9.1.5	Sisal/Epoxy specimens, tensile strength results.....	153
9.1.6	Sisal/Epoxy specimens, flexural strength results.....	155

LIST OF FIGURES

<u>Figure No.</u>	<u>Title of Figure</u>	<u>Page</u>
2.1	Typical tensile stress-strain curve of sisal fibre.....	10
2.2	Epoxy group.....	18
2.3	Cross-linking of epoxy resins.....	19
2.4	Uni-directional aligned continuous fibre composite.....	21
2.5	The variation of stresses along a fibre.....	22
2.6	Possible fibre reinforced cement stress-strain curves.....	26
2.7	Composite fractures indicating different fibre/matrix bond strengths.....	32
2.8	Variation of the composite tensile modulus of elasticity with the angle between the applied stress and principal fibre direction.....	36
2.9	Determination of the toughness index from a load-deflection curve using ASTM C1018 approach.....	41
3.1	Steel moulds for casting sisal/epoxy tensile test specimens.....	45
3.2	Steel moulds for casting sisal/epoxy flexure test specimens.....	46
3.3	Wooden moulds for casting sisal/RHAC tensile test specimens.....	47
3.4	Wooden moulds for casting sisal/RHAC flexure test specimens.....	47
3.5	Tensile test rig proposed by Bessel and Mutuli [38]	53
3.6	Flexural strength test rig.....	58
3.7	Arrangement of flexural loading on a sisal/RHAC composite beam test piece (two point loading).....	59
3.8	Dimensions of sisal/epoxy tensile test specimens.....	62
3.9	Schematic diagram of the flexure test arrangement on sisal/epoxy test piece.....	65
4.1	Variation of the flexural strength with fibre volume fraction in continuous fibre sisal/RHAC composites.....	70
4.2	Variation of the first crack flexural strength with fibre volume fraction in continuous fibre sisal/RHAC composites.....	71
4.3	Variation of the flexural strength with fibre aspect ratio in sisal/RHAC composites.....	71
4.4	Crack patterns in sisal/RHAC composite flexural failure.....	72
4.5	Variation of flexural strength with fibre volume fraction in 20 mm length chopped fibre sisal/RHAC composites.....	74

4.6	Variation of flexural strength with fibre volume fraction in 30 mm length chopped fibre sisal/RHAC composites.....	74
4.7	Variation of flexural strength with fibre volume fraction at different fibre lengths.....	75
4.8	Variation of the composite tensile strength with fibre volume fraction in continuous sisal/RHAC composites.....	77
4.9	Variation of the composite tensile strength with fibre volume fraction at different fibre lengths.....	77
4.10	Typical tensile stress-strain curves of continuous parallel aligned sisal fibre reinforced RHAC composites.....	78
4.11	Variation of the tensile modulus of elasticity with fibre volume fraction in continuous fibre sisal/RHAC composites.....	79
4.12	Variation of the tensile Modulus of Elasticity with fibre reinforcing index in continuous fibre sisal/RHAC composites.....	79
4.13	Variation of the mean modular ratio with fibre reinforcing index in continuous fibre sisal/RHAC composites.....	80
4.14	Variation of the composite Modulus of Elasticity with the tensile strength in continuous fibre sisal/RHAC composites.....	81
4.15	Variation of the tensile strength with fibre volume fraction in 20 mm length chopped fibre sisal/RHAC composites.....	83
4.16	Variation of the tensile strength with fibre volume fraction in 30 mm length chopped fibre sisal/RHAC composites.....	84
4.17	Typical stress-strain curves of discontinuous randomly aligned sisal fibre reinforced RHAC composites.....	85
4.18	Variation of the tensile Modulus of Elasticity with fibre contents in 30 mm length chopped fibre sisal/RHAC composites.....	85
4.19	Variation of the composite modulus of elasticity with the tensile strength in 30 mm length chopped fibre sisal/RHAC composites.....	86
4.20	Variation of the interfacial bond strength with fibre volume fractions in continuous fibre sisal/RHAC composites.....	88
4.21	Variation of the interfacial bond strength with fibre volume fractions in 30 mm length chopped fibre sisal/RHAC composites.....	88
4.22	Average crack spacing length in continuous fibre sisal/RHAC composites.....	89

4.23	Load-deflection curves of sisal/RHAC composites at varying fibre volume fractions.....	90
4.24	Bar chart of toughness indexes at varying fibre volume fractions in sisal/RHAC composites.....	91
4.25	Variation of the toughness indexes with fibre volume fraction.....	91
4.26	Load-deflection curves of sisal/RHAC composites at varying W/C ratios.....	93
4.27	Load-deflection curves of sisal/RHAC composites at varying curing ages.....	94
4.28	Variation of the composite density with fibre volume fraction in chopped fibre sisal/RHAC composites.....	96
4.29	Variation of the void volume value with fibre volume fraction in chopped fibre sisal/RHAC composites.....	96
4.30	Tensile stress-strain curves of sisal fibre reinforced epoxy resin	98
4.31	Combined tensile stress-strain curves of sisal fibre reinforced epoxy resin for varying fibre volume fractions.....	99
4.32	Variation of the tensile strength with fibre volume fractions for varying fibre lengths in sisal fibre reinforced epoxy resin composites.....	100
4.33	Variation of the tensile Modulus of Elasticity with fibre volume fractions in sisal fibre reinforced epoxy resin composites.....	101
4.34	Variation of the tensile strain with fibre volume fractions in continuous parallel aligned sisal fibre reinforced epoxy resin composites.....	102
4.35	Variation of the flexural strength with fibre volume fractions at different fibre lengths in sisal fibre reinforced epoxy resin composites.....	103
4.36	Variation of the flexural Modulus of Elasticity with fibre volume fractions at varying fibre lengths in sisal fibre reinforced epoxy resin composites.....	104
5.1	Load-deflection behaviour of unreinforced and fibre reinforced cement mortar with chopped and continuous long fibres.....	120
5.2	Variation of the density of wood pulp reinforced cement mortar with the reinforcement volume fraction.....	123
5.3	Variation of the density of glass fibre reinforced cement with fibre volume fractions at different fibre lengths.....	123

LIST OF TABLES

<u>Table No.</u>	<u>Title of Table</u>	<u>Page</u>
2.1	Composition of sisal fibre.....	10
2.2	Mechanical properties of commonly used artificial fibres.....	11
2.3	Mechanical properties of commonly used natural fibres.....	12
2.4	Mechanical properties of sisal fibres.....	12
2.5	Chemical composition of RHA for the husk obtained from Kisumu, Kenya.....	17
2.6	Typical properties of epoxy resins used in composite materials.....	20
2.7	Efficiency factors for different fibre orientations.....	37
4.1	Static flexural first crack strength values for continuous parallel aligned sisal fibre reinforced RHAC composites.....	68
4.2	Static flexural first crack strength values for 30 mm length discontinuous randomly aligned sisal fibre reinforced RHAC composites...	69
4.3	Toughness indexes at varying fibre contents in sisal/RHAC composites.....	90
4.4	Toughness indexes at various W/C ratios in sisal/RHAC composites.....	93
4.5	Toughness indexes at varying curing ages in sisal/RHAC composites.....	94
5.1	Critical fibre volume fraction of some common fibres in cement matrices.....	109
5.2	Interfacial bond strength values of common fibre/cement composites.....	118

LIST OF PLATES

<u>Plate No.</u>	<u>Title of Plate</u>	<u>Page</u>
3.1	Torsee Senstar (Tokyo) type sc 10 cs electronic universal testing machine.....	54
3.2	Sisal/RHAC composite beam, tensile test in progress.....	55
3.3	Flexural strength test of sisal/RHAC composite beam in progress,	59
3.4	Tensile test on sisal/epoxy specimen in progress.....	62
3.5	Flexure test on sisal/epoxy specimen in progress.....	64

ABBREVIATIONS

RHA	-Rice Husk Ash
OPC	-Ordinary Portland Cement
HABRI	-Housing and Building Research Institute
FAO	-Food and Agriculture Organisation
UNO	-United Nations Organization
RHAC	-Rice Husk Ash Cement
BRE	-Building Research Establishment
BS	-British Standards
W/C	-Water to Cement Ratio
FRC	-Fibre reinforced composite
LOP	-Limit of proportionality
L-D	-Load-deflection
MMF	-Multiple matrix cracking
MOR	-Modulus of Rupture
UTS	-Ultimate Tensile Strength
UG	-Universal grade

NOMENCLATURE

The subscripts f,m,c represents fibre, matrix and composites respectively.

σ_t - tensile strength

σ_b -flexural strength

P -applied load

ε -strain

E -modulus of elasticity

V - volume fraction

σ_{cu} -ultimate tensile strength of the composite

σ_m' -flow stress in matrix at fracture strain of the fibres

σ_{fu} -fibre fracture strength

σ_f' -stress in the fibre at the failure strain of the matrix

σ_{mu} -ultimate tensile strength of the matrix

σ_{mu} -first crack strength of the matrix

ε_{mu} -failure strain of the matrix

$\varepsilon_{f(max)}$ -maximum strain carried by the fibres

l_c -critical fibre volume fraction

τ_b -interfacial bond strength

$V_{f(crit)}$ -critical fibre volume fraction

r -fibre radius

d_f -fibre diameter

X -length of inter-crack spacing

$V_{f(min)}$ -minimum fibre volume fraction

δ -deflection

L -distance between the supporting rollers (span)

b -breadth of the specimen

d -depth of the specimen

A -original cross-section area of the composite

1. INTRODUCTION

A composite material is a combination of two or more materials each with its own distinct properties for the purpose of producing a superior material whose properties are a combination of the constituent materials. A fibre reinforced composite is defined as a material comprising a large number of strong stiff fibres embedded in a continuous phase of a second material known as the matrix. The fibre can be natural, man-made, metallic, inorganic or organic. Likewise the matrix can be a metal, metallic alloy, ceramic, inorganic cement, glass, natural or synthetic polymer [4].

Composite materials can be classified into two groups; namely those that are natural and those that are man-made. Examples of natural composites include wood, bone, bamboo, muscles and other body tissues. An early application of composite technology was in the construction of traditional huts, where a network of sticks was used as a reinforcement in mud. Mud cracks easily upon drying and in the absence of the reinforcing framework, crumbles and falls off the wall structure. The use of straw to reinforce mud bricks and hair in mortar are other examples [5]. Today many engineering components consist of two or more materials combined to give a better performance in service as well as having superior properties to those of the constituent elements. These are termed as man-made composites. The need for man-made composites arose due to the difficulty in getting a single phase material with unique properties to fulfil particular practical design requirements and specifications.

Most fibre reinforced composites consist of a plastic matrix reinforced with different types of fibres such as carbon, glass, polypropylene and aramid [4, 6-8]. The main advantage of such composites is the high strength-to-weight ratios associated with them. They therefore find

wide spread use in the aircraft and automotive (modern car bodies) industries, which have typically weight sensitive structures [6]. Other advantages of fibre-reinforced plastic composite materials include ease of fabrication, resistance to corrosion and reduced cost.

Another category of composites is designed to overcome certain basic weaknesses in, for example, unreinforced cement matrices. Building materials such as mortar and concrete have excellent compressive strength and stiffness, but are hampered in some applications by their brittleness and low fracture toughness. Asbestos [9], steel [10-12], glass [13-16] and polypropylene [17-19] fibres are typical examples of reinforcements used in cement paste, mortar and concrete so as to gain more strength in tension and impact loading conditions.

In fibre-reinforced composites the main load bearing component is the fibre. The fibres should have high strength and high elastic modulus, while the matrix should be ductile and should not react with the fibres. The matrix serves to transmit the load to the fibres and to protect fibres from surface damage [20]. The mechanical properties of a composite are a function of the properties of the constituent elements namely; fibre volume fraction, fibre/matrix interfacial bond strength, length and orientation of fibres [4-7].

The majority of the fibre reinforced plastic composites in the industrial market are made of epoxy resin reinforced with carbon, aramid and glass fibres [4]. In certain applications natural fibres can be used to reinforce plastics. Therefore research on reinforcing fibres has now been directed to natural fibres namely jute, hemp, coconut, coir, sisal etc which are available in developing countries. They can also be used as a reinforcement in cement-based matrices. Sisal is a tropical plant that is fibrous in nature, besides being exceptionally strong compared to other natural fibres. When it is embedded in an epoxy resin or inorganic cement

matrix, the resulting composites have a wide variety of applications notably in the construction industry as roofing materials. The main advantages of sisal fibre for reinforcement include; equivalent strength values to most synthetic fibre composites, lower cost, easy to cut, light weight, abundant availability and environmental benefits.

The change in research emphasis to natural fibres came in the wake of an appeal by the Food and Agriculture Organisation (FAO), (an organ of the United Nations Organisation (UNO)), to researchers to find alternative uses of sisal fibres and wastes which are being replaced in the hard fibre industry by synthetic fibres [21]. The aforesaid competition from synthetic fibres led to a decrease in world's demand and consequently a reduction in the world prices of sisal fibres.

One such alternative application is the use of sisal fibres as a reinforcement in plastics, cements and other brittle matrices. Sisal fibre reinforced polyester sheets can be used in the production of flat and corrugated roofing sheets [21-23]. The application of this natural fibre in the reinforcement of thin cement products such as roofing sheets, tiles, partitioning blocks and panels is also being tried out [24]. This is because affordable roofing is a necessity for the vast majority of the population in developing countries. Importing iron sheets or asbestos for asbestos/cement sheets is being tried as a solution. However with the increased economic burden it is becoming increasingly difficult to meet vital needs such as roofing from imports. Attention has therefore been focussed on finding appropriate solutions based on locally available raw materials. In this regard many different solutions based on natural fibres are being tried to solve the roofing problem. These include sisal, coconut husk, rice straw, sugar-cane bagasse, jute, hemp, coir and banana racquis [24].

Some researchers have reported a limited amount of embrittlement in these natural fibre reinforced OPC composites with time [25-26]. This can lead to cracking in roofing materials. The embrittlement of sisal fibre reinforced OPC mortar or concrete can be delayed by impregnating the fibres [27]. Sealing the pore system of the cement matrix with wax, zinc stearate or sulphur may also improve the durability of the fibres. A more effective method of avoiding the embrittlement of sisal/cement composites is by replacing part of the ordinary portland cement with fine grained pozzolanas, for instance silica fume, diatomite or rice husk ash [25-27].

An extensive research study conducted on cheap building materials by the Housing and Building Research Institute (HABRI) at the University of Nairobi produced roofing tiles and sheets from sisal fibre reinforced OPC mortars. The products were tested and applied at various pilot stations countrywide. Despite the on-going research work, these materials are already being produced in the informal sector of Kenya, and are finding applications in small but increasing scale in the building industry. There is therefore an urgent need for further research to ascertain the mechanical properties of these composites. This will also provide a source of reliable data for publication and design before these products can be put into wide-scale use. In this research an attempt has therefore been made to establish the mechanical properties of sisal fibre reinforced composites of epoxy resin and RHA cement matrices.

2. LITERATURE REVIEW

2.1 FIBRE REINFORCEMENT

Materials of high strength to weight ratio can be produced by incorporating fibres in a ductile matrix. In fibre reinforced plastics the main load-bearing component is the fibre. Therefore the fibre should have a high strength and high elastic modulus, while the matrix should be ductile and non-reactive with the fibres. The fibres may be long and continuous or they may be short and discontinuous. So in fibre strengthening of composites, the high modulus fibres carry essentially all the load. The matrix serves to transmit the load to the fibres, to protect the fibres from surface damage and to separate individual fibres and blunt cracks which arise from fibre breakage [5,20,28].

The purpose of reinforcing a cement matrix is not the same as that of reinforcing a plastic. In the case of a plastic, fibres are added to strengthen and stiffen the matrix. On the other hand cement is relatively stiff but brittle, therefore fibres are added to inhibit crack propagation, increase the tensile strength and fracture energy as well as to provide a degree of ductility in the behaviour of the material [5,11, 29-31].

Microscopically, cement has a porous structure, which changes with age due to continuing hydration of the cement. The size and extent of porosity in the fibre/cement composites depends on the W/C ratio, fabrication and curing methods employed. The Modulus of Elasticity, shear modulus, compressive and flexural strengths of cement mortar also vary with porosity.

2.1.1 FIBRES

Fibres incorporated in a cement matrix are utilised in a number of ways. First the reinforcing fibres lead to improved strength properties as well as providing higher toughness or energy absorbing capability. The main function of the fibres is to inhibit the propagation of cracks through the matrix. Fibres also allow the composite to retain some post-cracking strength and withstand deformations much greater than can be sustained by the matrix alone [20]. The pull-out process in which fibres bridge across the cracks starts at the onset of cracking. The composite therefore maintains some residual strength even at large displacements and thus continues to absorb energy with increasing deformations [19].

Typical applications of natural fibre reinforced cement and concrete include wood wool slabs covered with a thin layer of cement paste usually used as an insulation material, bamboo reinforcement in concrete slabs and natural fibre reinforced cement products such as roofing sheets and tiles. The use of high modulus fibres in reinforcing cement paste or mortar has also been tried in a number of applications [5,18,29,30]. Common applications includes alkali resistant glass fibre reinforced materials used in building applications and pipe constructions; steel fibre reinforced concrete finds extensive use in making concrete pipes, car park deck slabs, boat hulls, highways, street and air field pavement overlays. The use of low modulus fibres like polypropylene in the making of decorative building panels has also been reported by Zonsveld [18].

Typical fibres used in the reinforcement of epoxy resin include carbon, aramid, boron, glass and of late natural fibres such as sisal, jute, coconut, coir and hemp. Other fibres such as nylon, polyethylene, rayon and E-glass have been investigated in the past [6] but have been

ruled out of serious consideration due to either high cost, low effectiveness or inadequate resistance to alkaline cement environment [5].

The use of carbon in concrete results in low shrinkage, high resistance against freezing and thawing and high durability in hot environments. However glass fibres usually deteriorate at an early stage in alkaline atmospheres. Low frost resistance in cold climates has also been noted in glass/cement composites [5]. More so, carbon and glass are expensive in comparison to natural fibres. The health hazard associated with asbestos and the resulting pollution problem to the surrounding atmosphere were mapped out with clarity in the 1970's. Asbestos fibre producers therefore began looking for a replacement to asbestos and found cellulose based fibres. This effort succeeded in Finland where asbestos was completely replaced by combining cellulose fibres with a small quantity of polypropylene [5,25,30]

2.2 SISAL

2.2.1 HISTORICAL BACKGROUND

Sisal (*Agave Sisalana*), was first introduced into East Africa in 1893 at Kikogwe Tanzania by Dr. Richard Hindorf after procuring the planting materials from Florida. Seven years later the first shipment of sisal from East Africa was made when 7½ tons of fibre was sent from Kikogwe to Hamburg [32]. In Kenya sisal was introduced by the Department of Agriculture in 1903. The plants were obtained from Tanzania and then planted at the Nairobi experimental farm. Further importation of bulbils was made from the West Indies in 1904. These were planted in trial plots at Nairobi, Rabai near the coast and Kibos not far from Kisumu in 1905 and 1906. The first commercial sisal plantation of 1000 acres, was established by R. Swift and E. D. Rutherford in 1907 at Punda Milia between Thika and

Muranga. They had imported 375,000 sisal bulbils from Moa in Tanzania. During the next fifty years, the area planted in sisal had increased to over 250,000 acres and a production rate of 70,000 tons annually had been achieved [22].

Sisal fibre is classified as a hard fibre by virtue of its physical properties. It is coarse, long and has good strength that makes it suitable for spinning coarse yarns used in the manufacture of ropes and cordage where fineness and texture are relatively unimportant. Sisal is a drought resistant plant and is tolerant to a wide variety of soils [23]. It can therefore enable arid regions to be brought into productivity as would not be possible with most other crops. In general the durability of any natural fibre is affected by both the composition of the fibre as well as the environment surrounding the fibres.

2.2.2 MORPHOLOGY

Sisal is a monocotyledonous plant. It has a fibrous, spreading root system and no tap root. The leaf margins are roughly parallel for most of their length and the leaf is many times longer than its breadth. A sisal leaf has an average length of between 1.2 and 2 metres [33]. The leaf is thick at the butt end, fleshy and more or less triangular in cross-section particularly at the neck. The leaf gradually broadens out to a point about halfway along its length becoming thinner and concave on the upper surface. This region is referred to as the lamina, has a boomerang shaped cross-section and narrows down towards the tip. The outside of a sisal leaf is covered by a well developed epidermis having a waxy cuticle which repels water easily [32].

A leaf one meter or more in length contains approximately 1100 fibres, 770 of these being mechanical fibres that are found in the peripheral zone below the epidermis arranged in three or four rows. They reinforce the leaf and help to keep it rigid. The second type are the ribbon fibres, which occur in a median line that runs across the leaf from one margin to the other [33]. To obtain sisal fibres, the leaves are passed through a decorticating machine, which breaks and squeezes out the fleshy tissue. This exposes the fibres which are then washed, dried naturally or artificially and finally brushed.

A single sisal fibre is constructed of numerous elongated fusiform cells known as ultimates that taper at each end. They are closely packed and bonded together. A cross-sectional view shows that about 100 ultimates form a mechanical fibre. The ultimates are largest at the butt end, their sizes however diminishes at the neck and gradually becomes smaller towards the tip of the leaf. Other properties of sisal fibres such as texture, strength, elasticity and rigidity have been discussed in Wilson [34]. The fibre is composed of a complex substance termed as ligno-cellulose. Lock [32] gave the representative analysis of the composition of sisal fibre as shown in table 2.1.

The physical and mechanical properties of the 'UG' grade sisal fibres used in the present work had been researched by Mutuli [1]. Tables 2.2 – 2.4 give the comparison of strength properties between sisal and other commonly used artificial and natural fibres. A typical stress-strain curve of sisal fibre loaded in uniaxial tension as presented by Mutuli [1] is shown in figure 2.1. The curve has a continuous constant gradient and it can be seen that the fibre exhibits brittle failure with no plastic deformation.

Percentage by weight of oven dried material

Cellulose	78
Lignin	8
Waxes	2
Other Carbohydrates, hemicelluloses, pectins etc	10
Ash	1
Loss during analysis	1

Table 2.1 Composition of sisal fibre

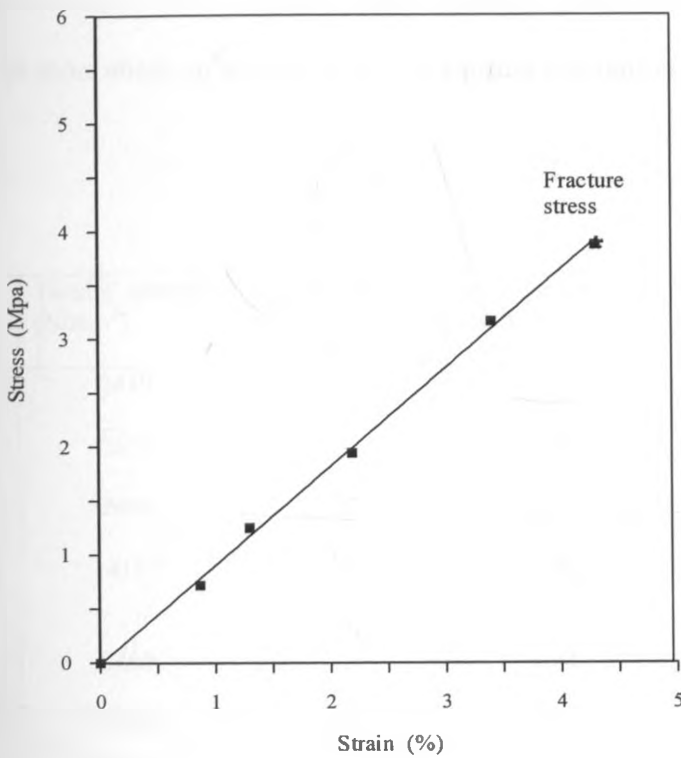


Figure 2.1 Typical tensile stress-strain curve of sisal fibre {after Mutuli [1]}

It can be seen from tables 2.2-2.4 that sisal fibres have comparatively low strength and Modulus of Elasticity compared to some synthetic fibres. However sisal fibres also have some important advantages. The fibre strength is independent of its length as opposed to other synthetic fibres like glass and carbon which gives a pronounced length–strength effect.

The cross-sectional area has an irregular shape, which aids in bonding and consequently improving the fibre/matrix bond strength. Further more sisal fibres appear to be little damaged by the composite production method. In addition the fibres are long and thin giving higher aspect ratios with the overall result of a good bond strength in the composite as discussed in Bessel et al [38] and Mutuli [1].

Fibre treatment provides an effective way of improving the mechanical properties of sisal fibre reinforced polymers. The various treatment methods ensure increased fibre/matrix interfacial bond strength. These include alkali treatment, acid treatment, copper coating and grafting of vinyl monomers on to sisal fibres by gamma irradiation techniques as discussed in Bisanda [39].

Fibre	Tensile strength (N/mm ²)	Modulus of Elasticity (GN/mm ²) X 10 ⁶	Specific gravity (g/cm ³)	Elongation to failure (%)	Source
E-glass	2410	69	2.54	-	Hull [6]
S-glass	2620	87	2.49	-	Hull [6]
Carbon type-2	2410	241	1.75	-	Hull [6]
Steel (structural)	413	207	7.85	-	Hull [6]
Aramid (high modulus)	3450	124	1.44	-	Holister [7]
Boron	2760	379	2.63	-	Holister [7]
Alumina	3000	297	3.30	-	Holister [7]
Asbestos	1490	183	2.40	-	Holister [7]
Titanium alloy	711	117	4.52	-	Majumdar [5]
Polypropylene	500	5	0.9	20	Majumdar [5]

- means the value is not available from literature

Table 2.2 Mechanical properties of commonly used artificial fibres

Fibre	Tensile strength (N/mm ²)	Modulus of Elasticity (GN/mm ²) X10 ⁶	Specific gravity (g/cm ³)	Elongation to failure (%)	Water absorption in 24 hrs (%)	Cross-sectional area (mm ²)	Source
Coconut	159.3 (70.38)	4.02 (2.26)	-	24.20 (8.15)	-	0.08 (0.04)	Kirima [3]
Piassava	143	5.6	1.054	5.99	34.4-108	-	Agopyan [35]
Bamboo sticks	575	28.8	1.158	3.2	145	-	Agopyan [35]
Jute	-	-	0.301	3.7-6.5	214.1	-	Agopyan [35]
Coir	105.3	-	-	41.8	140.3	0.232	Agopyan [35]
Wood	69	7	-	0.50	-	-	Majumdar [5]
Henequen	91-307	-	1.395	2.3-7.6	163.1	-	Agopyan [35]
Malva	300-500	10-40	1.2-1.5	-	400	-	Agopyan [35]
Banana	110-130	20-51	1.3	1.8-3.5	400	-	Rehsi [36]
Castor	25-40	-	1.01	-	235	-	Rehsi [36]
Hemp	40-200	-	1.36	-	140	-	Rehsi [36]
Pineapple Leaf	360-740	24.3-35.1	1.44	2.0-2.8	-	-	Rehsi [36]

Table 2.3 Mechanical properties of commonly used natural fibres

Source	Tensile strength (N/mm ²)	Modulus of Elasticity (GN/mm ²) X10 ⁶	Mean density of fibre (g/cm ³)	Elongation to failure (%)	Fibre cross-sectional area (mm ²) X 10 ⁻²	Breaking length (Km)	Water absorption (%)	Fibre diameter (mm)
Mutuli [1]	347 (118)	14.26 (3.14)	0.70 (0.127)	4	4.95 (1.38)	-	-	-
Maringa [2]	275.77 (90.69)	10.55 (3.13)	0.75	2.60 (0.32)	7.44 (4.71)	32.09 (5.50)	-	-
Nutman adapted from [1]	557 (34)	26.47 (0.057)	0.75	-	-	-	-	-
Agopyan [35]	458	15.2	1.27	4.3	-	-	239	-
Swift [37]	331 (65)	13.2 (0.3)	-	-	-	-	-	-
Majumdar [5]	800	-	1.5	3	-	-	-	0.01-0.05

The numbers in brackets are standard deviations

Table 2.4 Mechanical properties of sisal fibres

One of the important aspects considered in the design of sisal/cement composites is the durability of fibres. Some researchers have reported a limited amount of embrittlement in natural fibre reinforced OPC composites with time [26,35,36]. This can lead to cracks in roofing materials. Gram [25] reported that durability of fibres in alkaline environments can be improved by;

- Using bundled fibres
- Fibre impregnation with blocking agents
- Fibre impregnation with water repellent agents
- Fibre impregnation with both water repellent and blocking agents
- Use of a sealed matrix
- Reducing the alkalinity of the cement matrix.

The embrittlement of sisal fibre reinforced concrete can be delayed by impregnating the fibres. Sealing the pore system of the cement matrix with wax, zinc stearate or sulphur may also improve the durability of the fibres. A more effective method of avoiding the embrittlement of sisal/cement composites is by reducing the alkalinity of the concrete pore water. This reduction can be achieved by replacing part of the ordinary portland cement with fine grained pozzolanas, for instance silica fume, rice husk ash or diatomite [25, 27].

As previously stated, the preparation of sisal fibres involves squeezing out the fleshy tissue through a decorticator [34]. This can introduce a number of flaws (or points of weaknesses) in the fibre morphology.

2.3

MATRICES

2.3.1

RICE HUSK ASH POZZOLANIC CEMENT

2.3.1.1

BACKGROUND, AVAILABILITY AND SOURCES

Although rice husk ash cement has been used in many parts of the world as a pozzolana (cement extender), its potential for use in Kenya has remained largely untapped. This is despite the ever increasing accumulation of rice husks which are a major agro-waste from rice processing regions in this country. However there have been serious attempts recently to investigate the economic and technical feasibility of using RHA cement as a pozzolana in Kenya by the Housing and Building Research Institute (HABRI) at the University of Nairobi. The results so far show positive indications of commercial and technical feasibility.

Pozzolanas have been defined as non-cementitious materials, which in finely divided form react with lime in the presence of water to form cementitious compounds which harden and develop strength with time [40]. There are two types of pozzolanas. The natural pozzolanas have their origin from eruptive volcanic action, where less violent eruptions produces volcanic ash which is a less reactive pozzolana. Artificial pozzolanas are derived from clays, shales, bauxite and many other agricultural wastes such as rice husks, coffee hulls and groundnut shells. The artificial pozzolanas have been manufactured and used widely in many rice growing areas such as China, India, Pakistan, Nepal and Malaysia [40-41]. They have properties that can resist sulphate attack and reduce the occurrence of alkali-aggregate reactions as well as an increase in durability [41]. They are therefore used with lime to supplement the supply of ordinary portland cement (OPC). The main rice growing areas in Kenya includes Mwea, Ahero, West Kano, Bunyala and river Tana delta. The RHAC used in the present work was obtained from HABRI, University of Nairobi.

2.3.1.2 PRODUCTION

2.3.1.2.1 RAW MATERIAL

The raw material for RHA cement production is rice husks. Rice husk is the outermost cover of the rice grain produced after milling and constitutes about 20-30% by weight of the rice grain. Its abrasiveness is due to the presence of silica lodged in the cellulosic structure of the husk [41]. Soluble silica from the soil enters the rice plant through its roots and is accumulated in the husk as amorphous silica. Chemical analysis on the rice husks from Mwea and Ahero in Kenya revealed a high amount of silica (82.3-89.9%) [42]. Oxides of aluminium, iron and calcium are also present in the rice husks [42-43].

2.3.1.2.2 THE PRODUCTION PROCESS

There are two major processes in the production of RHA pozzolana, namely burning and grinding using a kiln and a ball mill type grinder respectively [42].

(i) Burning

The husks can be burned in the open in a heap or under controlled conditions in a special type incinerator. Controlled burning in an incinerator increases the reactivity of the ash [40,42]. Research has shown that reactive ash can be obtained at burning temperatures between 500 and 700° C. If the burning temperatures are too high such as above 750°C, a crystalline and less reactive silica that is much harder to grind develops [41]. Rice husks burn by themselves once started and so no fuel is required.

(ii) Grinding

The ash produced from the kiln is still coarse. In order to bring the constituents close together and to provide a large surface area for reactions to take place, dry grinding of the resulting ash is done in a ball mill for about 5 hours to the required fineness. Since the ash is to be blended with OPC or lime, the fineness achieved should resemble that of the two binders [40-44]. Grinding action takes place between steel balls in a rotating cylindrical drum. The reactivity of RHA is related to the fineness achieved during the grinding period. This in turn depends on the grinding time [43].

2.3.1.3 PROPERTIES

(i) Chemical Analysis

Hammond [40] gave the chemical composition of RHA cement after samples of ground RHA from Kisumu in Kenya were subjected to chemical analysis. This is shown in table 2.5. The Silica content was found to be slightly below 75%. This may be accounted for by the high percentage of ignition loss (21.45%) attributed to the substantial amount of carbon in the ash [40].

(ii) Crushing Strength

Tuts [44] reported on the basis of his compressive strength results that it is possible to add up to 30% of RHA to the OPC in a mortar matrix without losing any strength. According to Dulo [45] a decrease in mortar crushing strength is realised at 20% RHA, then an increase at 30% followed by another decrease at 40% RHA. It was therefore concluded that a mixture of 30:70 RHA to OPC or lime would be suitable for most common applications [45].

CONSTITUENT	% COMPOSITION
SiO ₂	74.50
Fe ₂ O	0.20
Al ₂ O ₃	0.37
CaO	0.80
MgO	0.37
Na ₂ O	0.13
Mn ₂ O ₃	0.14
K ₂ O	1.72
TiO ₂	0.27
P ₂ O ₅	0.05
Ignition loss	21.45

Table 2.5 Chemical composition of RHA for the husk obtained from Kisumu, Kenya.

2.3.2 EPOXY RESIN

Plastics can be broadly classified into two classes; namely thermoplastics and thermosets. Thermoplastics are anisotropic, high molecular weight strong solids and do not cross-link. They soften on heating but upon cooling regain their original mechanical properties. Typical examples include nylon 6-6, polypropylene and polycarbonates among others. They yield and undergo a large deformation before final fracture. Their mechanical properties are however dependent on the temperature and applied strain rate so they creep under constant load. This means that in a composite system there will be a redistribution of the load between the resin and fibres during deformation [6,8]. Thermosetting resins on the other hand are isotropic and brittle. They harden by a process of chemical cross-linking and do not melt on heating. Examples in this category include polyester, epoxy, phenolics, silicones and polyamides [8,46].

Epoxy resins may be defined as resins in which chain extension and cross-linking occurs through the reactions of epoxide group resident on the epoxy polymer chain [47].

The majority of epoxy resins used in composites are manufactured by the reaction of epichlorhydrin with materials such as bisphenol A or aromatic amines [46].

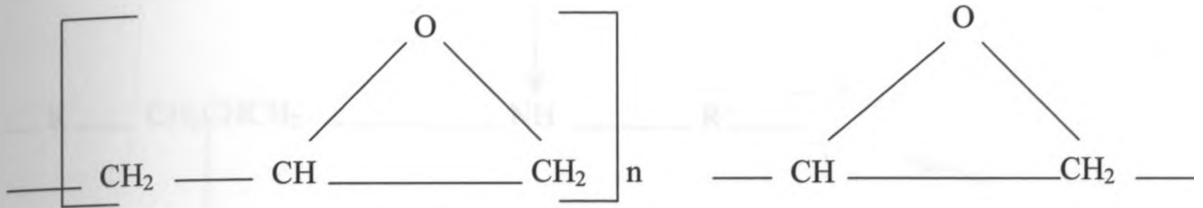


Fig 2.2 Epoxy group.

All epoxy resins contain the epoxy or glycidyl group as shown in figure 2.2. This can react with a number of compounds containing an active hydrogen atom such as phenols, amines and carboxylic acids. The reaction is an addition polymerisation which does not produce any side products and finally epoxy resins cure to give a three dimensional stable network with a relatively low shrinkage, typically 2-3% [4,46-47].

Cross-linking of epoxy resins by amines proceeds as illustrated in figure 2.3. The epoxy ring is opened by the primary amine group to give a secondary hydroxyl group. Thus when the amines and epoxy resins possessing a functionality greater than two react together, they cross-link to give a three-dimensional polymer network containing ether bridges, secondary hydroxyl groups and tertiary amine groups [4]. Epoxy resin hardening occurs through the reaction of epoxy group aided by selective use of hardeners, curing agents or catalysts. The liquid resins are converted into hard brittle solids by chemical cross-linking which leads to

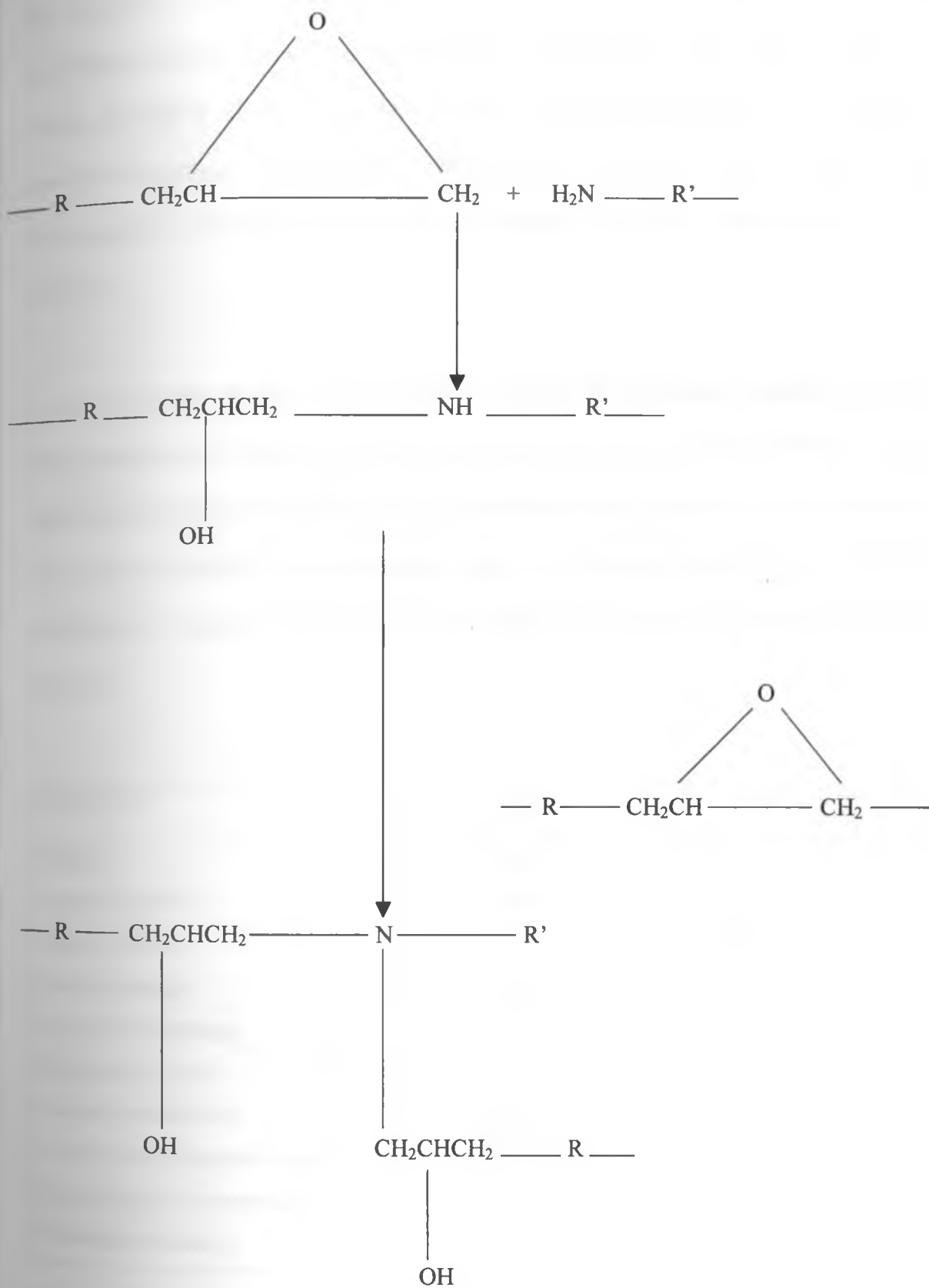


Figure 2.3 Cross-linking of epoxy resins

the formation of a tightly bound three dimensional network of polymer chains. The mechanical properties depend on the molecular units making up the network and on the length and density of cross links [46]. Epoxy resins are extensively used in advanced structural composites. For example by 1989, more than two thirds of the aerospace market for composites utilised epoxy resin matrices reinforced with either carbon, glass or aramid fibres [4].

A set of properties of epoxy resin is given in Table 2.6, which was compiled by Johnson from manufacturer's literature {Adapted from Hull [6]}. The overall key features of epoxy resin that lead them to be selected for high performance application of composite materials are: extreme versatility of processing and curing, low shrinkage, high adhesive strength, low co-efficient of thermal expansion, excellent mechanical strength and chemical resistance [6,8,47].

PROPERTY	UNITS	VALUE
Density	Mgm^{-3}	1.1 – 1.4
Young's modulus	GNm^{-2}	2 – 6
Poisson's ratio		0.38 – 0.4
Tensile strength	N/mm^2	35 – 100
Compressive strength	N/mm^2	100 – 200
Elongation to break	%	1 – 6
Thermal conductivity	$\text{WM}^{-1} \text{ } ^\circ\text{C}$	0.1
Co-efficient of thermal expansion	$10^{-6} \text{ } ^\circ\text{C}^{-1}$	60
Heat distortion temperature	$^\circ\text{C}$	50 – 300
Shrinkage on curing	%	1 – 2

Table 2.6 Typical properties of epoxy resins used in composite materials {after Johnson, Adapted from Hull [6]}

2.4 MECHANICAL PROPERTIES OF FIBRE REINFORCED COMPOSITES

2.4.1 STRENGTH CHARACTERISTICS OF FIBRE REINFORCED COMPOSITES

2.4.1.1 STRESS DISTRIBUTION IN FIBRE REINFORCED COMPOSITES

The stress system in a component of composite material can be regarded as comprising two parts namely:

- (i) The macroscopic system associated with external loading computed with the assumption that the material is uniform and homogenous.
- (ii) The microscopic system associated with the transfer of loads between the components of the composite.

At the microscopic level the mechanisms of fibre reinforced composites is well explained considering unidirectional continuous fibres [6-8] as shown in figure 2.4. Since the fibres and the matrix have quite different elastic moduli, a complex state of stress distribution will be developed when a composite is loaded uniaxially in the direction of the fibres. Analysis has shown that shear stresses develop at the fibre/matrix interface [20]. The distribution of this shear stress and the axial tensile stress along the length of the fibre is given in figure 2.5.

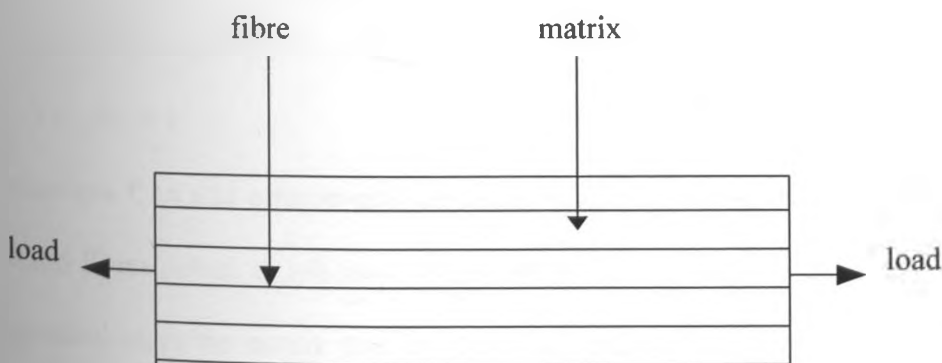


Figure 2.4 Uni-directional aligned continuous fibre composite

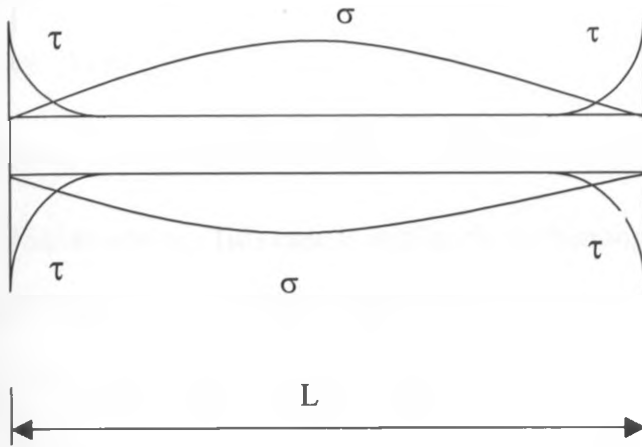


Figure 2.5 The variation of stresses along a fibre

2.4.1.2 RULE OF MIXTURES

A reasonable approximation of the modulus and strength of a fibre reinforced composite is given by the rule of mixtures [6,20,48] using the model in figure 2.4. If a tensile force P is applied in the direction of the fibres, it can be assumed that the fibres and the matrix will strain equally and that the load carried by the composite is the sum of the loads carried individually by the matrix and the fibres.

$$\epsilon_f = \epsilon_m = \epsilon_c \quad (2.1)$$

$$P_c = \sigma_f A_f + \sigma_m A_m \quad (2.2)$$

$$E_c = E_f V_f + E_m (1 - V_f) \quad (2.3)$$

$$\sigma_c = \sigma_f V_f + \sigma_m (1 - V_f) \quad (2.4)$$

$$V_f + V_m = 1 \quad (2.5)$$

The subscripts f , m and c represents the fibre, matrix and composite respectively with both matrix and fibres acting simultaneously as a two phase composite until failure. However in most practical cases the matrix does not fracture simultaneously with the fibres [37]. Hence

equation (2.4) is modified to give the ultimate strength of the composite as:

$$\sigma_{cu} = V_f \sigma_{fu} + (1 - V_f) \sigma_m' \quad (2.6)$$

Where σ_m' represents the flow stress in the matrix at the fracture strain of the fibres and σ_{fu} represents the fibre fracture stress. This case is applicable to thermoplastic composites where the fibres fracture first. In the case of brittle matrices such as cement or concrete, the matrix will fracture first and so equation (2.4) is modified to:

$$\sigma_{cu} = V_f \sigma_f' + (1 - V_f) \sigma_{mu} \quad (2.7)$$

Where σ_f' is the stress in the fibre at the failure strain of the matrix [20,37]. Fibre additions to the cement paste or mortar offer a convenient and practical means of achieving improvements in many engineering properties of the material such as fracture toughness, fatigue resistance, impact resistance and flexural strength. The concept of providing reinforcement as an integral part of the fresh mortar mass also provides advantages in terms of fabrications of products and components [30].

It can be shown theoretically that a large increase in strength can be obtained as a result of the inclusion of low-modulus fibres in epoxy resin [6]. It has also been shown that continuous low-modulus polypropylene fibrillated fibres in OPC mortar and paste can more than double the load capacity of beams [37]. In the present work the results of a theoretical analysis of flexure in references [28,37,49] were confirmed experimentally, showing that such increases are possible using sisal, a cheap, low modulus fibre whose use in the manufacture of cement-mortar composites has great potential in the building and construction industry of developing countries.

2.4.1.3 FIRST CRACK STRENGTH UNDER AXIAL TENSION

The cracking strength of a brittle matrix is given by Dieter [20] as

$$\sigma_{m(cr)} = E_m \epsilon_{mu} = \sigma_{mu} \quad (2.8)$$

If this matrix is reinforced with fibres, volume fraction V_f and modulus E_f , then the first crack strength of the composite is given by the rule of mixtures as

$$\sigma_{c(cr)} = V_f E_f \epsilon_{mu} + (1 - V_f) E_m \epsilon_{mu} \quad (2.9)$$

For strengthening due to fibre reinforcement to occur

$$\sigma_{c(cr)} - \sigma_{m(cr)} = V_f (E_f - E_m) \epsilon_{mu} > 0 \quad (2.10)$$

Thus for an increase in first crack strength to occur, the modulus of the fibres must exceed that of the matrix [37].

2.4.1.4 ULTIMATE TENSILE STRENGTH

Once the matrix has cracked, the greatest strain that can be carried by the fibres is denoted by $\epsilon_{f(max)}$. If the composite continues to bear increasing loads after the matrix has visibly cracked and no longer contributes to the strength of the composite [5,16,48] then the ultimate tensile strength is given by

$$\sigma_{cu} = V_f E_f \epsilon_{f(max)} \quad (2.11)$$

Thus Swift [49] and Kelly [50] concluded that for strengthening to occur

$$\frac{\epsilon_{f(max)}}{\epsilon_{mu}} > \frac{E_m}{V_f} \quad (2.12)$$

2.4.1.5 ULTIMATE FLEXURAL FAILURE

Swift and Smith [37] pointed out that in flexure additional effects have to be considered.

These include the redistribution of stress and movement of the neutral axis, arising from the changes in the local stress-strain behaviour. A similar observation was also made by Nair [13] suggesting that in the tensile zone, micro and visible crack lower the elastic modulus of the material giving a form of plastic behaviour as fibres pull out. As the neutral axis approaches the compressive surface, a non-linear compressive behaviour is likely to occur [14]. On complete cracking when the entire load is carried by fibres only, the effective modulus of the cracked region is given by Kelly [50] as

$$E_1 = \eta V_f E_f \quad (2.13)$$

Where η is a factor that allows for disorientation of fibres (taking values of $2/\pi$ and 0.5 for planar and three-dimensional random orientations respectively) and the length of fibres.

2.4.2 STRESS-STRAIN CURVE

When a fibre reinforced brittle matrix is loaded, the matrix will crack long before the fibre can be fractured. Once the matrix is cracked, one of the following types of composite failure (stress-strain curves) shown in figure 2.6 may occur [16].

- (a) The composite fractures immediately after matrix cracking. The composite does not carry any further load after the first crack.
- (b) The maximum load the composite can withstand is equal to the matrix strength. However the composite continues to carry decreasing loads after the peak stress. Pulling out of fibres from the cracked surfaces provides the post-cracking resistance. No considerable increase in tensile strength is observed but a remarkable increase in toughness (area under the load extension curve) is noted.
- (c) The composite continues to carry increasing loads even after matrix cracking. Both the composite tensile strength and percentage elongation to failure is greater than

those of the matrix alone. This is attributed to the energy absorbing mechanism of multiple-matrix fracture (MMF) and it ensures the optimum performance of both matrix and fibres.

If the fibre pull-out strength is greater than the matrix-cracking strength, the composite will absorb energy on loading even after first cracking. With increasing loads the composite transfers this energy to the matrix through the bond stresses. If the energy transferred is less than the fibre/matrix bond strength, then multiple cracking occurs. The process of multiple cracking continues until the fibre fractures or accumulated debonding leads to fibre pull-out.

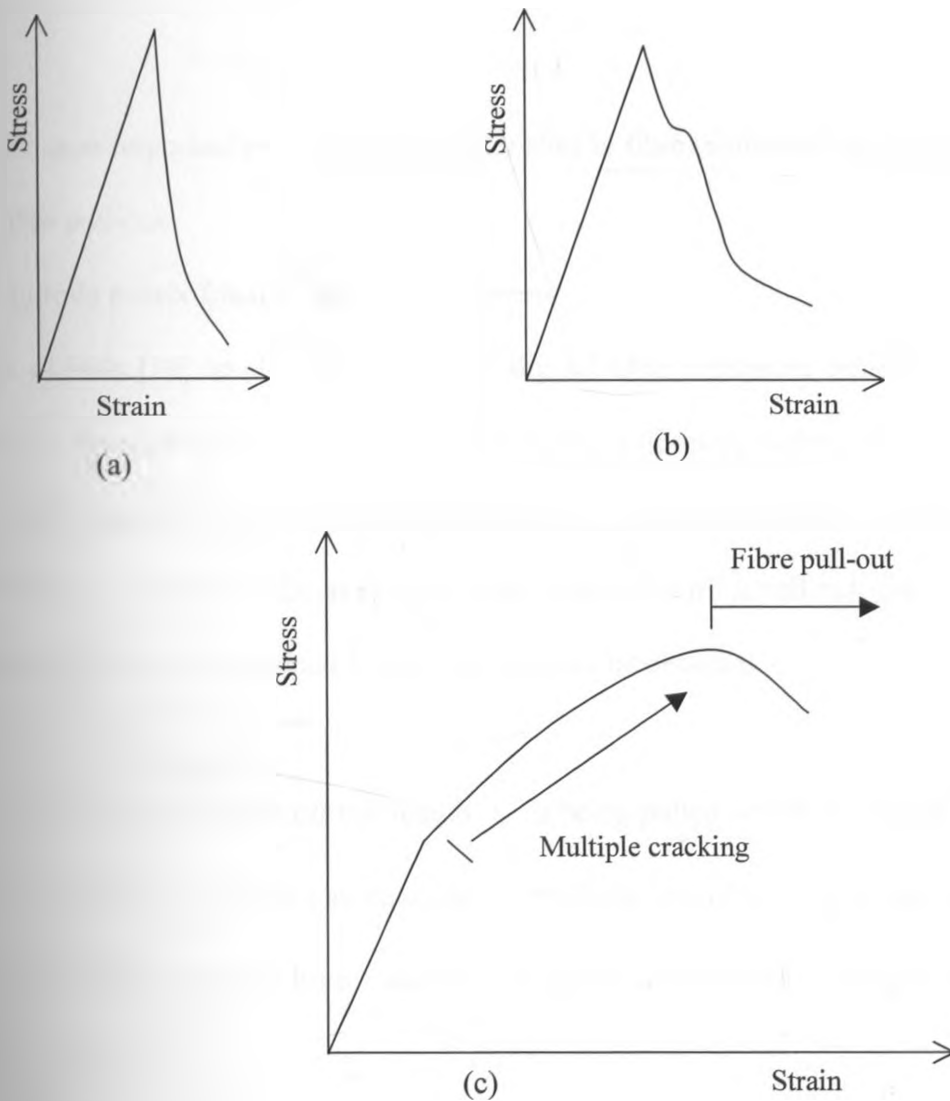


Figure 2.6 Possible fibre reinforced cement stress-strain curves

POST CRACKING DUCTILE BEHAVIOUR

2.4.3

One of the advantages of fibre reinforcement in composite materials is to impart additional energy absorbing capability thereby transforming a brittle cement material into a pseudo ductile material. Fibres in cement composites act as crack arrestors, which creates a stage of slow crack propagation and gradual failure. Aziz et al [51] observed that the presence of fibres spanning across the cracks at the post-cracking stage usually inhibits the sudden collapse of a member. This gives ample warning of imminent failure. It was also reported in [51] that this improvement in strength property can also be imparted by natural fibres in cement paste, mortar or concrete.

Two of the most important post ductile characteristics in fibre reinforced composites includes

- (i) Fibre pull-out
- (ii) Multiple matrix fracture (MMF) phenomena

The work of Hale [14] on chopped, randomly aligned fibre reinforced cements showed that fibre pull-out occurs preferentially at a single crack when fibres of uniform cross-section are used. Further research by Majumdar [5] pointed out that if the radius of fibre increases towards the ends so that interfacial pressure also increases during pull out, then the increase in maximum shear stress sustained by the interface can be obtained.

If a fibre of length equal to its critical length ' l_c ' is being pulled out of the matrix, the tensile strength of the fibre at cracking is equal to its breaking strength ' σ_{fu} '. The critical fibre length is the shortest length of fibre, which can be loaded to fracture in a composite [5].

$$\sigma_{fu} = \tau_b \frac{l_c}{r} \quad (2.14)$$

where τ_b is the interfacial bond strength and 'r' the fibre radius. Therefore no fibre will be broken if fibre lengths are less than l_c . Pull-out will initially occur at composite stress σ_p^o given by Hale [14] as

$$\sigma_p^o = \frac{1}{2} \sigma_{fu} V_f \frac{l_f}{l_c} \quad (2.15)$$

Oakley and proctor [16] stated that in cases where the fibre breaks before pulling out, frictional forces play a big role in maintaining a high proportion of strand fracture. The work of Parameswaran and Rajagopalan [10] showed that in cases where beams failed by the fibre pull-out mode, a single crack traversing through the neutral axis of the beam at matrix cracking load was noticed. Similar results were also obtained by Swift and Smith [49] who observed that as fibres gradually pull out of the matrix, there is a progressive diminution in the load giving the composite a superior post-cracking ductility and energy absorption characteristics. The essential condition for MMF to occur is that the fibres reinforcing the matrix should be sufficiently strong and numerous to sustain the load even after the matrix has failed, as discussed in Forsyth [28]. The stress in the composite immediately before the composite cracks was given by Oakley and Proctor [16] as

$$\sigma_c = V_f \sigma_f' + (1 - V_f) \sigma_{mu} \quad (2.16)$$

$$= V_f E_f \varepsilon_f (1 + \alpha) \quad (2.17)$$

Where
$$\alpha = \frac{1 - V_f}{V_f} \frac{E_m}{E_f} \quad (2.18)$$

Multiple fracture is therefore expected if fibre lengths exceed a value ' l_m ' given in Aveston et al [52] such that

$$\frac{l_m}{l_c} = 2 \frac{\varepsilon_{mu}}{\varepsilon_{fu}} (1 + \alpha) \quad (2.19)$$

If ' l_m ' is less than ' l_c ' then MMF followed by fibre pull-out will occur in discontinuous fibre composites.

Once multiple cracking is complete the matrix cannot carry any additional load. Fibres carry the entire load. The slope of the stress-strain curve after multiple cracking is complete ' E_α ' was given by Oakley and Proctor [16] as

$$E_\alpha = V_f E_f \quad (2.20)$$

The strength of the composite at failure then becomes

$$\sigma_c = V_f \sigma_f \quad (2.21)$$

MMF has also been investigated by Kelly and Zwebeden [50] who reported an increase in strength of hardened OPC due to this phenomenon. This occurs if the negative effects of shrinkage stresses and fibre surface asperities are eliminated.

2.4.4 ENERGY ABSORBING MECHANISMS

Various forms of energy absorbing mechanisms occur in composites during fracture. These include matrix fracture, fibre fracture, bond failure and fibre pull-out. Different researchers have developed a number of energy absorbing mechanisms as given below.

(i) Energy absorbed in cracking the matrix, (Kelly and Zwebeden [50])

$$\gamma_m = \frac{V_m^2 \sigma_m r U_m}{2V_f \tau_s} \quad (2.22)$$

Where U_m is the work done to deform a unit volume of matrix to failure and τ_s is the shear stress.

- (ii) Energy absorbed by the composite due to debonding of fibres, (Hale [14])

$$\gamma_b = \frac{\sigma_f^2}{2V_f} \frac{r}{E_f \tau_s} \left[\frac{\sigma_f}{V_f} - \frac{(4\tau_b E_f)^{\frac{1}{2}}}{r} \right] \quad (2.23)$$

Where τ_b is the interfacial bond strength.

- (iii) Energy absorbed in fracturing the fibres, (Nair [13])

$$\sigma_{fu} = \frac{V_f \sigma_f^2 l_c}{6E_f} \quad (2.24)$$

2.4.5 FRACTURING ENERGY

Two forms of fracture can occur in FRC

- (i) Fibres pull-out before fracture (fracture type I)
 - (ii) Fibres fracture followed by pull out of some of them (fracture type II)
- (a) The first case occurs when short fibres are used as a reinforcement. Three stages can be distinguished namely; debonding, pull-out and then secondary redistribution of stresses. Hence the total energy absorbed by the composite at fracture is the sum of these three components [19]

- After debonding fibres pull-out; the energy absorbed by composite during fibre pull-out

' γ_p ' is

$$\gamma_{p(I)} = \frac{V_f \tau l^2}{6 d_f} \quad (2.25)$$

where l is the length of fibre and d_f the fibre diameter.

- After both debonding and fibre pull-out the fibre ends are unable to absorb the excess energy stored in the deformation process. This energy ' γ_r ' is transferred to the matrix

$$\gamma_{r(l)} = \frac{V_f \tau^2 l^2}{6 E d_f} \quad (2.26)$$

- Finally the energy of the matrix fracture, considering the reinforcement volume fraction, is given by

$$\gamma_{s(l)} = (1 - V_f) \gamma_m \quad (2.27)$$

Therefore the total energy in a pull-out dominated process is:

$$\gamma_{tot(l)} = \gamma_{p(l)} + \gamma_{r(l)} + \gamma_{s(l)} \quad (2.28)$$

- (b) The second case occurs when long continuous fibres are used as a reinforcement.

2.4.6 INTERFACIAL BOND STRENGTH

Interfacial bond strength refers to the strength of the bond between the fibre and the matrix. The strength of a composite greatly depends on the fibre/matrix bond strength [15]. It was also observed by Dyczek and Petri [19] that the strength of a fibre/matrix bond is a quality which determines to a considerable degree such properties as strength, modulus of rupture and fracture energy of the composite.

In the case of polymeric matrices the fibre/matrix bond is frictional, meaning that its strength depends on the surface roughness of the fibre. In glass fibre reinforced cements, a chemical bond is formed due to nucleophilic attack of OH^- on the Si-O bond. The work of Majumdar [5] on steel wire reinforced cements showed that the fibre/matrix interface is a zone in which a transition of properties occurs from the fibre to the matrix. Further work by Broutman and

Krock [53] pointed out that fracture surface can indicate the type of fibre/matrix bond that existed as shown in figure 2.7.

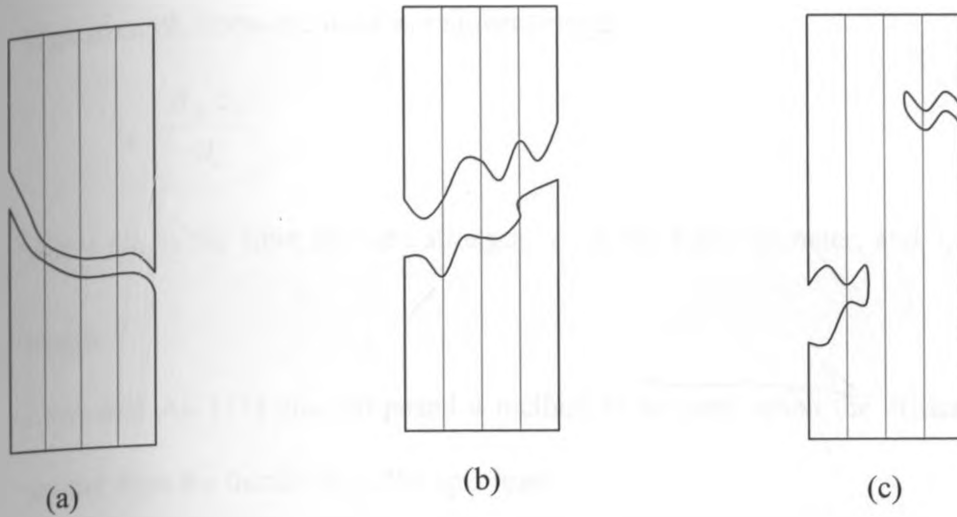


Figure 2.7 Composite fractures indicating different fibre/matrix bond strengths

- (a) Strong fibre/matrix bond strength
- (b) Intermediate fibre/matrix bond strength
- (c) Poor fibre/matrix bond strength

A low bond strength is associated with large impact resistance and poor tensile strength of the composite. Several researchers have proposed different methods of determining the fibre/matrix bond strength. These include;

1. Oakley and Proctor [16] proposed a method used when the fibre/matrix bond is frictional in nature. In this case the shear stress along the fibre in a pull-out test is constant and equal to the bond strength. The bond strength is given by

$$\tau_b = \frac{F}{tp} \quad (2.29)$$

where τ_b is the interfacial bond strength, F is pull-out load, t is the embedded length or

disk thickness and p the strand perimeter.

2. Laws and Ali [15] gave the average fibre/matrix interfacial bond strength when very thin, high strength fibres are used as reinforcements.

$$\tau_b = \frac{\sigma_{fu} d_f}{4l_c} \quad (2.30)$$

where σ_{fu} is the fibre fracture strength, d_f is the fibre diameter, and l_c the critical fibre length.

3. Laws and Ali [15] also proposed a method to be used when the critical fibre length is greater than the thickness of the specimen.

$$\tau_b = \frac{F}{\Pi d_f b} \quad (2.31)$$

where b is the specimen thickness and F is the pull-out load.

4. Dyczek and Petri [19] developed a method which is applicable when a fibre that is fastened to a matrix along a length X is being pulled out of the matrix.

$$\tau_b = \frac{\sigma_f d_f}{4X} \quad (2.32)$$

where $d_f = \frac{4A_f}{p_f}$ = fibre diameter, A_f is the fibre cross-sectional area, p_f is the fibre perimeter and X is the length of fibre embedded in the matrix.

5. Aveston et al [52] proposed a method that measures the bond strength by use of crack spacings. According to their theory during multiple cracking, the cement matrix is broken into a series of blocks of lengths X' and $2X'$.

$$\tau_b = \frac{V_m \sigma_{mu} r}{V_f 2X'} \quad (2.33)$$

Where σ_{mu} is the ultimate strength of matrix, r is the fibre radius and X^1 is the length of inter-crack spacing.

The equation proposed by Aveston uses parameters that can be directly measured and therefore becomes more practical in most common applications. It was therefore used to determine the interfacial bond strength of sisal fibre reinforced RHAC composites fabricated in the present work.

2.4.7 EFFICIENCY FACTORS

The fibre reinforcement arrangement that has a particular importance in reinforced cements, concrete or polymeric matrices are discontinuous, randomly aligned fibres arranged in two or three dimensions. To deal with such cases the concept of efficiency factors was introduced by Krenchel [54]. Efficiency factors give an estimate of how efficient discontinuous randomly aligned fibres are as reinforcements when compared to continuous parallel aligned ones.

2.4.7.1 FIBRE LENGTH EFFICIENCY FACTOR

Allen [55] and Laws [56] gave the expressions for the failure stress of the composite when fibres are sufficiently long relative to the critical length ' l_c ' (l_c is the shortest length of fibre which can be loaded to failure in the composite) as

$$\sigma_c = \left(1 - \frac{l_c}{2l_f}\right) V_f \sigma_f + V_m \sigma_m \quad (2.34)$$

$$E_c = \left(1 - \frac{l_c}{2l_f}\right) V_f E_f + V_m E_m \quad (2.35)$$

The co-efficient $\left(1 - \frac{l_c}{2l_f}\right)$ is the length efficiency factor η_l . It is determined by the length of the fibre in relation to the critical fibre length l_c [5].

$$\eta_l = \left(1 - \frac{l_c}{2l_f}\right) \text{ for } l_f > l_c \quad (2.36)$$

2.4.7.2 FIBRE ORIENTATION EFFICIENCY FACTOR

Tsai [57] analysed unidirectional fibre reinforced composites. A misalignment factor K was used to correct for non-parallelism of the fibres. The misalignment factor is usually less than unity, the rule of mixtures equations 2.3 and 2.4 are therefore modified to

$$\sigma_c = KV_f \sigma_f + V_m \sigma_m \quad (2.37)$$

$$E_c = KV_f E_f + V_m E_m \quad (2.38)$$

A more general form of the longitudinal modulus and stress at an arbitrary angle θ to the fibre direction was given by Nielson [58] as

$$\frac{1}{E_c} = \frac{\cos^4 \theta}{E_{11}} + \frac{\sin^4 \theta}{E_{22}} + \left[\frac{1}{G_{12}} - \frac{2\nu_{12}}{E_{11}} \right] \cos^2 \theta \sin^2 \theta \quad (2.39)$$

$$\frac{1}{\sigma_c} = \frac{\cos^4 \theta}{\sigma_{11}} + \frac{\sin^4 \theta}{\sigma_{22}} + \left[\frac{1}{\tau_{12}} - \frac{2\nu_{12}}{\sigma_{11}} \right] \cos^2 \theta \sin^2 \theta \quad (2.40)$$

A plot of the variation of the tensile modulus of elasticity with the angle between the applied stress and the principal fibre direction is shown in figure 2.8.

fibre direction

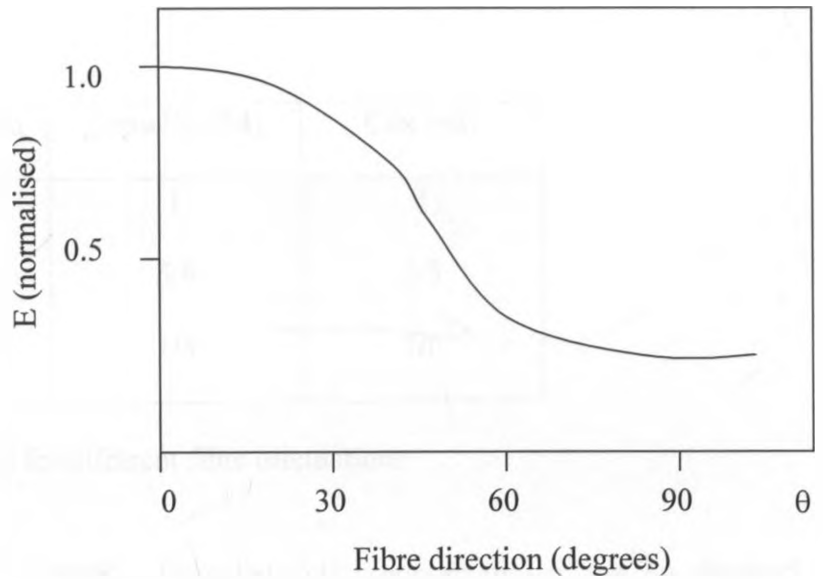
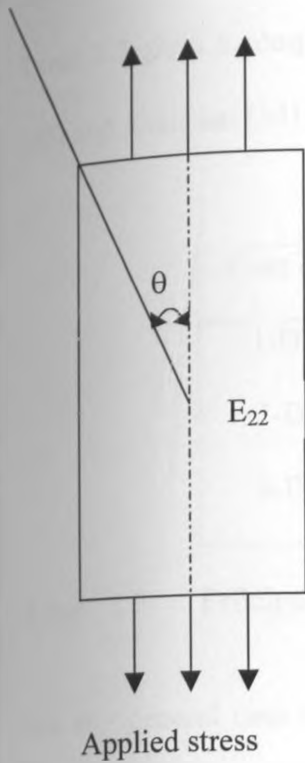


Figure 2.8 Variation of the composite tensile modulus of elasticity with the angle between the applied stress and principal fibre direction

2.4.7.3 FIBRE RANDOMNESS EFFICIENCY FACTOR

The concept of randomness efficiency factor was studied by Cox [48]. He used a randomness efficiency factor η_o to take into account the dependence of the modulus on randomness and orientation. The rule of mixtures equations 2.3 and 2.4 then become

$$\sigma_c = \eta_o V_f \sigma_f + V_m \sigma_m \quad (2.41)$$

$$E_c = \eta_o V_f E_f + V_m E_m \quad (2.42)$$

The work of Cox [48] also showed that η_o took values of 1/3 and 1/6 for two and three dimensional fibre distributions respectively.

However Nielson [58] argued that the value of η_o depends on the method of analysis used.

Table 2.7 gives a comparison of the values of η_o obtained by two different researchers Cox [48] and Krenchel [54].

Fibre orientation	Krenchel [54]	Cox [48]
1-D aligned	1	1
2-D aligned	3/8	1/3
3-D aligned	1/5	1/6

Table 2.7 Efficiency factors for different fibre orientations

For any general case of fibre orientation, Krenchel [54] proposed that η_o can be obtained from the equation

$$\eta_o = \sum_{j=1}^m V_{ij} \cos^4 \theta_j \quad (2.43)$$

Where V_{ij} is the fibre volume fraction at an angle θ to the principal axis, and m is the number of intervals in θ .

When all the three efficiency factors are used together, the rule of mixtures equations 2.3 and 2.4 are modified to

$$\sigma_c = K \eta_o \eta_l V_f \sigma_f + (1 - V_f) \sigma_m \quad (2.44)$$

$$E_c = K \eta_o \eta_l V_f E_f + (1 - V_f) E_m \quad (2.45)$$

2.4.8 CRITICAL FIBRE LENGTH

Majumdar [5] defined the critical fibre length as the shortest length of fibre which can be loaded to fracture in a composite. The critical fibre length also plays an important role in the determination of the fibre fracture strength and fibre/matrix interfacial bond strength. The work of Hale [14] showed that when a fibre of length equal to its critical length is being pulled out of a matrix, then the tensile strength σ_f of the fibre at the crack surface becomes equal to the fibre fracture strength σ_{fu} given in equation 2.14. The fibre pull-out stress that initially occurs in the composite σ_p^o was given by Hale [14] in equation 2.15. It gives the relationship between the critical fibre length and the initial fibre pull-out stress in the composite.

Dyczek and Petri [19] gave the expression for evaluating the fibre critical length as

$$l_c = \frac{\sigma_f d_f}{2\tau_b} \quad (2.46)$$

where σ_f is the tensile strength of the fibre, d_f is the fibre diameter and τ_b is the interfacial bond strength.

2.4.9 CRITICAL FIBRE VOLUME FRACTION

Critical fibre volume fraction is defined as the volume fraction which must be exceeded in a composite system before fibre strengthening of the composite can occur [20]. Therefore in order to obtain any benefit from the use of fibres as a reinforcement, the composite strength must be greater than that of the strain hardened matrix [28] such that

$$\sigma_{cu} \geq \sigma_{mu} \quad (2.47)$$

$$\sigma_{fu} V_f + \sigma'_m (1 - V_f) \geq \sigma_{mu} \quad (2.48)$$

This means that a critical fibre volume fraction that must be exceeded for strengthening to occur can be obtained from equation 2.48. This critical fibre volume fraction was given by Dieter [20] as

$$V_{f(crit)} = \frac{\sigma_{mu} - \sigma'_m}{\sigma_{fu} - \sigma'_m} \quad (2.49)$$

The strength of the composite may not follow equation 2.48 in very low fibre volume fraction composites. The reason for this was given by Hull [6] as being because there would be an insufficient number of fibres to effectively restrain the elongation of the matrix. As a result the fibres are rapidly stressed to fracture and the matrix carries part of the load by strain hardening. Assuming that this happens, when all the fibres fracture ($V_f = 0$), equation 2.48 becomes

$$\sigma_{cu} \geq \sigma_{mu} (1 - V_f) \quad (2.50)$$

The minimum fibre volume fraction which must be exceeded to have real reinforcement is given in Dieter [20] as

$$V_{f(min)} = \frac{\sigma_{mu} - \sigma'_m}{\sigma_{fu} + \sigma_{mu} - \sigma'_m} \quad (2.51)$$

Aveston et al [52] in the characterisation of the stress-strain curve of a fibre reinforced composite explained that after the LOP, a regime of multiple cracking can follow provided that there are sufficient fibres to support the stress after the matrix has failed. The critical fibre volume fraction which must be exceeded for this to take place is given by the inequality

$$V_{f(crit)} \sigma_{fu} > E_c \varepsilon_{mu} \quad (2.52)$$

Where ε_{mu} is the matrix failure strain, σ_{fu} is the fibre fracture strength, and E_c is the composite modulus of elasticity.

The critical fibre volume fraction in fibre reinforced cements can also be evaluated from the fibre/matrix interfacial bond strength and fibre aspect ratio. This expression was given by Hannant [59] as

$$V_{f(crit)} = \frac{2\sigma_{cu}d_f}{\tau_b l_f} = \frac{2\sigma_{cu}}{\tau_b(l_f/d_f)} \quad (2.53)$$

Where σ_{cu} is the ultimate composite strength in direct tension, τ_b is the interfacial bond strength, l_f is the fibre length, d_f is the fibre diameter and l_f/d_f is the fibre aspect ratio.

2.4.10 FLEXURAL TOUGHNESS

Flexural toughness measurements are made from load-deflection curves during flexural testing of beams. The standard method for measuring flexural toughness is ASTM C1018 [74]. This standard is based upon a specimen and loading geometry taken from its related standard ASTM C78 [75] for flexural strength.

One of the important properties of fibre reinforced cements is toughness. It could reduce the risk of structural failure especially in areas where earthquakes frequently occur. Toughness is a measure of the energy absorption capacity. The toughness of a fibre reinforced cement composite is represented by the area under the load-deflection curve. However this property is better quantified by another material property known as a toughness index [31,74].

The toughness index is defined as a measure of the amount of energy required to deflect the (100 × 100 × 500) mm beams used in the MOR tests up to a certain multiple of first crack displacement, compared to the energy required to bring the fibre beam to the point of first crack deflection (proportional limit, defined as the deviation from linearity). Toughness

index therefore is the number obtained by dividing the area under the load-deflection curve of a flexural strength specimen up to a specified multiple of first crack deflection, by the area up to the deflection at which first crack is deemed to have occurred. Toughness indexes are expressed by subscripts 5,10,30 etc [31,60,74].

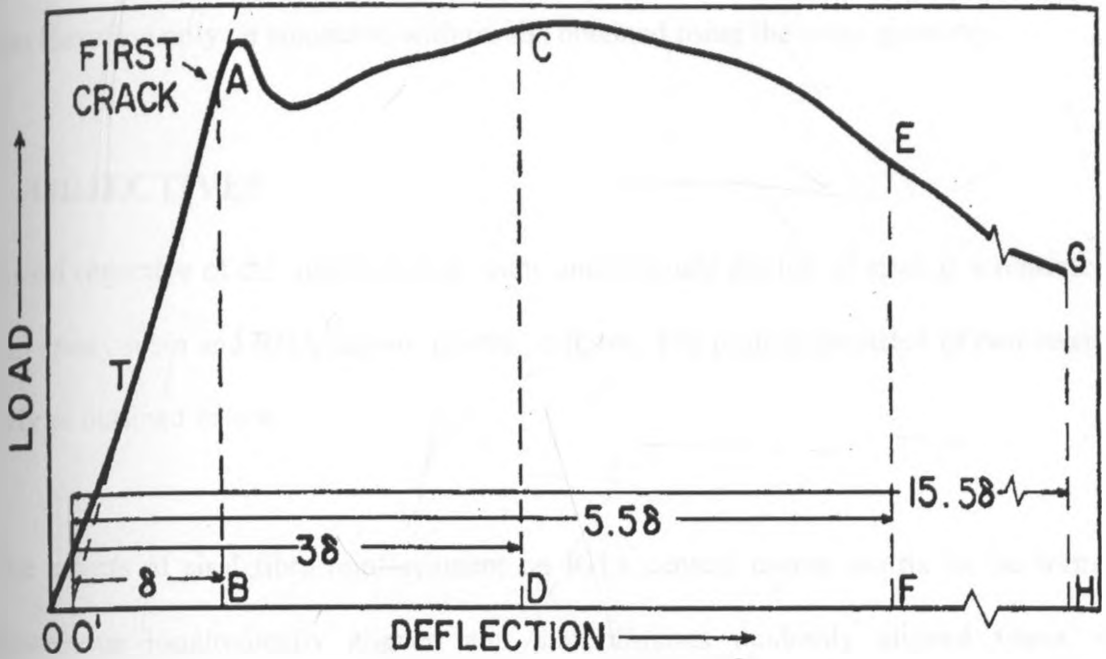


Figure 2.9 Determination of toughness index from a load deflection curve using ASTM C1018

Referring to figure 2.9

$$I_1 = \frac{\text{Area under the } L - D \text{ curve, up to a specified multiple } \delta}{\text{Area under the } L - D \text{ curve up to } \delta} \quad (2.54)$$

$$I_5 = \frac{\text{Area under the curve to } 3\delta}{\text{Area under the curve to } \delta} \quad (2.55)$$

$$I_{10} = \frac{\text{Area under the curve up to } 5.5\delta}{\text{Area under the curve to } \delta} \quad (2.56)$$

Flexural toughness index I_5 is defined as the area under the load deflection curve up to 3δ divided by the area up to δ [60,61]. For a perfectly elastic-plastic material, the flexural

toughness index I_5 would equal 5. Index I_{10} would be equal to 10 in the elastic-plastic material. A toughness index I_5 greater than 5 indicates that the area under the load-deflection curve is greater than for the elastic-plastic material behaviour. This could be an indication of increased load carrying capacity beyond matrix cracking. The reverse could be the same for toughness index less than 5 [60]. Toughness values are dependent on specimen geometry and can therefore only be compared with results obtained using the same geometry.

2.5 OBJECTIVES

The broad objective of this research is to study and evaluate the use of sisal as a reinforcing fibre in epoxy resin and RHA cement mortar matrices. The project consisted of two sections of study as outlined below.

1. The effects of sisal fibre reinforcement on RHA cement mortar matrix in the form of continuous longitudinally aligned and discontinuous randomly aligned fibres was examined with respect to the reinforcement volume fraction and fibre aspect ratios on the following;
 - (a) Flexural strength
 - (b) Tensile strength
 - (c) Tensile Modulus of Elasticity
 - (d) Density and void volume
 - (e) Fibre/matrix interfacial bond strength
 - (f) Flexural toughness, while varying fibre volume fraction, water/cement ratio and curing age.

2. The effects of sisal fibre reinforcement on epoxy resin matrix was investigated with respect to the fibre content, aspect ratios and incorporation techniques on the following composite mechanical properties.

- (a) Tensile strength and tensile strain
- (b) Tensile Modulus of Elasticity
- (c) Flexural strength
- (d) Flexural Modulus of Elasticity

3 EXPERIMENTAL PROCEDURE

3.1 MOULDS

The preparation of specimens involved casting by laying and curing in moulds. Moulds for casting sisal fibre reinforced epoxy resin specimens consisted of top and bottom faces made from a black mild steel plate and an open ended frame, also made from black mild steel flat bars. The moulds for casting RHAC mortar specimens were made from timber. All the mould surfaces that were expected to come into contact with the specimens were ground finished. The moulds are shown in figures 3.1 to 3.4.

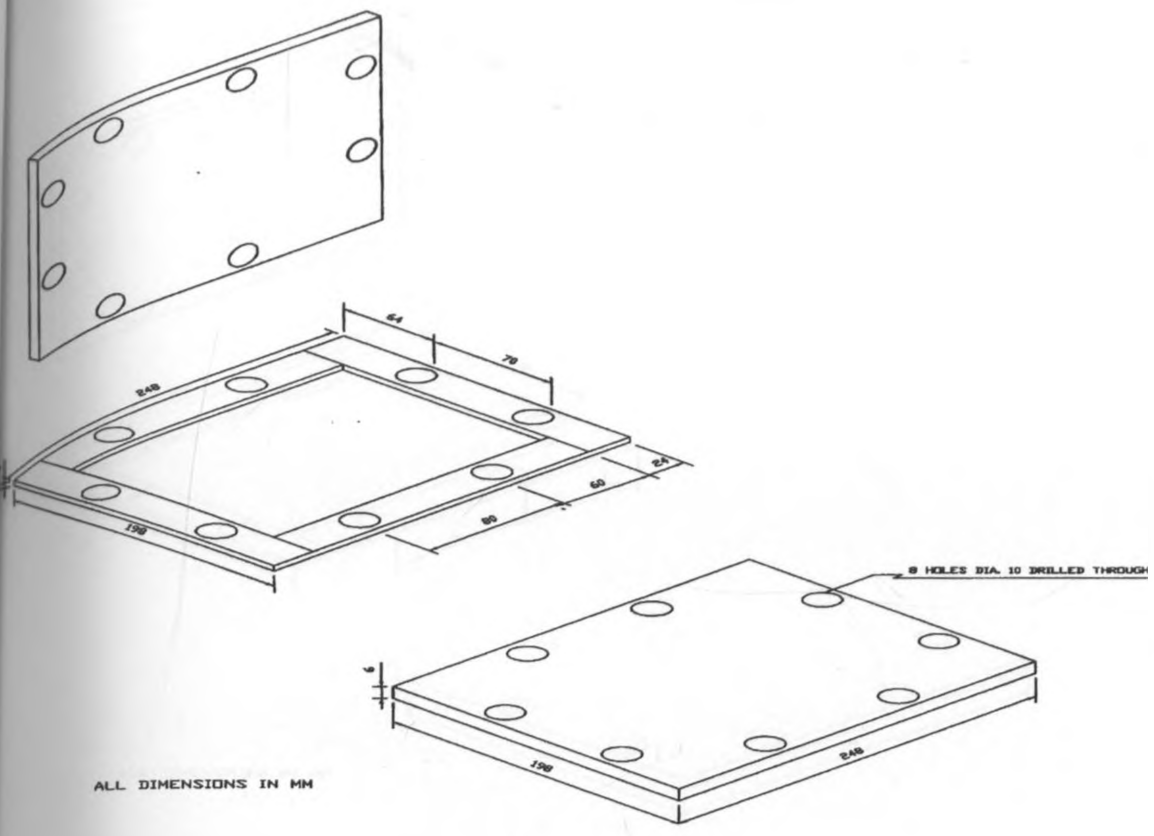
3.2 SPECIMEN PREPARATION

3.2.1 PREPARATION OF SISAL FIBRES

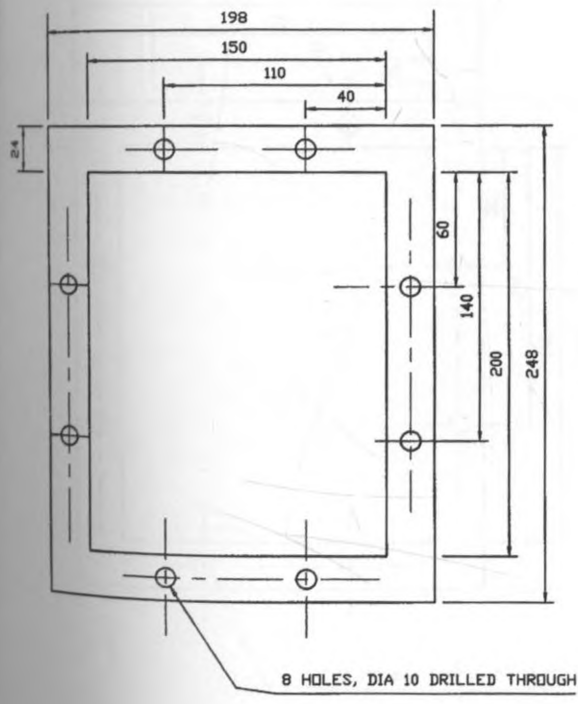
A number of sisal fibres were picked at random from a large bulk. These were cut to the required length from the butt-end, middle portion and apex. Fibres for reinforcement were then picked randomly from the cut pieces.

3.2.2 PREPARATION OF PURE EPOXY RESIN SPECIMENS

The epoxy resin and hardener were both weighed on an electronic balance and mixed in proportions as recommended by the supplier. Thorough mixing was achieved after stirring properly with a spoon. A thin layer of petroleum jelly was then smeared on all the inner surfaces of the moulds. This ensured that the specimens did not stick on to the moulds as well as producing smooth surface specimens. The resin was poured into the moulds centrally and allowed to spread out till it filled the mould. Two methods of eliminating entrapped air bubbles were used. These included (i) pinching of air bubbles with a sharp needle and (ii) allowing a breathing time of approximately thirty minutes to the mixture. Finally the top



ALL DIMENSIONS IN MM



ALL SURFACES TO COME INTO CONTACT WITH SPECIMEN ARE TO BE GROUND FINISHED

ALL DIMENSIONS IN MM

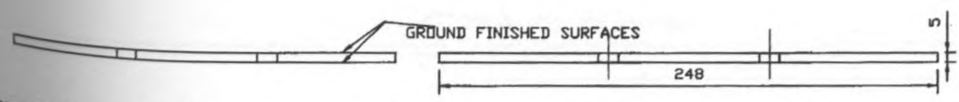
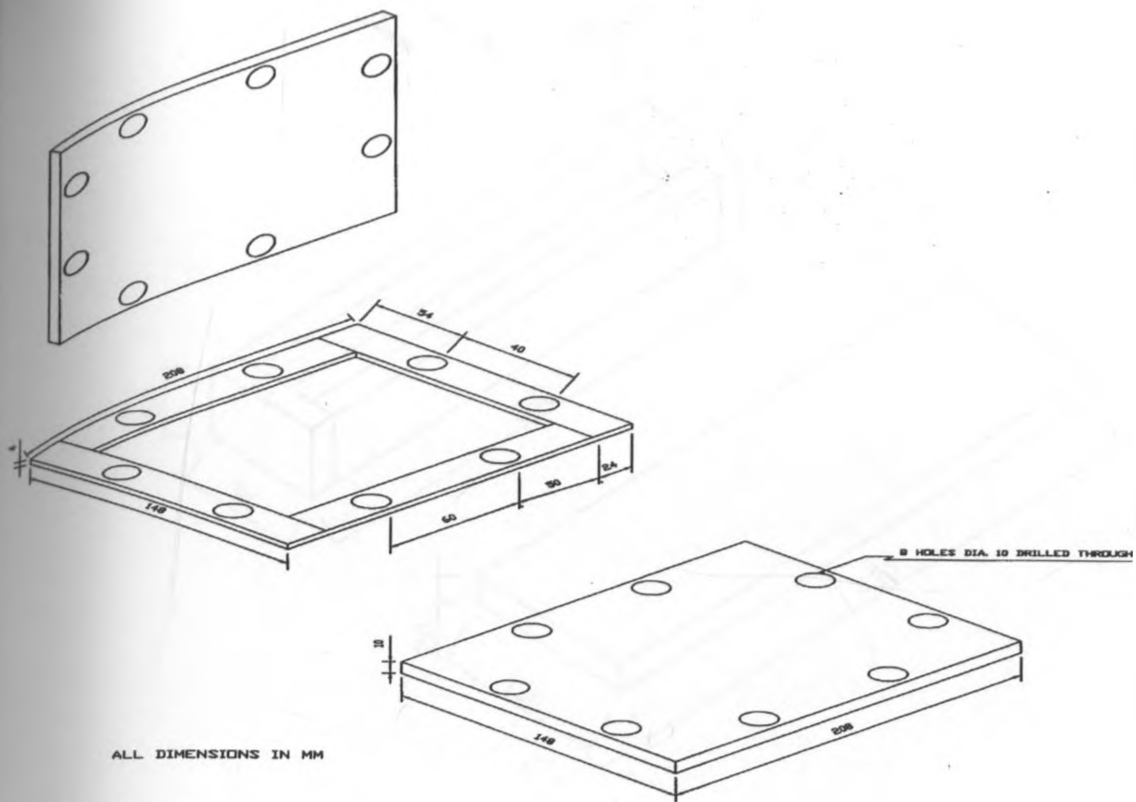
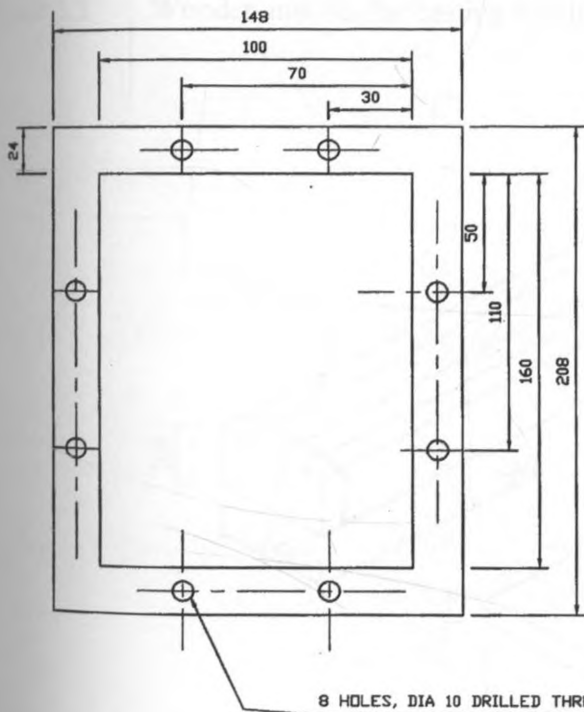


Figure 3.1 Steel moulds for casting Sisal/Epoxy tensile test specimens



ALL DIMENSIONS IN MM



ALL SURFACES TO COME INTO CONTACT WITH SPECIMEN ARE TO BE GROUND FINISHED

ALL DIMENSIONS IN MM

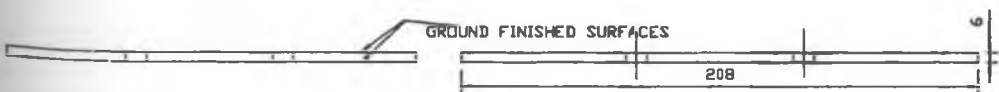
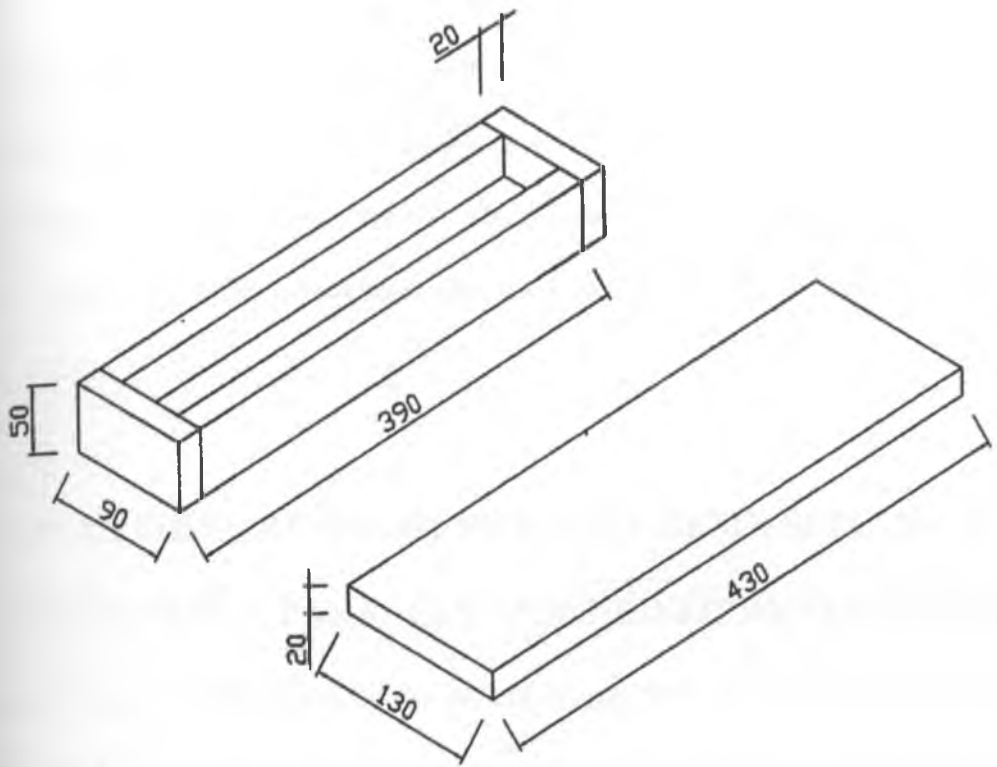
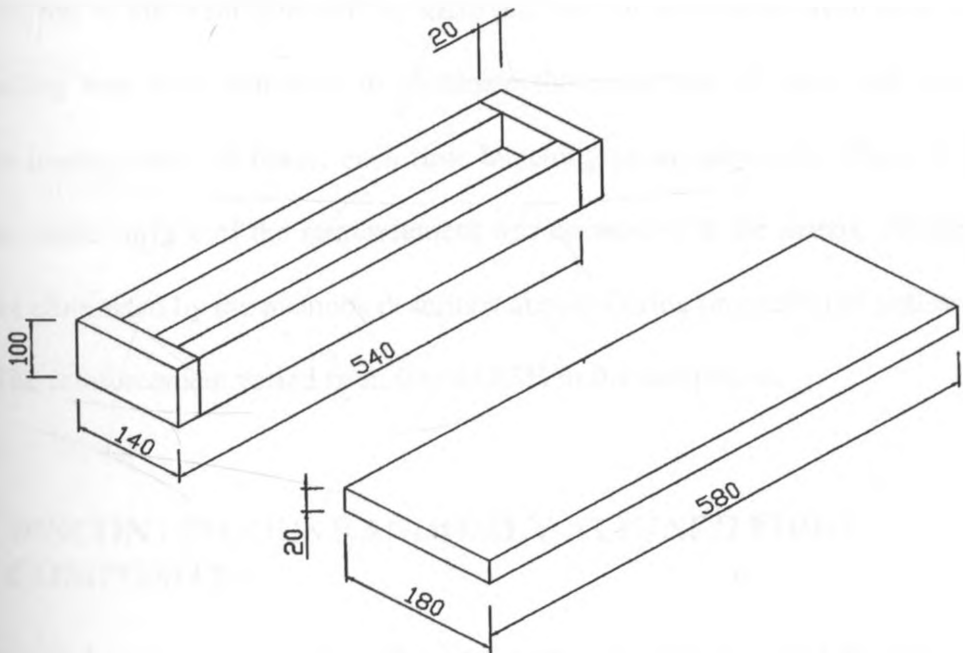


Figure 3.2 Steel moulds for casting Sisal/Epoxy flexure test specimens



ALL DIMENSIONS IN MM

Figure 3.3 Wooden moulds for casting Sisal/RHAC tensile test specimens



ALL DIMENSIONS IN MM

Figure 3.4 Wooden moulds for casting Sisal/RHAC flexure test specimens

cover was put in place and pressure exerted on it, by tightening the nuts and bolts assembly. The mixture was then allowed to cure for 24 hours at room temperature and pressure, after which the castings were removed from the moulds by light tapping. A circular saw mounted on a Victoria horizontal milling machine was used to cut the test pieces to specified dimensions.

3.2.3 SISAL FIBRE REINFORCED EPOXY RESIN SPECIMENS

3.2.3.1 CONTINUOUS PARALLEL ALIGNED FIBRE COMPOSITES

Sisal fibres were cut into lengths equal to the internal length dimension of the mould using a hand-shearing machine. These were weighed on an electronic balance and grouped into various masses corresponding to different fibre volume fractions. A thin layer of resin was then poured onto the base of the mould. Pre-determined weights of sisal fibres were spread longitudinally on top of the resin followed by small amounts of resin in between each layer of fibres. Soaking was done manually to eliminate the formation of voids and also to facilitate proper impregnation of fibres, each time bunching to straighten the fibres. It was ensured that the entire surface of the reinforcement was covered with the matrix. Entrapped air bubbles were eliminated by the methods described above. Curing proceeded as outlined in section 3.2.2. The reinforcement varied from 0 to 44.83% in the composites.

3.2.3.2 DISCONTINUOUS RANDOMLY ALIGNED FIBRE COMPOSITES

First the inner mould surfaces were smeared with a petroleum jelly to avoid sticking. This was followed by gently pouring a thin layer of epoxy resin into the base of the moulds. Pre-determined weights of discontinuous fibres of given lengths were then randomly spread and soaked manually to facilitate proper impregnation. Again elimination of air bubbles was done

as described above. The rest of the casting procedure proceeded as outlined in section 3.2.2. Increasing the weight of embedded fibres varied the reinforcement volume fraction. Finally curing took place at normal room conditions for 24 hours.

3.2.4 UNREINFORCED RHAC MORTAR SPECIMENS

Sand was vibrated through a series of screens to obtain a maximum particle size of 2 mm. Sand was then dried in an oven at 100°C for 12 hours to attain a uniform moisture content. This was followed by spreading the hot sand in a tray and allowing it to cool for another 12 hours. To avoid sticking, all the mould surfaces expected to come into contact with the specimen were smeared with oil.

The sand, OPC and water ratio of 5:2:1 used by HABRI in the fabrication of sisal/OPC roofing materials was adopted in the present work. Mixing pre-weighed quantities of RHAC and sand took place in a horizontal, rotating counter flow, electric-motor driven mixer for one minute. Mixing continued for another two minutes as a weighed quantity of water was gently added. Then the mixer was switched off. Finally all the dry and unmixed material clogged in the mixer blades or pan surfaces were mixed with a hand trowel. By a feel of hand the resulting mortar was considered ready for use.

From the mixer, mortar was poured into the moulds and levelled with a trowel. Moulds were then placed on a vibration table for compaction and elimination of entrapped air bubbles. Vibration was done for about two minutes, each time filling the moulds and checking for any overflow. The top surfaces were then levelled to a smooth finish using a hand trowel when compaction was over. Finally the mixture in the moulds was covered with polythene papers

to control the evaporation rate. Initial curing took place in a wet room for 24 hours, after which the specimens were demoulded and polythene papers replaced with wet cotton cloths. Curing continued in the wet room for the next 28 days before taking the specimens for laboratory tests. The making of these RHAC mortar test beams was done in accordance to BS: 1881: Part 109: 1983 [76].

3.2.5 SISAL FIBRE REINFORCED RHAC MORTAR SPECIMENS

3.2.5.1 CONTINUOUS PARALLEL ALIGNED FIBRE COMPOSITES

To avoid sticking a thin layer of oil was applied on all the internal mould surfaces, followed by a layer of RHAC mortar being spread on the mould base before vibrating slightly to attain a level surface. Each group of the pre-weighed (different fibre volume fractions) sisal fibre bundles were then subdivided into small portions. This was followed by spreading a layer of parallel fibres from the subdivided portions onto the mortar. The process was repeated until the whole bundle of fibres was fully embedded in the matrix. To ensure fibre parallelism is maintained, the moulds were vibrated slightly after each and every fibre addition. Care was taken to ensure that individual layers of each constituent were of the same weight. The mortar rich moulds were then vibrated again for another two minutes. This aided in the compaction and elimination of air bubbles before covering with polythene papers. Curing procedure was as outlined in section 3.2.4.

3.2.5.2 DISCONTINUOUS RANDOMLY ALIGNED FIBRE COMPOSITES

As before, a thin layer of oil was applied on all the internal mould surfaces. Pre-determined weights of chopped sisal fibres were mixed with mortar in the mixing container before

putting into the moulds. The moulds were then vibrated for two minutes. After compaction the specimens were covered with polythene papers and stored in a wet room for 24 hours. The specimens were demoulded after 24 hours, stripped of polythene papers and covered with wet cotton cloths. Curing took place in a wet room for 28 days.

3.3 MECHANICAL TESTING

3.3.1 SISAL FIBRE REINFORCED RHAC SPECIMENS

3.3.1.1 TENSILE TEST

The direct application of a tensile test to cement composites is very difficult for two reasons. First there could be sliding due to the gripping system, and second, secondary tension may appear in the adjacent zones. Concrete materials are usually brittle. Therefore when they are unconfined, the specimens cannot yield plastically to relieve the stress concentrations that are produced at localised points especially at the point of grip. Consequently premature failure may start at these points. There are also difficulties of ensuring a true axial loading to the specimens, so the specimens might twist or bend when gripped and pulled apart from either end.

Various direct and indirect methods have been developed to solve these problems so that the tensile strength of cement mortar and concrete can be determined [38,62,77]. In particular, the bid to solve the problem of non-uniform stress distribution and the difficulty in gripping has led to the development of a number of indirect methods. One such indirect method is given in ASTM C-496 [77] for the determination of the splitting tensile strength of cylindrical concrete specimens. It measures the splitting tensile strength by the application of a diametral compressive force on a cylindrical concrete specimen, placed with its axis

horizontal between the platens of the testing machine. The splitting tensile strength is then calculated from the maximum applied load, length and diameter of the specimen.

In the present work the difficulty of carrying out direct tensile tests on RHAC mortar composites, and that of achieving a uniform stress distribution without inducing stress concentration at the grips was overcome by using a tensile test rig proposed by Bessel and Mutuli [38]. The tensile test rig shown in figure 3.5 was fabricated. This gripping arrangement is used to grip the square section specimen on all its four sides. The grips consist of a square top plate with four slots at 90° to each other. Through these slots can be bolted four vertical plates which forms an open box section when in place. The inside surfaces of these plates were roughened to aid in gripping of the specimen. A high tensile pin on the top plate is gripped by the testing machine.

The faces of the specimens prepared as described in sections 3.2.4 and 3.2.5 were serrated slightly using a saw blade and then glued to the four plates using "Isopon" polyester paste popularly known as car body filler. The polyester paste was made by mixing the resin and hardener in proportions recommended by the manufacturer. The plates were then held in place using G-clamps. After "Isopon" had set, the gauge length of the specimen was measured using a steel rule accuracy ± 0.5 mm. Finally the vertical plates were bolted into place on the top and bottom plates. The upper and lower assemblies were then carefully aligned and mounted on to the Torsen Senstar (Tokyo) type SC 10 CS Electronic Universal Testing Machine. The specimens were tested at a cross-head speed of 2 mm/min.

The ultimate tensile loads were recorded from the digital read out of the testing machine. However its plotter was not in good working condition, therefore a different equipment

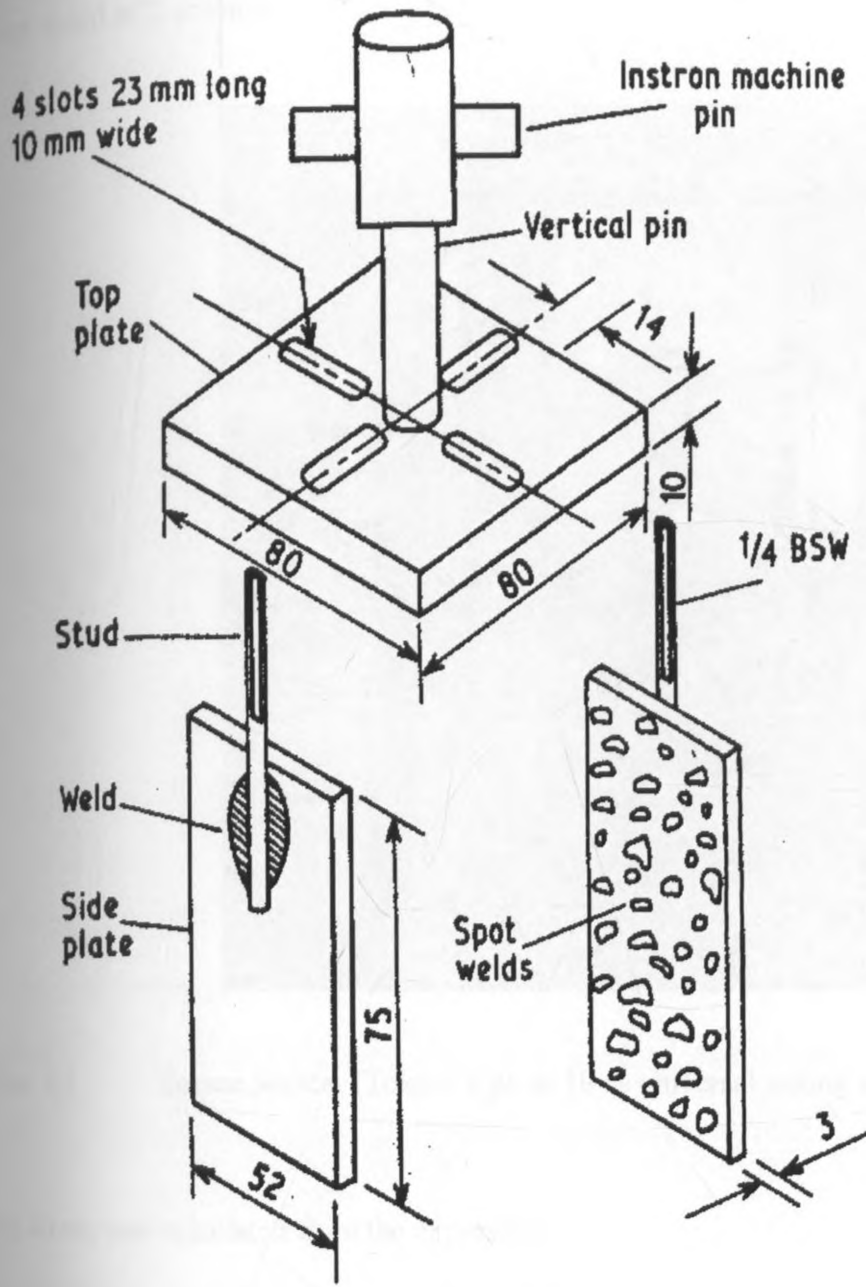


Figure 3.5 Tensile test rig proposed by Bessel and Mutuli [38]

Shimadzu UMH-30 Universal Testing Machine was used whenever load-extension or load-deflection plots were required. The load-extension curves were automatically plotted using the servo-drive mechanism of the Shimadzu UMH Universal Testing Machine. These were subsequently used to plot the stress-strain curves. In the Shimadzu UMH-30 Universal Testing Machine, a cross-head speed of 2 mm/min was used for transmission with a

chart speed of 2 cm/min.

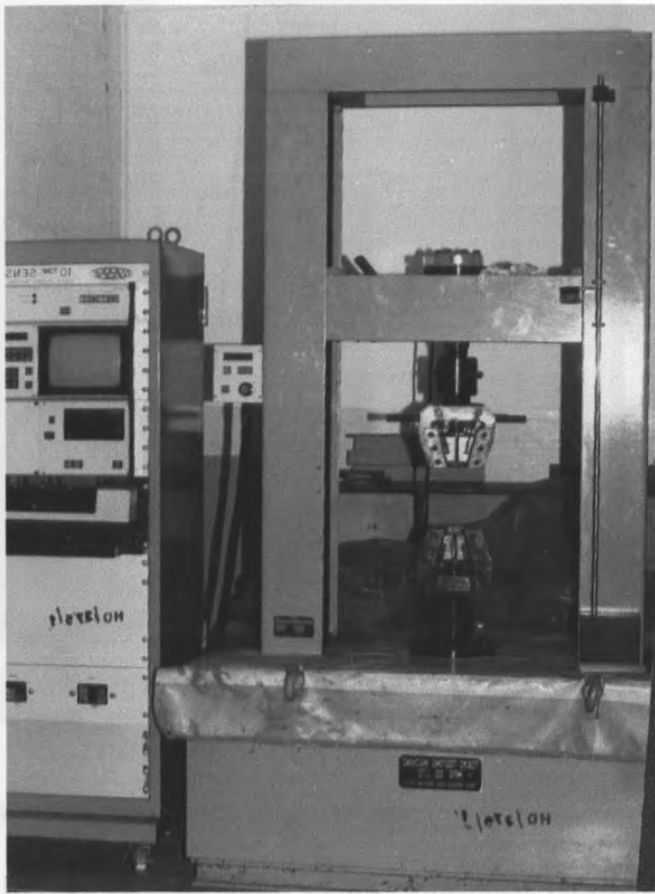


Plate 3.1 Torsee Senstar (Tokyo) type sc 10 cs universal testing machine

The strain was calculated from the expression

$$\text{Strain} = \frac{\text{Chart length}}{(\text{Magnification factor})(\text{Gauge length})} \quad (3.1)$$

Where

$$\text{Magnification factor} = \frac{\text{Chart speed}}{\text{Cross - head speed}}$$

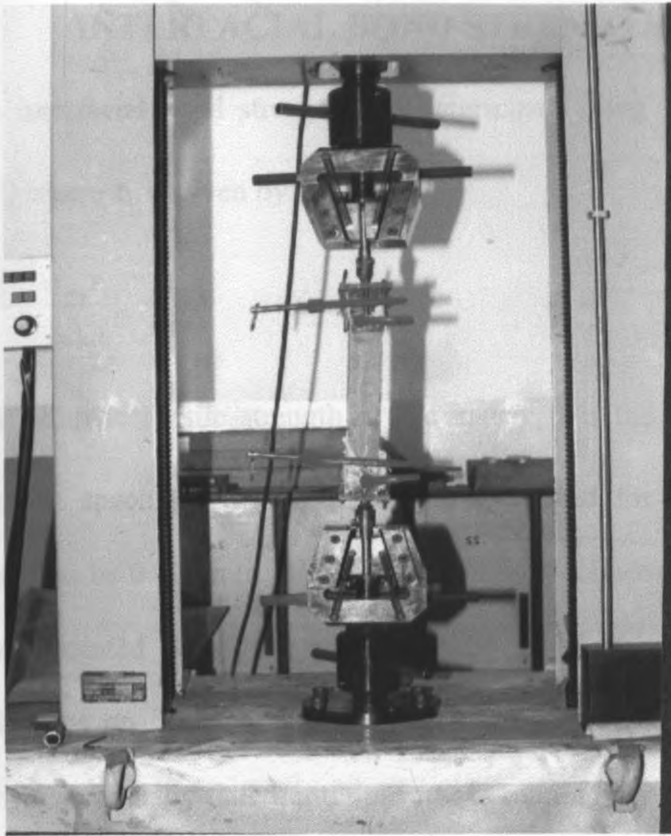


Plate 3.2 Sisal/RHAC composite beam, tensile test in progress

In order to obtain a good representation of the composite properties, a sample size of 5 specimens at every fibre volume fraction was chosen and subsequently used in the tests. The composite ultimate tensile strength was obtained from the expression

$$\sigma_{UTS} = \frac{P}{A} \quad (3.2)$$

Where σ_{UTS} is the ultimate tensile strength, P is the maximum applied load and A is the original cross-sectional area. The modulus of elasticity was obtained by getting the slope of the linear portion of the stress-strain curve. This is defined as an incremental stress divided by the corresponding incremental strain. Using this gripping method there was no obvious evidence of stress concentrations or fracture being initiated at or near the grips as approximately 95% of the specimens tested were observed to fracture within the central portion of the gauge length. Results of the remaining 5% were discarded.

3.3.1.2

INTERFACIAL BOND STRENGTH

The fibre/matrix interfacial bond strength was determined using the method proposed by Aveston et al [52] where τ_b is given by

$$\tau_b = \frac{(1-V_f) \sigma_{mu} r}{V_f 2X'} \quad (3.3)$$

where σ_{mu} is the ultimate tensile strength of the matrix, r is the fibre radius and X' the length of inter-crack spacing. This equation was developed for macro-cracks. The fibre radius 'r' was taken to be 0.126 mm [1]. The tensile test specimens prepared as described in section 3.2.5 were painted with three successive layers of white-wash to improve crack visibility. Tensile tests on the specimens were performed as described in section 3.3.1.1. When the composite eventually failed, multiple cracks running perpendicular to the direction of loading were observed in the matrix. The inter-crack spacings (macro-cracks) were measured accurately by the use of a vernier calliper (accuracy ± 0.05 mm) in each face. Then an average of all crack spacing lengths for all the four faces was obtained.

3.3.1.3

FLEXURE TEST

The flexural strength of sisal fibre reinforced RHAC mortar beams were determined by means of a two point loading system (four point bending test) in accordance to BS EN-12390: Part 5: 2000 [78]. An experimental flexure test rig used to apply the loads was fabricated according to specifications in [78]. It consisted of two support rollers and two load application rollers as shown in figure 3.6. All rollers were turned from bright mild steel on a lathe machine and then ground finished to a smooth surface on a cylindrical grinding machine, to a circular cross-section of diameter 25 mm and length 120 mm. The support rollers rested on a square cross-section bright mild steel bar machined on a vertical milling

machine and ground finished to final dimensions of (120 × 120 × 520) mm.

The top plate (200 × 120 × 20) mm was machined on a shaper and then ground to a smooth finish on a surface grinder. The slots in both the top plate and bottom bar were cut to a 10 mm radius on a vertical milling machine. In order to apply a point load on the top plate, a hemispherical slot on which a high tensile strength steel ball rests was cut on the top plate. The distance between the outer rollers (span) was equal to 3d, while the distance between the inner rollers was maintained at d. The inner rollers were equally spaced between the outer rollers as shown in figure 3.7.

The sisal fibre reinforced RHAC composite beams made and cured as described in sections 3.2.4 and 3.2.5 had a nominal depth d of 100 mm, with a square cross-section over a length of 5d i.e. 500 mm. The specimens were submerged in water at room temperature for approximately 48 hours before testing. Specimens were tested immediately after removal from water when they were still wet, but water and grit were first wiped off the specimen surface using a piece of cotton cloth. The bearing surfaces of the loading rollers were also wiped clean before the test commenced.

The flexural strength tests were done on a Torse Senstar (Tokyo) type SC 10 CS Electronic Universal Testing Machine. The specimen was placed in the testing machine correctly centred, with the longitudinal axis of the specimen at right angles to the rollers as shown in plate 3.3. A loading rate of 2 mm/min was maintained without change until fracture occurred.

The load indicator of the testing machine had a resettable device that permitted the recording of peak loads sustained by the composite beams. Therefore the ultimate flexural loads were

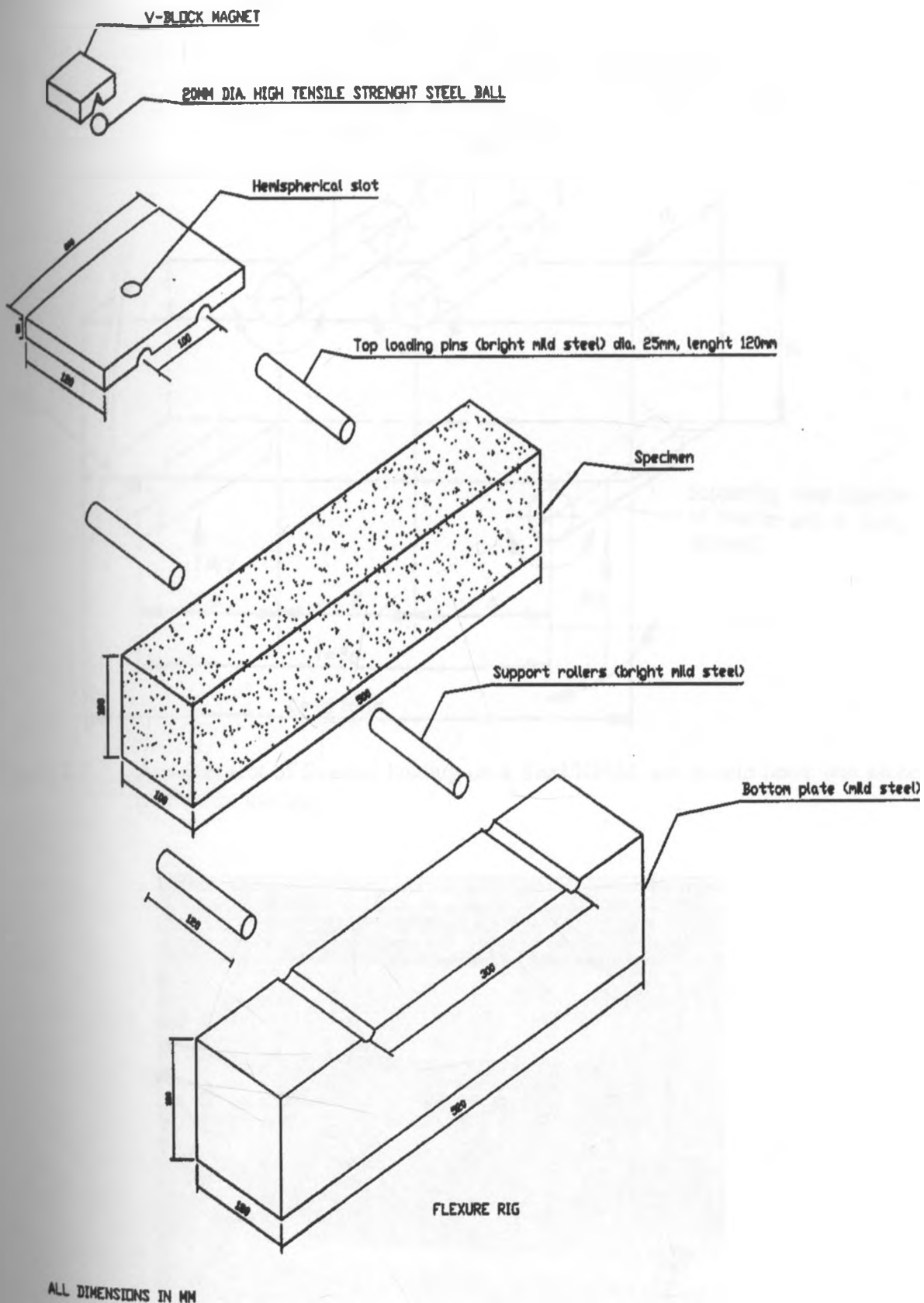


Figure 3.6 Flexural strength test rig

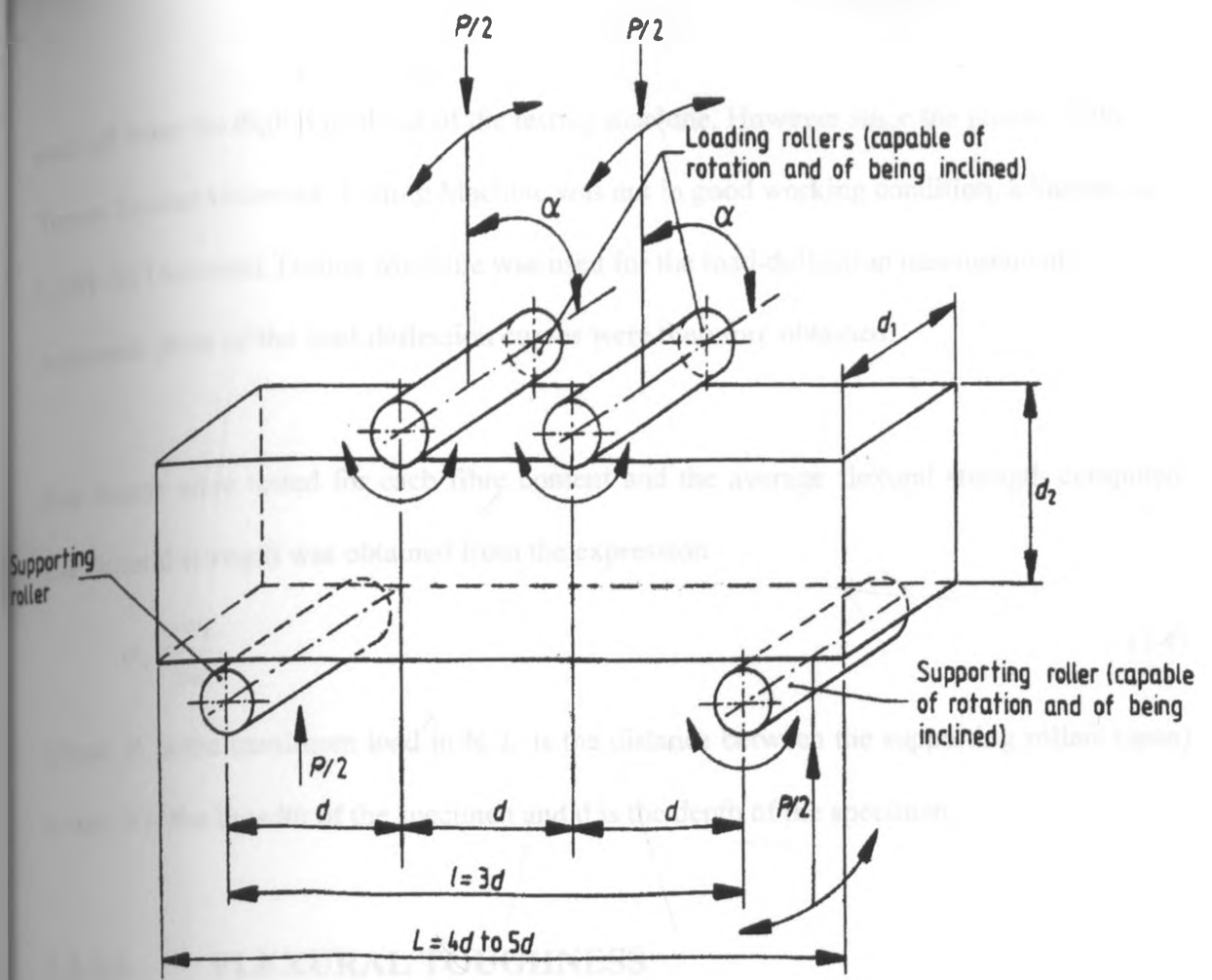


Figure 3.7 Arrangement of flexural loading on a Sisal/RHAC composite beam test piece (two point loading)



Plate 3.3 Flexural strength test of Sisal/RHAC composite beam in progress.

read off from the digital read-out of the testing machine. However since the plotter of the Torsee Senstar Universal Testing Machine was not in good working condition, a Shimadzu UMH-30 Universal Testing Machine was used for the load-deflection measurements. Automatic plots of the load-deflection curves were therefore obtained.

Five beams were tested for each fibre content and the average flexural strength computed. The flexural strength was obtained from the expression

$$\sigma_b = \frac{PL}{bd^2} \quad (3.4)$$

Where P is the maximum load in N, L is the distance between the supporting rollers (span) in mm, b is the breadth of the specimen and d is the depth of the specimen.

3.3.1.4 FLEXURAL TOUGHNESS

Sisal fibre reinforced RHAC mortar composite beams of dimensions (100 × 100 × 500) mm were tested in flexure on a 300 mm span as described in section 3.3.1.3. A span to depth ratio of 300/100 = 3 was used. Toughness values were calculated using the ASTM C1018 [74] approach. This method defines flexural toughness as the area under the load-deflection curve. The load-deflection plots were obtained automatically from the Shimadzu UMH-30 Universal Testing Machine for each of the specimens tested. The load-deflection plots were then analysed to characterise the material toughness as specified in [74]. The areas under the load-deflection curves were determined by the use of a planimeter for subsequent computations of first crack energy and toughness indexes.

3.3.1.5

COMPOSITE DENSITY AND VOID VOLUME VALUE

Oven dried specimens were immersed in tap water at 22°C for 48 hours. After removal from water, they were surface dried by removing the surface moisture with a towel and then weighed on a digital electronic balance. This gives the mass of the saturated specimen W_s . The saturated specimens were then dried in an electric oven at a temperature of 100°C for 24 hours. After removing the specimens from the oven, they were allowed to cool at room conditions for 12 hours and then weighed again. This gives the mass of the dry specimen w_d . The average amount of water absorbed at each fibre content was calculated. The percentage water absorption by weight w_a was obtained from the expression

$$w_a = \frac{W_s - w_d}{w_d} (100) \quad (3.5)$$

This was followed by the determination of the percentage void volume value in accordance to ASTM C 220 -75 [79] as given in equation 3.6.

$$V_v = \rho_c w_a \quad (3.6)$$

Where V_v is the void volume value and ρ_c is the density of the specimen. Composite density and void volume values were obtained as an average of five specimens at each fibre volume fraction. Finally the variations of ρ_c and V_v with the reinforcement volume fractions were plotted.

3.3.2 SISAL FIBRE REINFORCED EPOXY RESIN SPECIMENS

3.3.2.1 TENSILE TEST

The preparation of test pieces and tensile tests were performed in accordance to BS 2782, Part 3, method 320E: 1996 [80] specifications. Test pieces were subjected to a tensile force on a Torse Senstar (Tokyo) type SC 10 CS Electronic Universal Testing Machine. The

rectangular test pieces shown in figure 3.8 were cut from a cast specimen by means of a circular saw mounted on a victoria horizontal milling machine as described in section 3.2.2. These test pieces were then mounted on the testing machine in axial alignment with the direction of pull as shown in plate 3.4.

Testing was done under normal room conditions (22°C, 65% RH). A gauge length of 110 mm was maintained for all the test pieces. This was set as the distance between the gripping

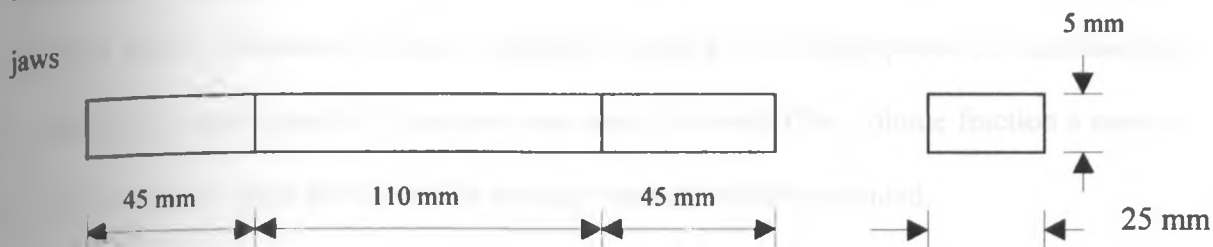


Figure 3.8 Dimensions of Sisal/Epoxy tensile test specimens

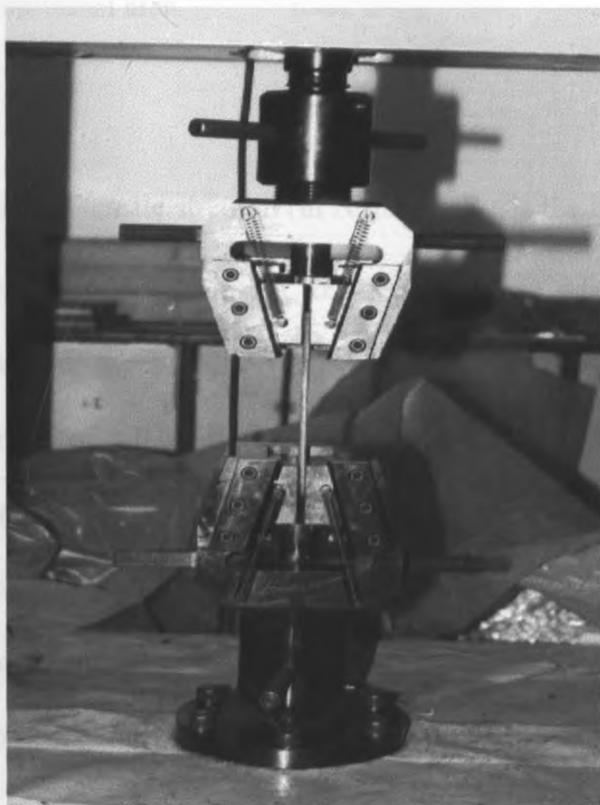


Plate 3.4 Tensile test on Sisal/Epoxy specimen in progress

before loading commenced. The grips were of constant position self-aligning wedge type that increased the grip pressure as force applied on the test piece increased. To ensure a constant gauge length, all specimens were initially marked at 45 mm from both ends. A cross-head speed of 2 mm/min was used through out the test. The ultimate tensile loads for each specimen were measured using the Torsen Senstar (Tokyo) type SC 10 CS Electronic Universal Testing Machine, while the load-extension curves were obtained from a Shimadzu UMH-30 Universal Testing Machine. This was used to plot the stress-strain curves of the composite. In the Shimadzu Universal Testing Machine a cross-head speed of 2 mm/min and a corresponding chart speed of 2 cm/min were used. For each fibre volume fraction a sample size of 5 test pieces were tested and the average strength values computed.

Tensile strength was obtained by dividing the maximum load the composite could withstand by the original cross-sectional area.

$$\sigma_{UTS} = \frac{P_{\max}}{A} \quad (3.7)$$

Where σ_{UTS} is the ultimate tensile strength (in N/mm^2), P_{\max} is the maximum load (N) and A is the initial cross-sectional area (mm^2). Cross-sectional area was calculated by taking an average of four readings of the width and thickness of the test pieces measured by a vernier calliper with an accuracy of ± 0.05 mm. Strain was calculated from the expression given in equation 3.1. The strain calculations were done with the assumptions that strain in the machine members was negligible compared to the specimen strain. The tensile modulus of elasticity was obtained from the slope of the linear portion of the stress-strain curve. It was calculated as the ratio of the incremental stress to the corresponding incremental strain.

3.3.2.2

FLEXURE TEST

The flexural strength test of sisal fibre reinforced epoxy resin test pieces is shown in plate 3.5. Test pieces were prepared and tested in accordance to the specifications of BS 2782: Part 3: Method 335 A: 1993 [81]. The test piece was tested as a freely supported beam loaded at mid-span (three point bending test). It was deflected at a constant rate at mid span until fracture. During this procedure the load and corresponding deflections were recorded from the digital read-out of the Torsee Senstar (Tokyo) type SC 10 CS Electronic Universal Testing Machine.

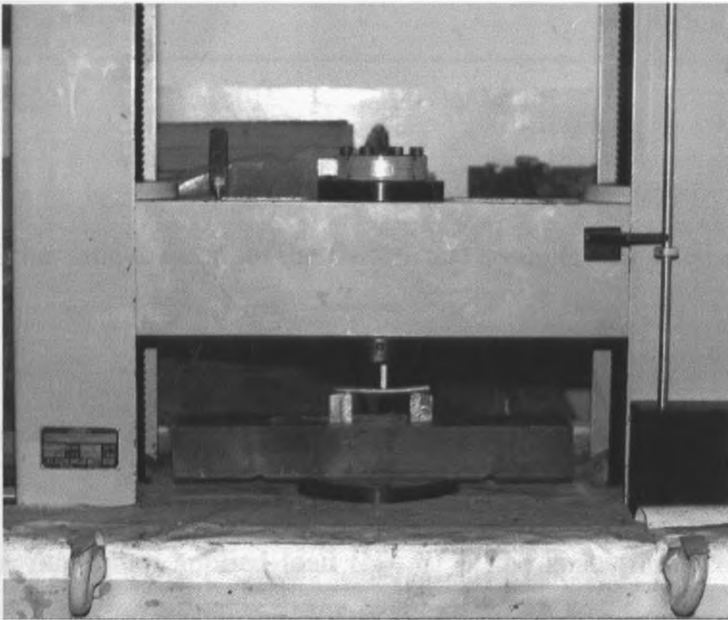


Plate 3.5 Flexure test of Sisal/Epoxy specimen in progress

The width b and thickness d of the test pieces were measured using a micrometer with an accuracy of ± 0.005 mm, while the span L was measured by a vernier calliper accuracy ± 0.05 mm. These measurements were done near the centre of the specimen. The mean thickness and breadth were taken as an average of four readings from the test piece. A span to depth ratio of $96/6 = 16$ was used. The test piece was then placed symmetrically on the

two supports and loads applied at mid-span as shown in the schematic diagram in figure 3.9. A cross-head speed of 2 mm/min was maintained throughout the test. Testing was done at normal room conditions (22°C, 65% RH), and results from any test piece that fractured outside the central third of its span were discarded.

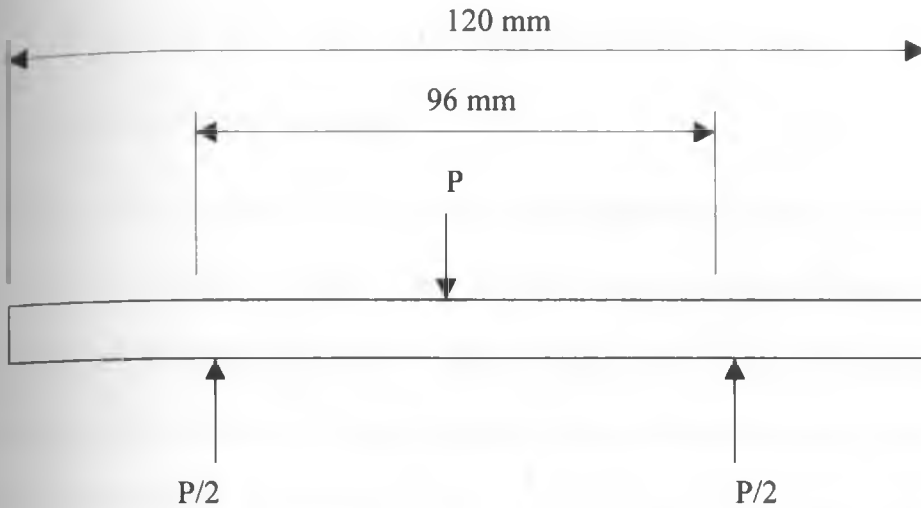


Figure 3.9 Schematic diagram of the flexure test arrangement on Sisal/Epoxy test piece

The composite flexural strength was obtained from the equation

$$\sigma_b = \frac{3PL}{2bd^2} \quad (3.8)$$

where P is the maximum applied load (N), L is the span (mm), b is the width of the specimen (mm) and d is the thickness (mm). The flexural modulus of elasticity was obtained

from the following expression

$$E_b = \frac{\sigma_{b2} - \sigma_{b1}}{\epsilon_{b2} - \epsilon_{b1}} \quad (3.9)$$

where $\epsilon_{b1} = 0.0005$ and $\epsilon_{b2} = 0.0025$. The flexural stress values σ_{b1} and σ_{b2} are calculated at deflections δ_1 and δ_2 corresponding to the strains ϵ_{b1} and ϵ_{b2} . These deflections were obtained as follows [81].

$$\delta_1 = \frac{\varepsilon_{b1} L^2}{6d} = \frac{0.0005(96)^2}{6(6)} = 0.128 \text{ mm} \quad (3.10)$$

$$\delta_2 = \frac{\varepsilon_{b2} L^2}{6d} = \frac{0.0025(96)^2}{6(6)} = 0.64 \text{ mm} \quad (3.11)$$

3.4 DESCRIPTION OF THE EQUIPMENTS USED

3.4.1 VIBRATION TABLE

The vibration table consisted of a horizontal table supported by compression springs and mounted with an off balance weight. The excitation motor was supplied from a 240 V mains supply. When the power is put on, the rotation of the motor excites the supporting springs. Due to the presence of the out-of-balance weights, this combination causes vertical vibrations which are transmitted to the horizontal table via the supporting springs. The system was provided with a non-variable frequency amplitude control.

3.4.2 TORSEE SENSTAR (TOKYO) TYPE SC 10 CS ELECTRONIC UNIVERSAL TESTING MACHINE

Test pieces were tested on a Torsee Senstar (Tokyo) type sc 10 cs electronic universal testing machine. The loading frame had a digital read-out for applied loads and their corresponding extensions. The grip was constant position wedge type serrated on the inner gripping surfaces. They consisted of self-tightening jaws that increased the grip pressure on the test piece with subsequent extensions. Initial tightening was done manually with a rotary handle to ensure the specimens did not slip. Loading was done manually using a dial knob. The loading frame had the provision of an automatic peak load indicator.

RESULTS

SISAL FIBRE REINFORCED RHAC MORTAR COMPOSITES

FLEXURAL STRENGTH

CONTINUOUS PARALLEL ALIGNED FIBRE REINFORCED SPECIMENS

The results of static flexural strength tests are shown in tables 4.1 and 4.2 for continuous parallel aligned and chopped randomly aligned sisal fibre reinforced RHAC mortar composites respectively. The tables show the first crack stress and the composite flexural strength. The ultimate flexural strengths were obtained from the peak loads recorded from the four point bending tests using a Torsen Senstar (Tokyo) type SC 10 CS Electronic Universal Testing machine.

The regression equation for the flexural strength of continuous sisal fibre reinforced RHAC mortar composites was found to be

$$\sigma_b = 2.0562 + 1.0476V_f - 0.0021V_f^2 - 0.004V_f^3 \quad (4.1)$$

Figure 4.1 shows the variation of the flexural strength with fibre content in parallel aligned fibre reinforced RHAC composites cured in air for 28 days. The flexural strength increased with the reinforcement volume fraction starting from a value of 1.946 N/mm² for unreinforced specimens to a maximum ultimate flexural strength of 8.61 N/mm² at a reinforcement volume fraction of 9.5%. Beyond a fibre content of about 9.5% in the case of parallel fibre reinforcement and 8.3% V_f in 30 mm length chopped fibre reinforcement, the composite flexural strength was seen to decrease with further fibre additions. It can be seen from figure 4.1 that the rate of increase of flexural strength with V_f is fairly rapid initially up to a fibre content of about 6.8%, then the rate of increase decreases with fibre additions up to

the maximum strength at 9.5% fibre content. A linear increase in flexural strength was observed up to about 6.8% V_f before deviations become apparent.

Fibre volume fraction (%)	I ST CRACK VALUES	ULTIMATE VALUES
	Stress (N/mm ²)	Flexural strength (N/mm ²)
0	1.706	1.946
1.672	3.896	3.924
2.691	4.635	4.962
3.355	4.838	5.346
4.711	6.120	6.444
5.754	5.538	7.189
6.750	7.041	7.524
7.783	7.402	8.285
8.516	7.660	8.494
9.505	7.825	8.610
11.200	7.297	7.810

Table 4.1 Static flexural first crack strength values for continuous parallel aligned sisal fibre reinforced RHAC composites

Results show that flexural strengths increased by 101%, 154%, 231%, 269% and 301% in parallel fibre reinforced composites at fibre contents of 1.67%, 2.69%, 4.71%, 5.75%, and 11.2% respectively. Standard deviations for all fibre volume fractions were found to be very low. However the variations between specimens at a given fibre volume fraction was found to be larger for fibre reinforced specimens than in unreinforced test pieces. This can be attributed to the difficulty in achieving the same uniform distribution and orientation of fibres.

Both the limit of proportionality (LOP) strength and the Modulus of Rupture were calculated. The relationship between the first crack strength and peak strength gives an indication of the effect of fibre reinforcement on the composite behaviour. Figure 4.2 shows the variation of first crack flexural strength with the fibre volume fraction. The first crack load increased

from 5685.47 N in unreinforced specimens to a maximum of 26083.52 N at 9.5% V_f before finally decreasing to 24322.82 N at 11.2% V_f .

Fibre volume fraction (%)	I ST CRACK VALUES	ULTIMATE VALUES
	Stress (N/mm ²)	Flexural strength (N/mm ²)
0	1.706	1.946
0.855	2.426	2.510
1.378	2.294	2.939
1.981	2.965	3.201
2.540	2.952	3.464
3.147	3.299	3.849
3.647	3.569	4.079
4.374	3.283	4.317
4.945	3.557	4.431
5.815	3.759	4.568
6.527	3.981	4.762
7.422	4.123	4.898
8.376	4.044	4.923
9.406	3.433	4.534
9.797	3.023	4.156
10.284	2.917	3.572

Table 4.2 Static flexural first crack strength values for 30 mm length discontinuous randomly aligned sisal fibre reinforced RHAC composites

The relationship between the composite flexural strength and fibre aspect ratio is shown in figure 4.3. It was seen that flexural strength increases gradually with the fibre aspect ratio. The unreinforced specimens failed without any warning exhibiting a brittle failure. On the other hand, fibre reinforced specimens had a slow ductile failure. Multiple cracking was observed with fibre pull-out taking place after visible cracks had appeared. The crack patterns observed at flexural failure of sisal fibre reinforced RHAC composites in a four point bending test is shown in figure 4.4. It was seen that a single crack perpendicular to the neutral axis was the dominant mode of failure for unreinforced and chopped fibre composite beams. For continuous parallel aligned fibre composites, multiple cracks parallel to the

neutral axis were seen exhibiting a shear mode of failure. In chopped fibre cement composites, the single crack was followed by fibre pull-out.

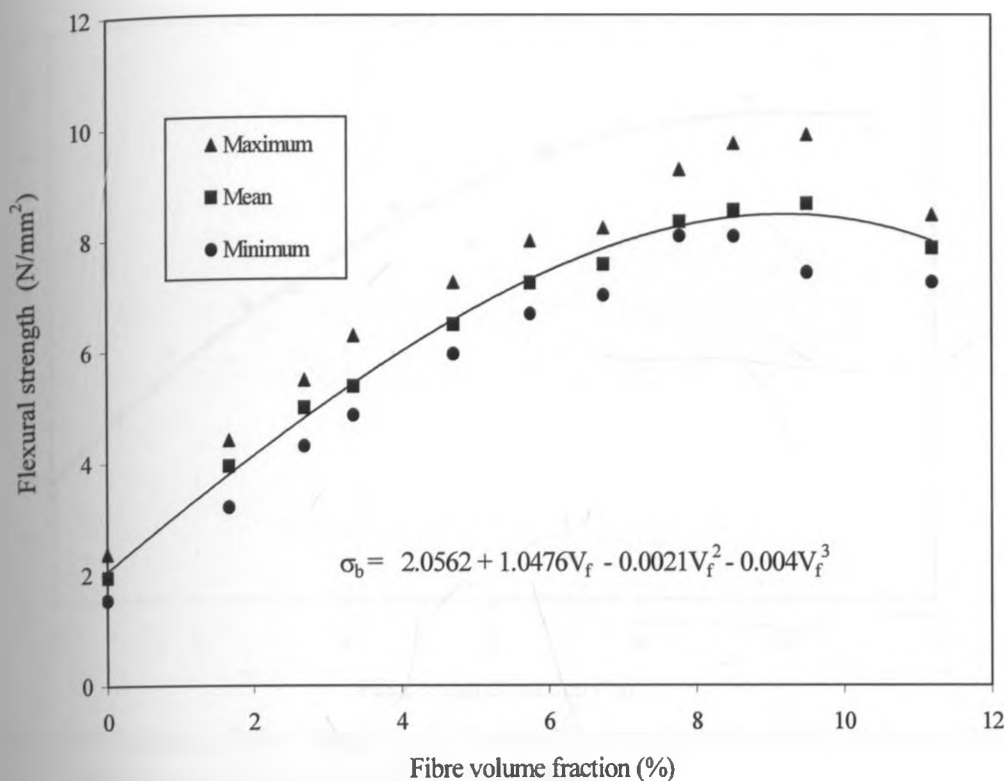


Figure 4.1 Variation of the flexural strength with fibre volume fraction in continuous fibre Sisal/RHAC composites

4.1.1.2 DISCONTINUOUS RANDOMLY ALIGNED FIBRE REINFORCED SPECIMENS

A plot of flexural strength versus fibre volume fraction of 20 mm and 30 mm length chopped fibre reinforced RHAC composites are presented in figures 4.5 and 4.6 respectively. A maximum value of 3.743 N/mm² and 4.923 N/mm² were obtained for the modulus of rupture in 20 mm and 30 mm length chopped fibres at fibre volume fractions of 5.88% and 8.38 % respectively. The flexural strength of unreinforced specimens was obtained as 1.946 N/mm².

The regression equation for the flexural strength of 20 mm length discontinuous randomly

aligned fibre reinforced composites is

$$\sigma_b = 1.793 + 0.245V_f + 0.0527V_f^2 - 0.0067V_f^3 \quad (4.2)$$

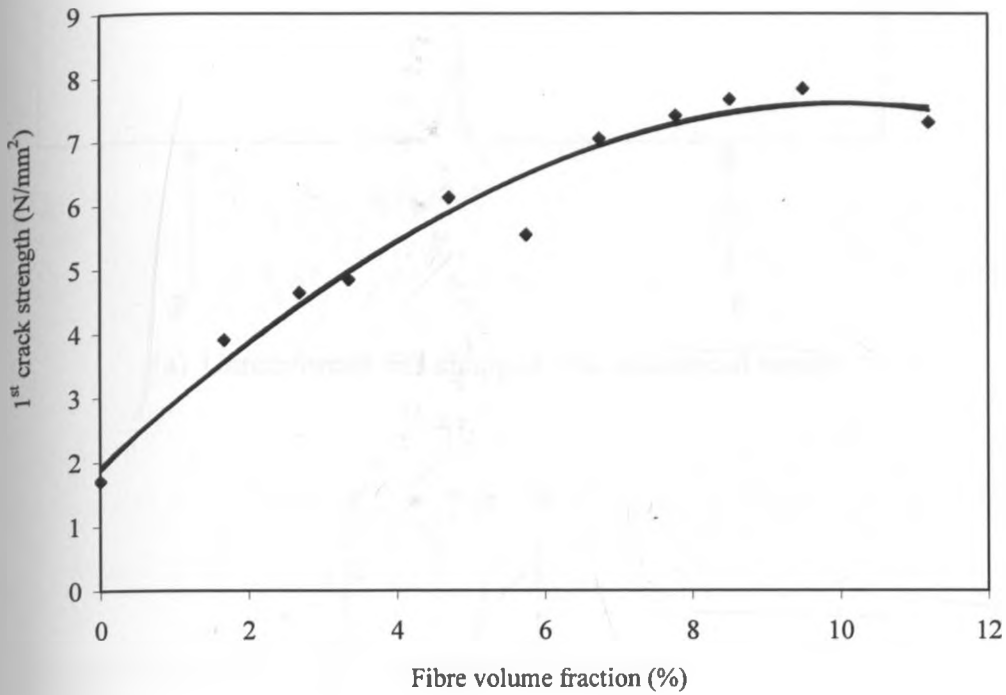


Figure 4.2 Variation of the first crack flexural strength with fibre volume fraction in continuous fibre Sisal/RHAC composites

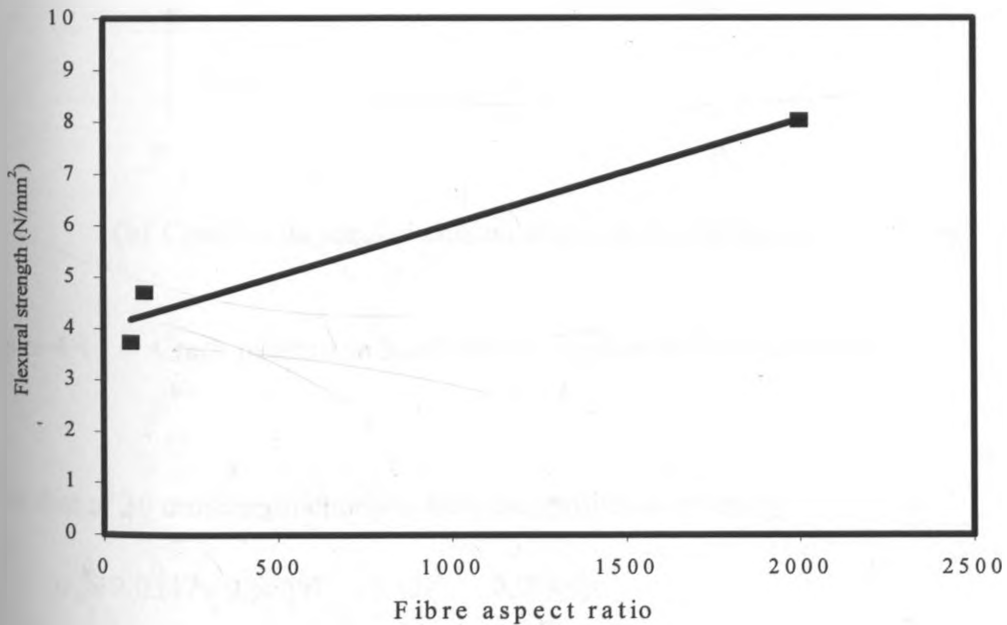
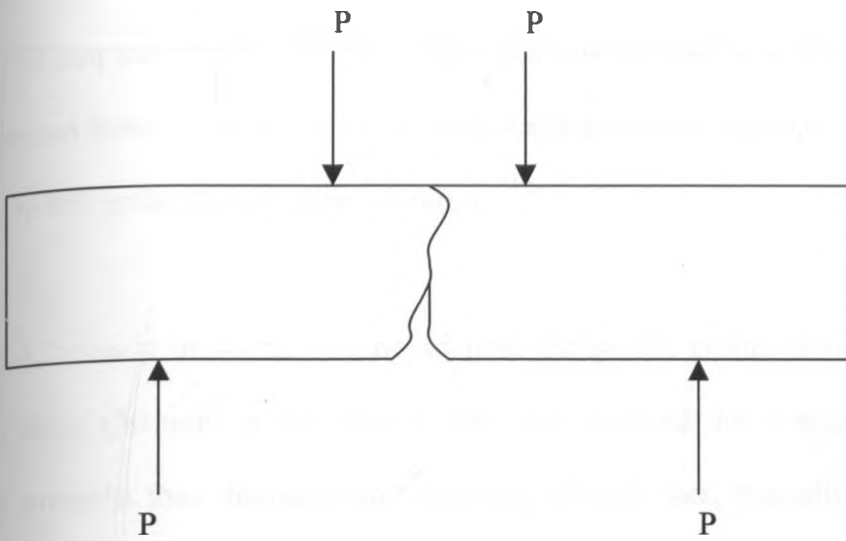
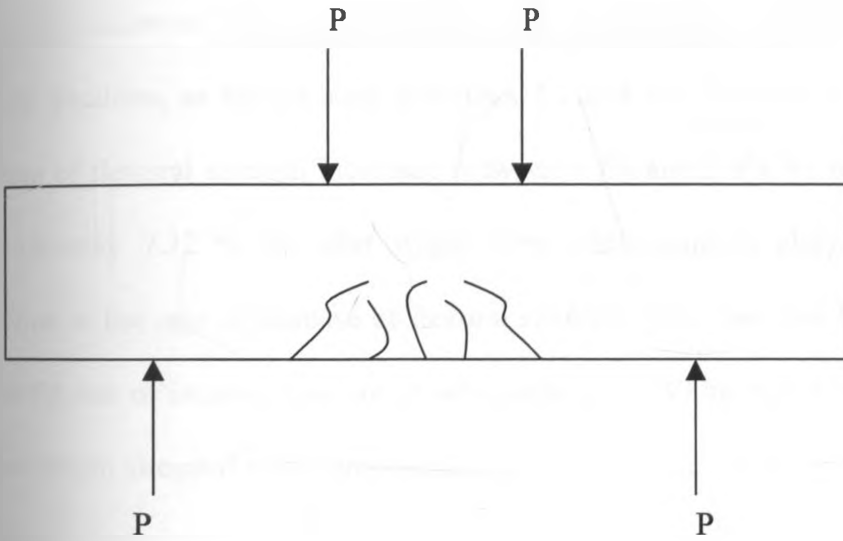


Figure 4.3 Variation of flexural strength with fibre aspect ratio in Sisal/RHAC composites



(a) Unreinforced and chopped fibre reinforced beams



(b) Continuous parallel aligned fibre reinforced beams

Figure 4.4 Crack patterns in Sisal/RHAC composite flexural failure

while that of 30 mm length chopped fibre composites is given by

$$\sigma_b = 2.0347 + 0.5669V_f + 0.11V_f^2 - 0.0048V_f^3 \quad (4.3)$$

A trend was seen of flexural strengths increasing with fibre additions. The optimum flexural strength of 30 mm length chopped fibre composites was realised at about 7.423 % V_f , while

that of 20 mm length chopped fibre composites was obtained at a slightly lower V_f of about 6%. Beyond these optimum values of reinforcement volume fractions, the flexural strengths started to fall gradually with fibre additions.

Figure 4.7 clearly show that in chopped fibre composite, greater strengths is obtained with longer fibres (30 mm) in this case. It was also observed that continuous fibres produced higher strengths than discontinuous randomly aligned ones, typically the difference being about 49%.

The rate of increase of flexural strength with fibre contents decreased at the higher fibre volume fractions, as can be seen in figures 4.5 and 4.6. Figure 4.5 shows that the rate of increase of flexural strength increased between 1.9% and 5.8% V_f , remained constant up to approximately 7.12 % V_f , after which fibre reinforcements above 7.12% resulted in a reduction in the rate of increase of flexural strength. This can also be seen from figure 4.6 where the rate of increase was not as substantial as the V_f increased from 5.81% to 7.42% in 30 mm length chopped fibre composites.

The specimens were seen to fail with a single crack traversing through the neutral axis. After the crack appeared, the load started decreasing progressively with more fibres pulling out the matrix. As loading continued, the crack widened exposing more fibres. The fibre pull-out phenomenon ensures a larger area under the load-deflection curve for chopped sisal fibre reinforced RHAC mortar composites compared to that of the unreinforced matrix. This results in an increased flexural toughness as well as increased post-cracking ductility.

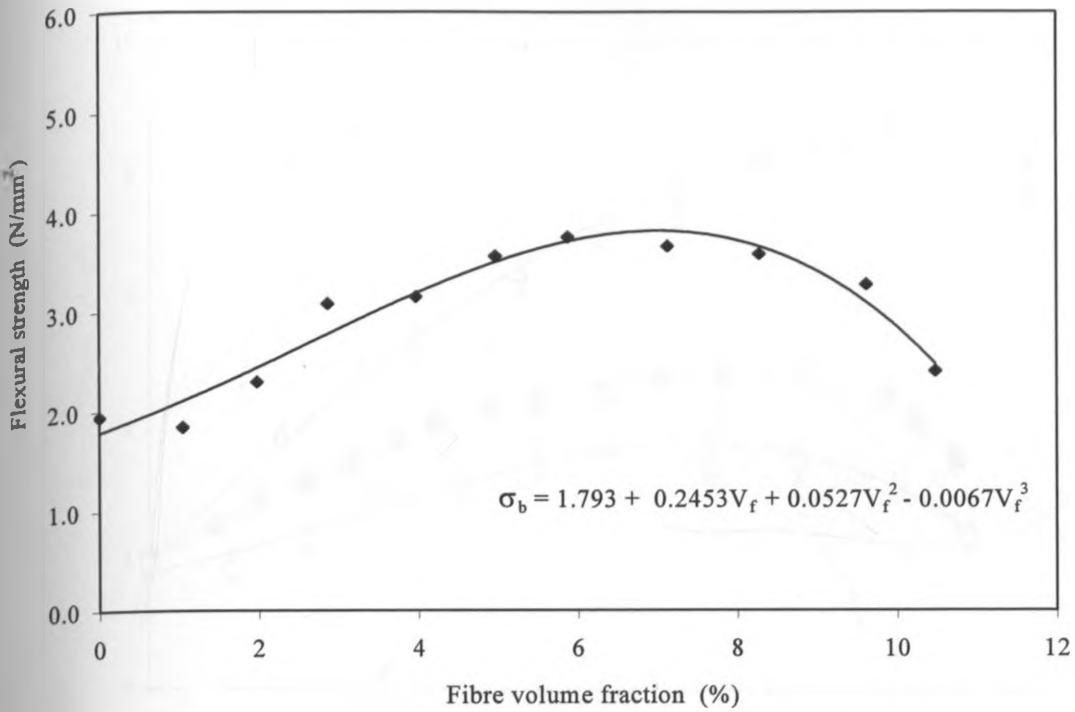


Figure 4.5 Variation of flexural strength with fibre volume fraction in 20 mm length chopped fibre Sisal/RHAC composites

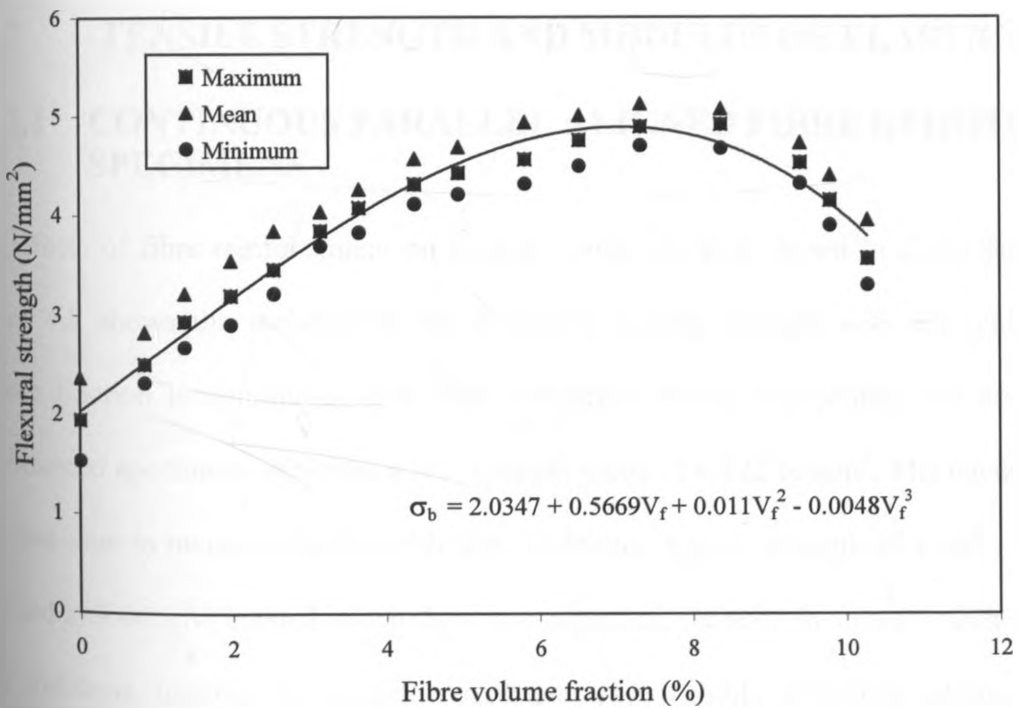


Figure 4.6 Variation of flexural strength with fibre volume fraction in 30 mm length chopped fibre Sisal/RHAC composites

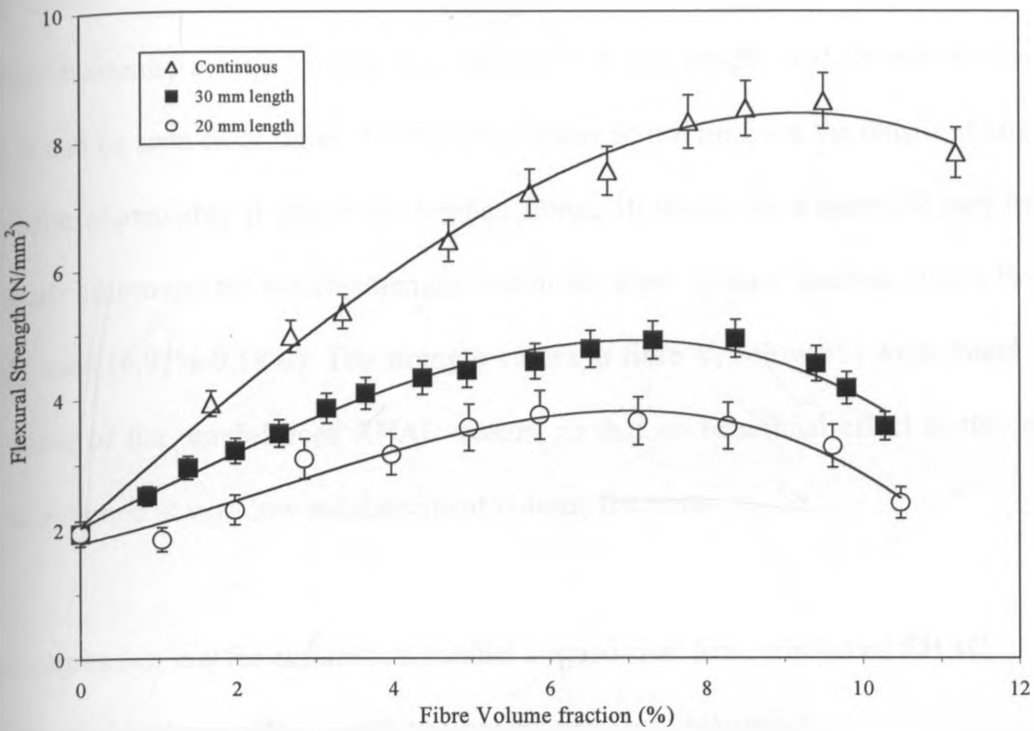


Figure 4.7 Variation of flexural strength with fibre volume fraction at different fibre lengths

4.1.2 TENSILE STRENGTH AND MODULUS OF ELASTICITY

4.1.2.1 CONTINUOUS PARALLEL ALIGNED FIBRE REINFORCED SPECIMENS

The effects of fibre reinforcement on cement mortar are best shown in direct tensile tests. Figure 4.8 shows the variation of the composite tensile strength with the reinforcement volume fraction in continuous sisal fibre reinforced RHAC composites. As expected the unreinforced specimens exhibited a low strength value of 0.922 N/mm^2 . The tensile strength was then seen to increase slightly with fibre additions. A peak strength of 3.642 N/mm^2 was obtained at $9.04\% V_f$ beyond which there was a gradual decrease in strength with successive fibre additions. Initially the tensile strength increased steadily with fibre additions but the trend changed at reinforcement volume fractions above 6.50% from where a slow rate of increase was observed. Beyond $9.04\% V_f$ no increase in strength with fibre additions was

recorded. Instead a gradual decrease in composite tensile strength occurred. More so at higher fibre contents, a large scatter was observed in the results and deviations became apparent. It can be seen from figure 4.9 that sisal fibres do not improve the tensile strength of the composite appreciably if added as chopped fibres. However the longer (30 mm length) fibres slightly improved the tensile strength within the fibre volume fraction ranges that are commonly used (6.97%-9.18%). The strength values at fibre V_f below 1% were found to be close to those of the unreinforced RHAC beams, so that no beneficial effect to the tensile strength is obtained at very low reinforcement volume fractions.

A general regression law for continuous parallel aligned sisal fibre reinforced RHAC composites relating the tensile strength to fibre content was obtained as

$$\sigma_t = 0.892 + 0.404V_f + 0.11V_f^2 - 0.0024V_f^3 \quad (4.4)$$

A maximum reinforcement volume fraction of 11.83% was realised for parallel fibre arrangement, while only 10.5% V_f was obtained for chopped randomly aligned fibres. Ductile failure was observed with fibres holding the composite together until the last fibres failed or pulled out, unlike the unreinforced beams that exhibited a sudden brittle failure.

The tensile stress-strain curves of continuous parallel aligned sisal fibre reinforced RHAC composites are shown in figure 4.10. The stress-strain curves indicates that inclusion of fibres leads to increased strains in comparison to unreinforced specimens at the same level of loading. At 4.19% V_f the maximum strain was more compared to that at 2.41% V_f . Similarly a larger strain was recorded at 9.082% V_f than at 7.36% V_f . It can be seen from figure 4.10 that the stress-strain curve of sisal fibre reinforced RHAC composites can be categorised into three distinct regions.

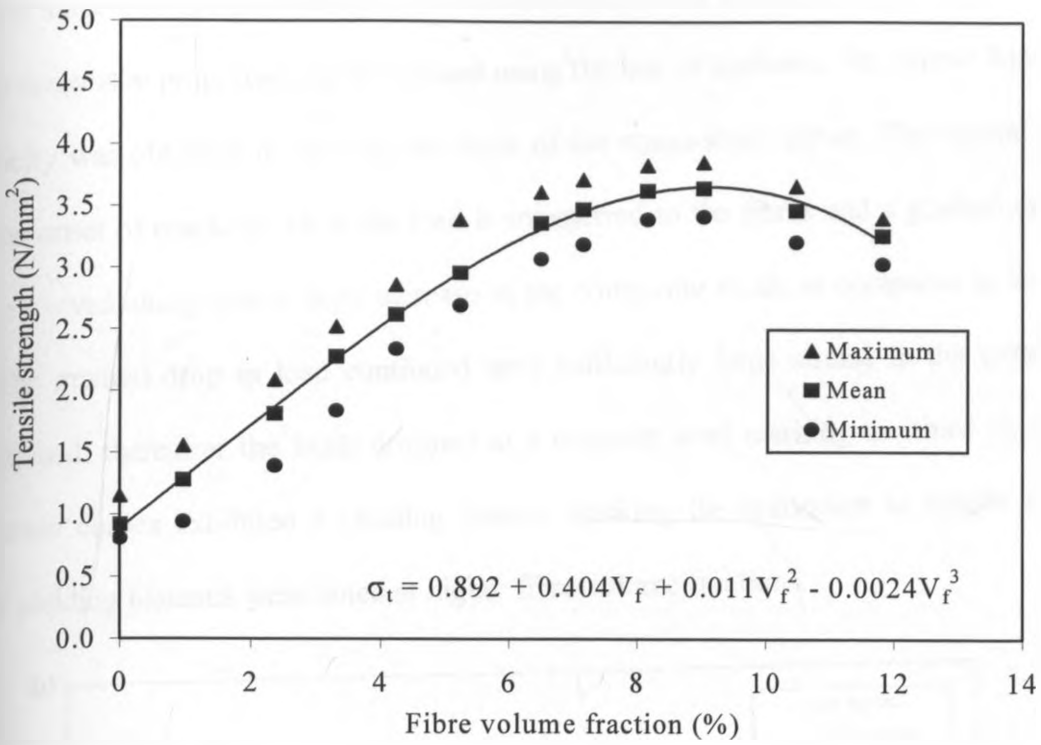


Figure 4.8 Variation of the composite tensile strength with fibre volume fraction in continuous sisal/RHAC composites

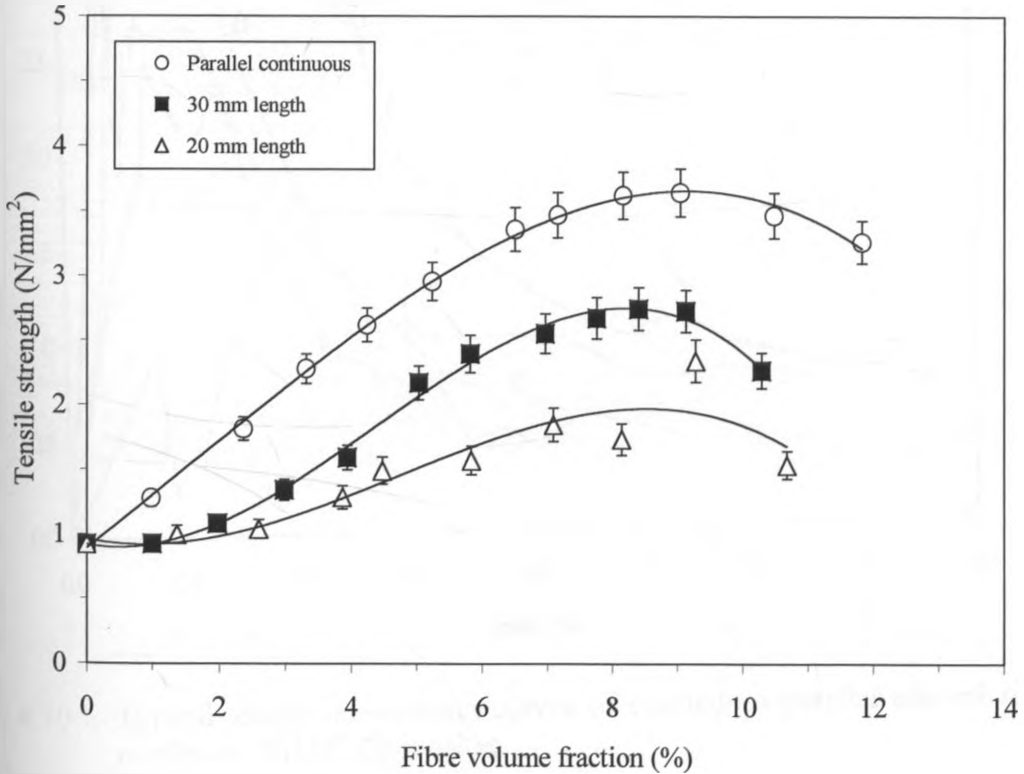


Figure 4.9 Variation of the composite tensile strength with fibre volume fraction at different fibre lengths

In the first stage a linear elastic response was observed till the matrix cracked. In this linear stage the composite properties can be defined using the law of mixtures. The tensile Modulus of Elasticity was obtained by finding the slope of the stress-strain curve. The second stage marks the onset of cracking. Here the load is transferred to the fibres and a gradual drop in load is observed along with a large increase in the composite strain as compared to the first stage. The gradual drop in load continued until sufficiently large strains in the composite were attained, thereafter the loads dropped to a constant level marking the third stage. All stress-strain curves exhibited a yielding plateau marking the resistance to tensile failure. Greater yielding plateaus were noted at higher fibre volume fractions.

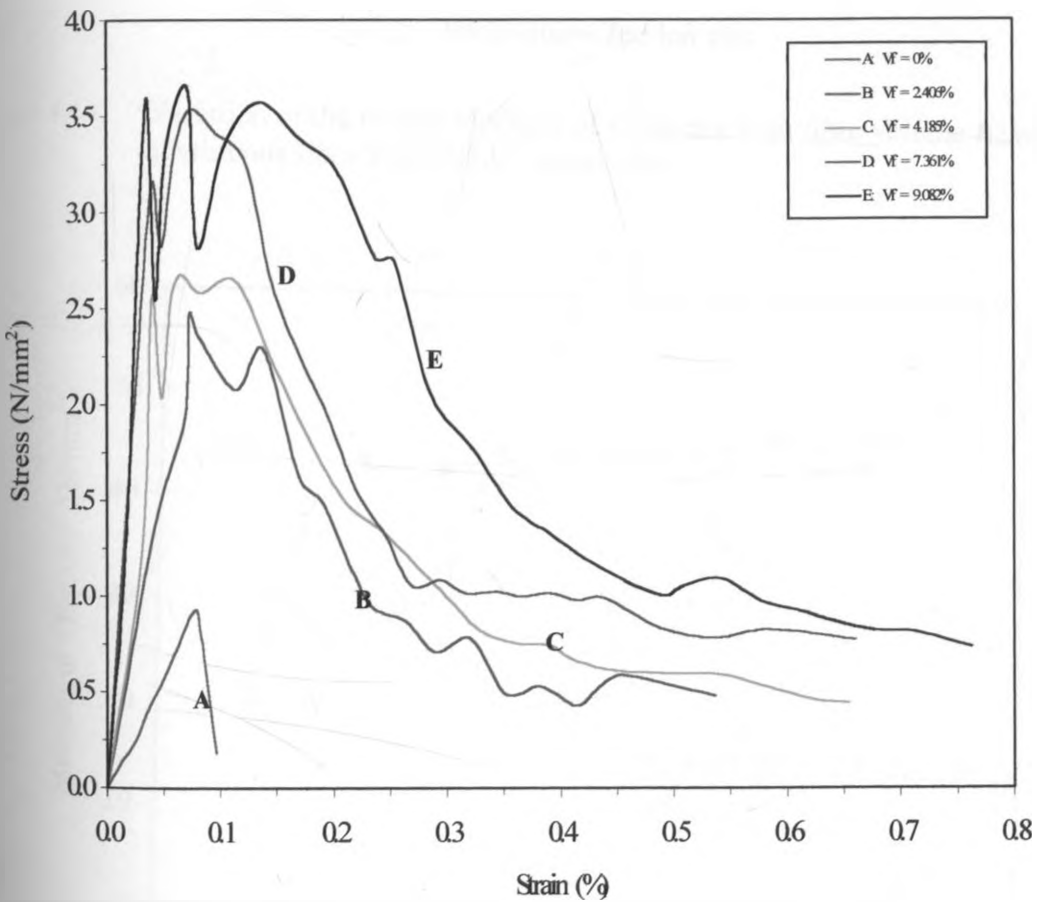


Figure 4.10 Typical tensile stress-strain curves of continuous parallel aligned sisal fibre reinforced RHAC composites

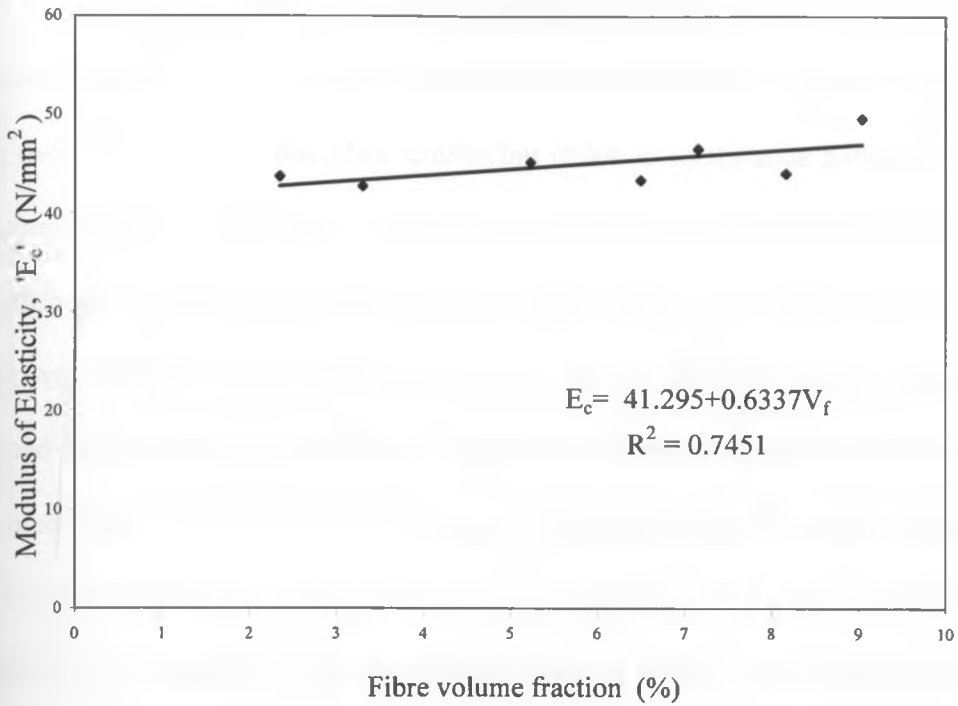


Figure 4.11 Variation of the tensile Modulus of Elasticity with fibre volume fraction in continuous fibre Sisal/RHAC composites

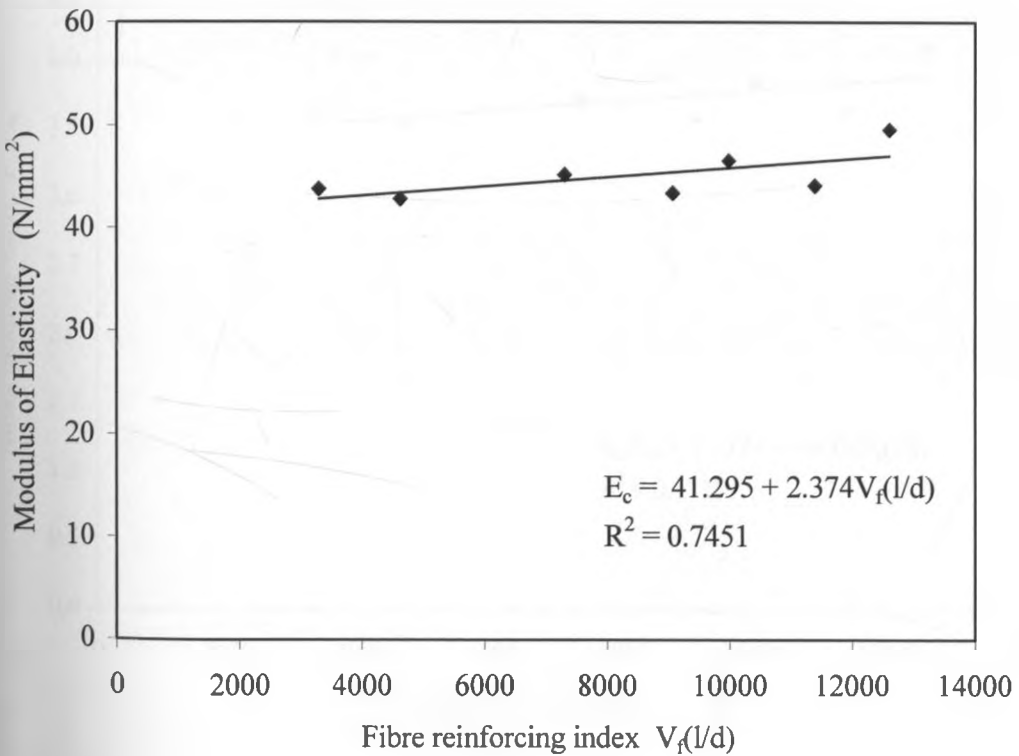


Figure 4.12 Variation of the tensile Modulus of Elasticity with fibre reinforcing index in continuous fibre Sisal/RHAC composites

Figures 4.11 and 4.12 shows the relationship between the tensile Modulus of Elasticity with fibre content and fibre reinforcing index respectively, while figure 4.13 gives the variation of the mean modular ratio with the fibre reinforcing index in continuous parallel aligned sisal fibre reinforced RHAC composites. The static Modulus of Elasticity was measured from the linear portion of the stress-strain curve up to the first crack. The modulus of elasticity of the composite was found to vary in the range of 42.84 MN/m² to 49.60 MN/m² with that of the unreinforced matrix being 12.12 MN/m². Only minor increases in stiffness of the composite was obtained with incremental fibre additions. This shows that the reinforcement volume fraction has no marked effect on the flexibility of specimens. The mean modular ratio also showed very slight variations with the fibre reinforcing index. The expressions correlating the Young's modulus to the amount of fibre in the composite is given in equations 4.5-4.7.

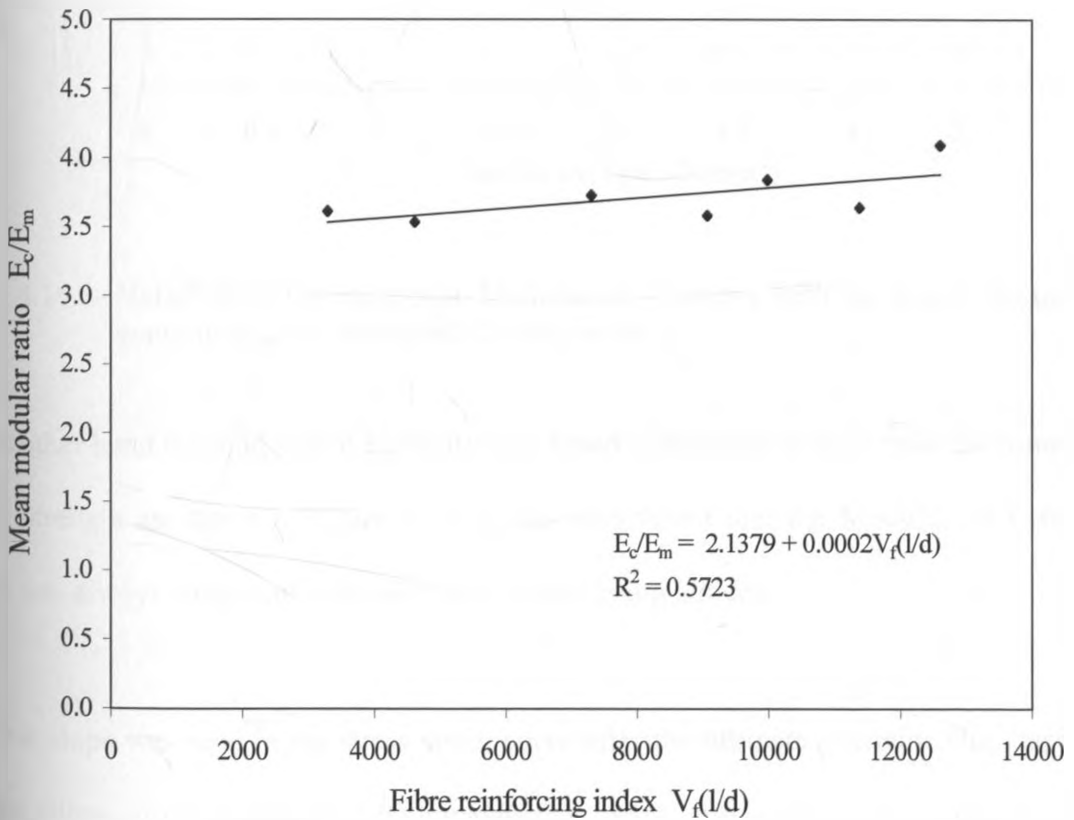


Figure 4.13 Variation of the mean modular ratio with fibre reinforcing index in continuous fibre Sisal/RHAC composites

$$E_c = 25.91 + 2.88V_f \quad (4.5)$$

$$E_c = 25.91 + 0.0021V_f \frac{l}{d} \quad (4.6)$$

$$\frac{E_c}{E_m} = 2.14 + 0.0002V_f \frac{l}{d} \quad (4.7)$$

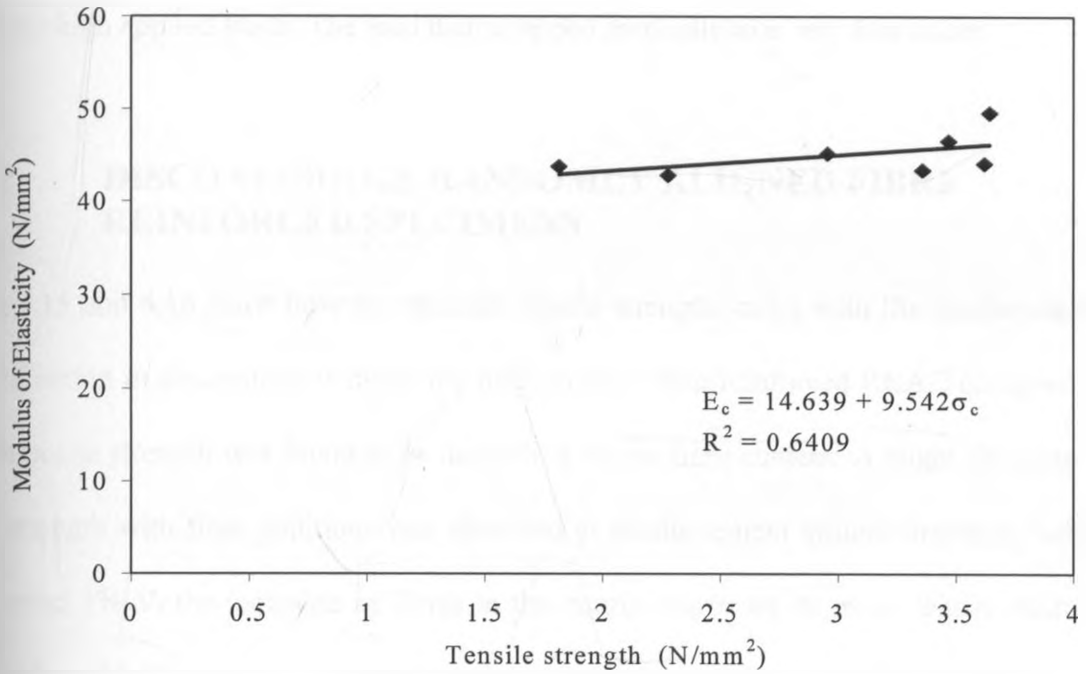


Figure 4.14 Variation of the composite Modulus of Elasticity with the tensile strength in continuous fibre Sisal/RHAC composites

On the other hand the modulus of elasticity was found to increase linearly with the composite tensile strength as shown in figure 4.14. It was also found that the Modulus of Elasticity values was always consistent with very little scatter being noticed.

A gentle slope was seen in the stress-strain curve after the ultimate strength. This implies a gradual failure of the composite which means that inclusion of sisal fibres greatly improves the structural integrity of the RHAC mortar. The specimens failed with multiple cracks appearing along the gauge length upon reaching the composite failure stress. The cracks

occurred perpendicular to the direction of loading spaced at almost regular intervals. The stress-strain curves exhibited a post ductile behaviour, with specimens carrying additional loads even after the advent of the first crack. However this ability of fractured specimens to carry higher loads diminished after crack opening became so large that fibres could not carry any additional load. Specimen fracture finally occurred when the remaining fibres could not sustain the high applied loads. The load then dropped gradually to a very low value.

4.1.2.2 DISCONTINUOUS RANDOMLY ALIGNED FIBRE REINFORCED SPECIMENS

Figures 4.15 and 4.16 show how the ultimate tensile strength varies with the reinforcement volume fraction in discontinuous randomly aligned sisal fibre reinforced RHAC composites. The composite strength was found to be dependent on the fibre content. A slight decrease in tensile strength with fibre additions was observed at reinforcement volume fractions below 1%. Beyond 1% V_f the inclusion of fibres in the matrix improved its mean tensile strength from a value of 0.922 N/mm^2 in unreinforced specimens to a peak value of 2.744 N/mm^2 at a fibre volume fraction of 8.4% in 30 mm length chopped fibre/cement composites. The strength of 20 mm length chopped fibre/cement composites also improved slightly reaching a maximum of 2.342 N/mm^2 at 9.28% V_f . However reinforcement volume fractions above these values produced a drop in strength.

It can be seen from figure 4.15 that above 6% V_f the rate of strength increase with fibre additions reduced. Maximum reinforcement volume fractions of 10.69% and 10.29% were realised with 20 mm and 30 mm lengths respectively in sisal fibre reinforced RHAC mortar. The optimum fibre volume fraction was found to be in the range of 7.76% to 9.12%. In the experiments an increase in the composite tensile strength with fibre length was also noted.

However mixing was easier with shorter fibres. A large scatter was seen in the 30 mm length fibre/cement composites than the 20 mm length ones.

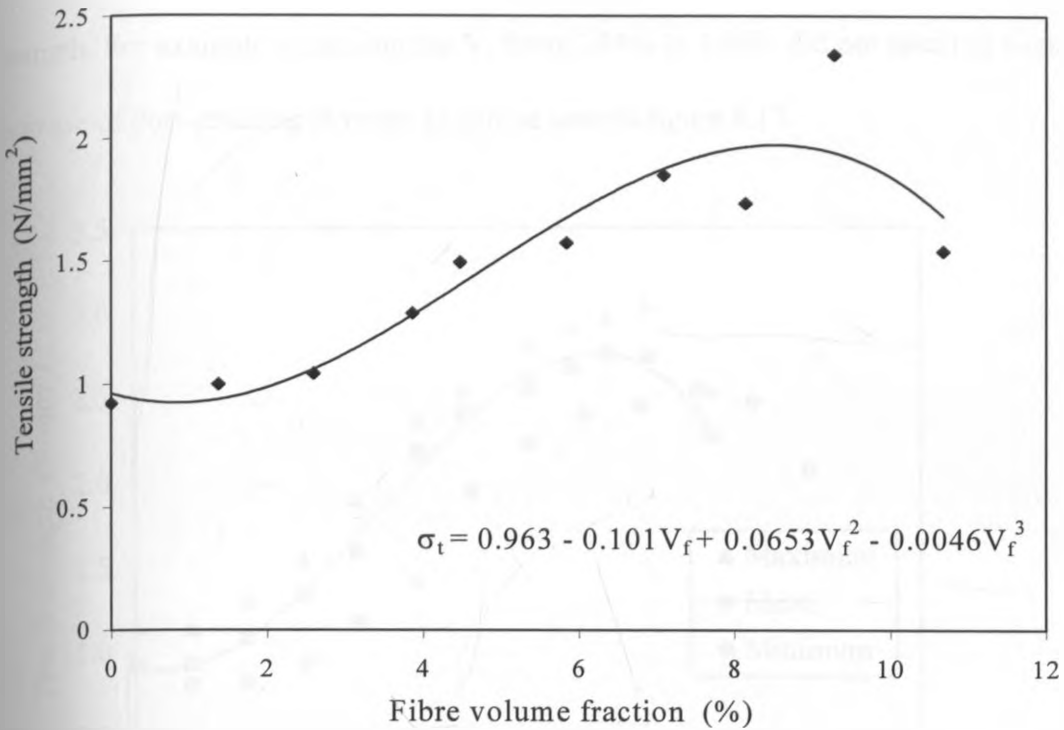


Figure 4.15 Variation of the tensile strength with fibre volume fraction in 20 mm length chopped fibre Sisal/RHAC composites

The regression equation predicting the relationship between the composite tensile strength and its fibre content in 20 mm length fibre/cement composites was found as

$$\sigma_t = 0.963 - 0.101V_f + 0.065V_f^2 - 0.0046V_f^3 \quad (4.8)$$

While that of 30 mm length chopped fibre/cement composites was obtained as

$$\sigma_t = 0.919 - 0.093V_f + 0.104V_f^2 - 0.008V_f^3 \quad (4.9)$$

The first cracks were observed to occur at strength values about 87% of the peak strengths on average. The stress-strain curve of 30 mm length chopped sisal fibre reinforced RHAC mortar composites is shown in figure 4.17. A gentle slope was observed after the first crack

in the stress-strain curve of chopped sisal fibre reinforced RHAC specimens. This indicates a slowly progressing cracking phenomenon. An important observation made was that increasing the fibre content does not result in a significant increase in the post-cracking strength. For example increasing the V_f from 2.04% to 3.86% did not result in a considerable increase of post cracking strength as can be seen in figure 4.17.

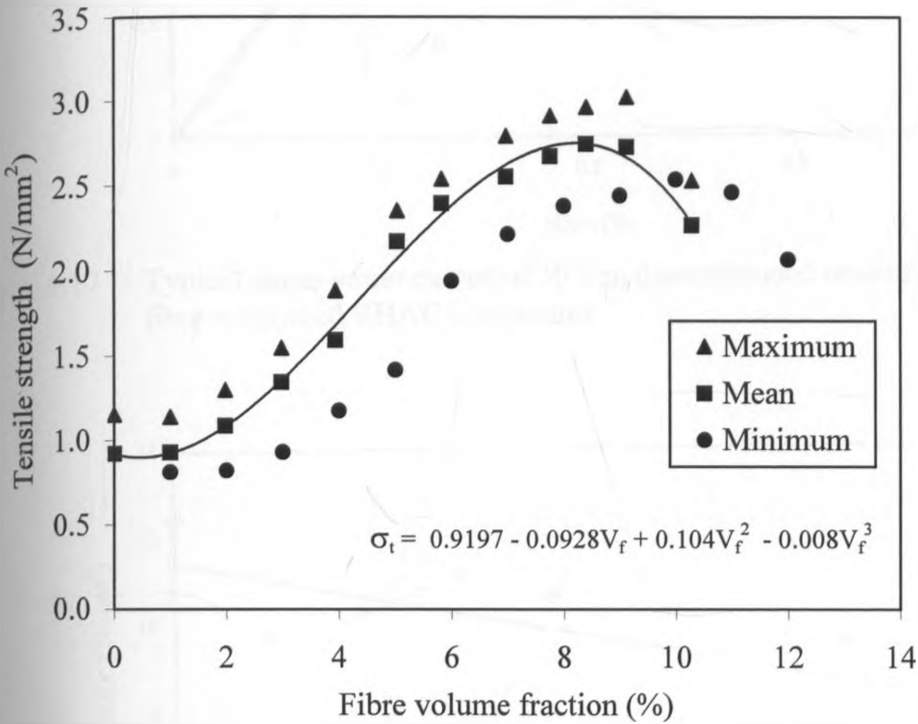


Figure 4.16 Variation of the tensile strength with fibre volume fraction in 30 mm length chopped fibre Sisal/RHAC composites

Figure 4.18 shows the variations of the tensile modulus of elasticity with fibre content in 30 mm length chopped fibre/cement composites. The tensile modulus of elasticity showed a linear decrease with fibre content. Their linear correlation is given in equation 4.10.

$$E_c = 11.42 - 0.40V_f \tag{4.10}$$

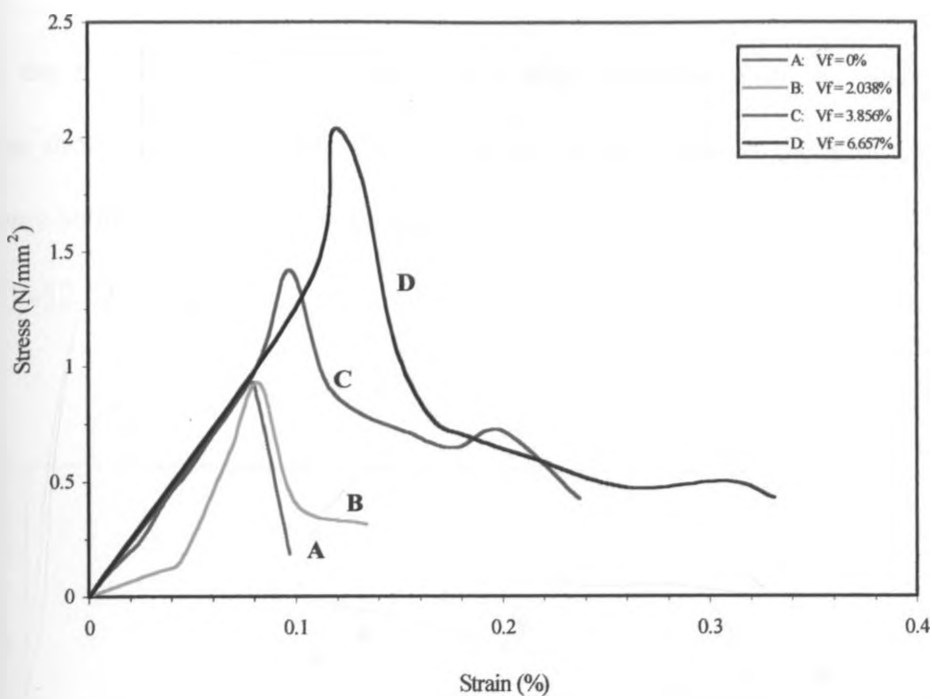


Figure 4.17 Typical stress-strain curves of 30 mm discontinuous randomly aligned sisal fibre reinforced RHAC composites

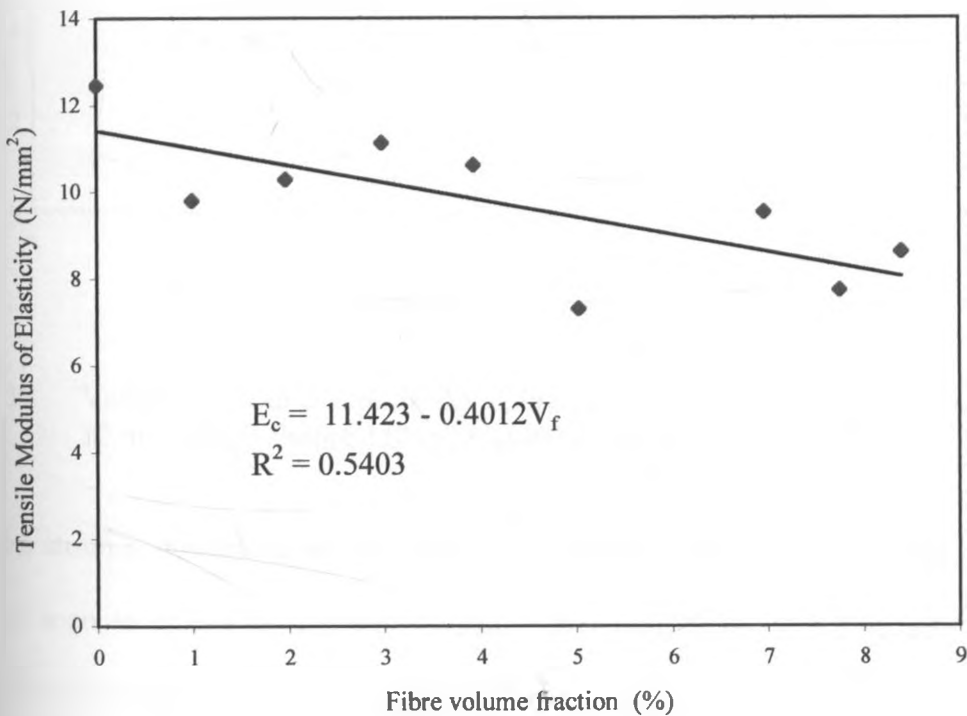


Figure 4.18 Variation of the tensile Modulus of Elasticity with fibre content in 30 mm length chopped fibre Sisal/RHAC composites

Likewise the modulus of elasticity showed a slight decrease with the composite tensile strength as shown in figure 4.19. The correlation of the Young's modulus and composite strength was obtained as given in equation 4.11.

$$E_c = 12.62 - 1.62\sigma_c \quad (4.11)$$

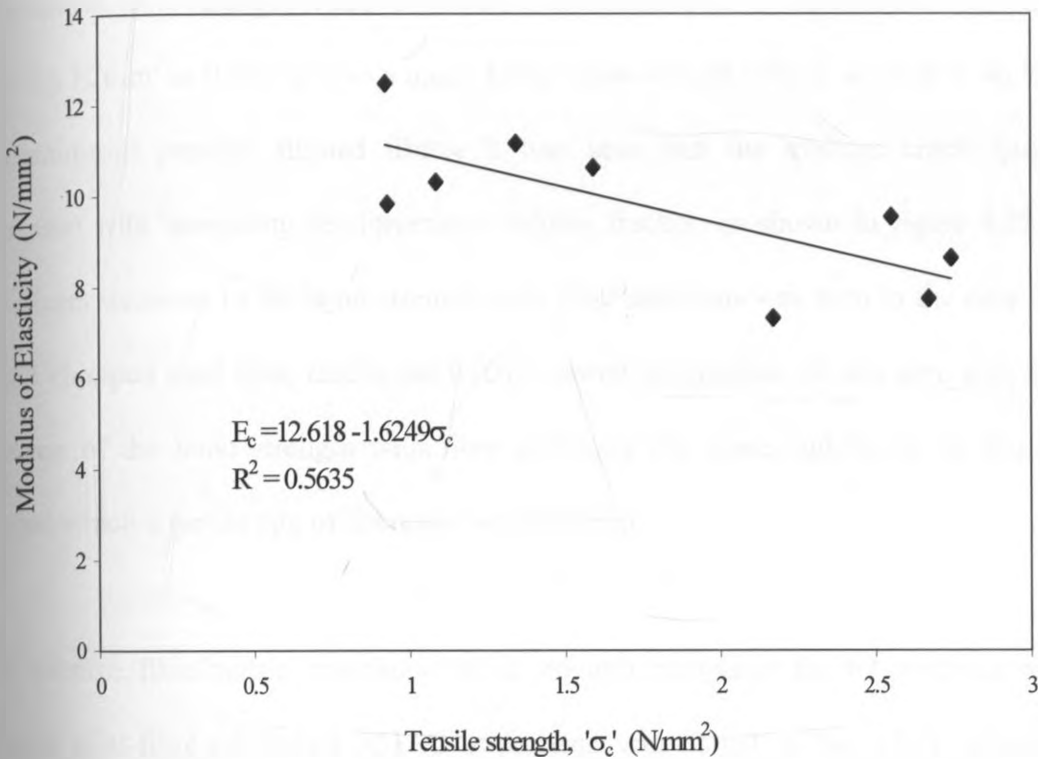


Figure 4.19 Variation of the composite Modulus of Elasticity with the tensile strength in 30 mm length chopped fibre Sisal/RHAC composites

The failure strain concentrated on one crack when chopped fibre reinforcements was used, but it was seen to spread to numerous cracks when long fibres and high reinforcement volume fractions were used. A catastrophic failure was observed in the tensile tests accompanied by the load falling suddenly to a very low value. The failed specimens showed no ability to sustain any load after the appearance of the failure crack traversing across the specimen with the failure surface in some cases exhibiting fibre pull-out.

The values of the fibre/matrix interfacial bond strength calculated on the basis of measured crack spacings are shown in figures 4.20 and 4.21 for continuous parallel and discontinuous randomly aligned sisal-fibre-reinforced RHAC mortar composites respectively. A significant effect of the variations of fibre content on the fibre/matrix bond strength was observed. The fibre/matrix bond strength reduced with fibre additions in the composite starting with a value of 0.453 N/mm^2 at $0.982\% V_f$ to a much lower value of 0.06 N/mm^2 at $11.83\% V_f$ in the case of continuous parallel aligned fibres. It was seen that the average crack spacing also decreased with increasing reinforcement volume fraction as shown in figure 4.22. A more significant decrease in the bond strength with fibre additions was seen in the case of 30 mm length chopped sisal fibre reinforced RHAC mortar composites. It was seen that the rate of decrease of the bond strength with fibre additions was quite sudden up to about $4\% V_f$, beyond which a gentle rate of decrease was observed.

The average fibre/matrix interfacial bond strength computed for 63 continuous parallel-aligned sisal-fibre-reinforced RHAC specimens was found to be 0.139 N/mm^2 with a standard deviation of 0.116 N/mm^2 , while that of discontinuous randomly aligned fibres was found to be 0.121 N/mm^2 with a standard deviation of 0.083 N/mm^2 . The minimum and maximum bond strength values obtained for parallel fibres in the cement matrix were found to be 0.061 N/mm^2 and 0.463 N/mm^2 respectively. Chopped fibre specimens however gave comparatively lower bond strength values in the range of 0.033 N/mm^2 to 0.317 N/mm^2 . The crack patterns on the composite systems showed that cracks appeared much earlier in low fibre content beams as compared to higher fibre volume fraction specimens.

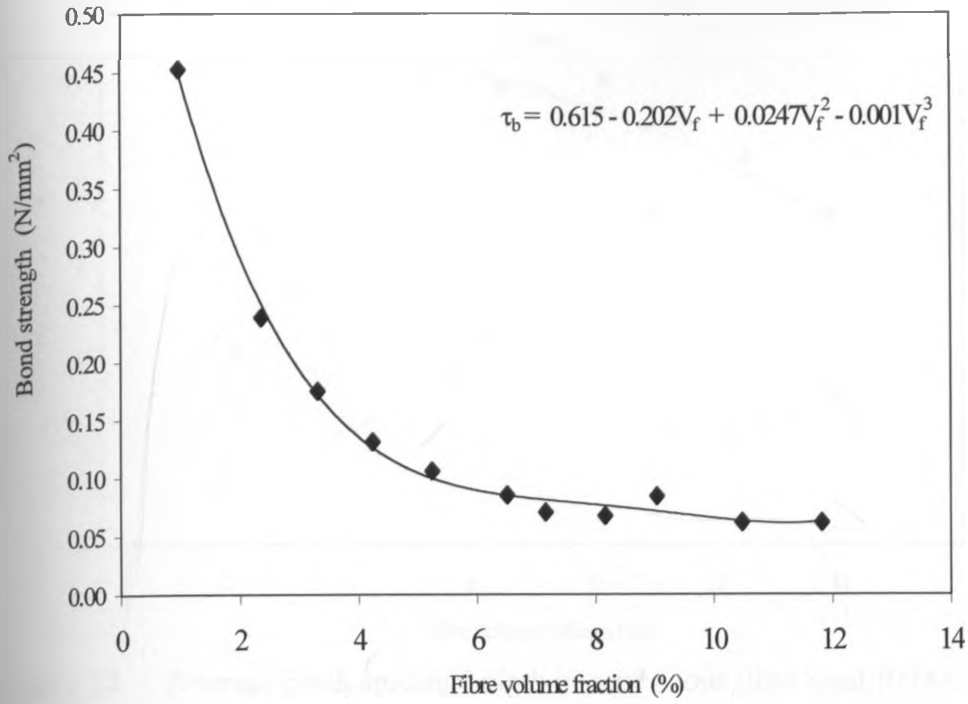


Figure 4.20 Variation of the interfacial bond strength with fibre volume fractions in continuous fibre Sisal/RHAC composites

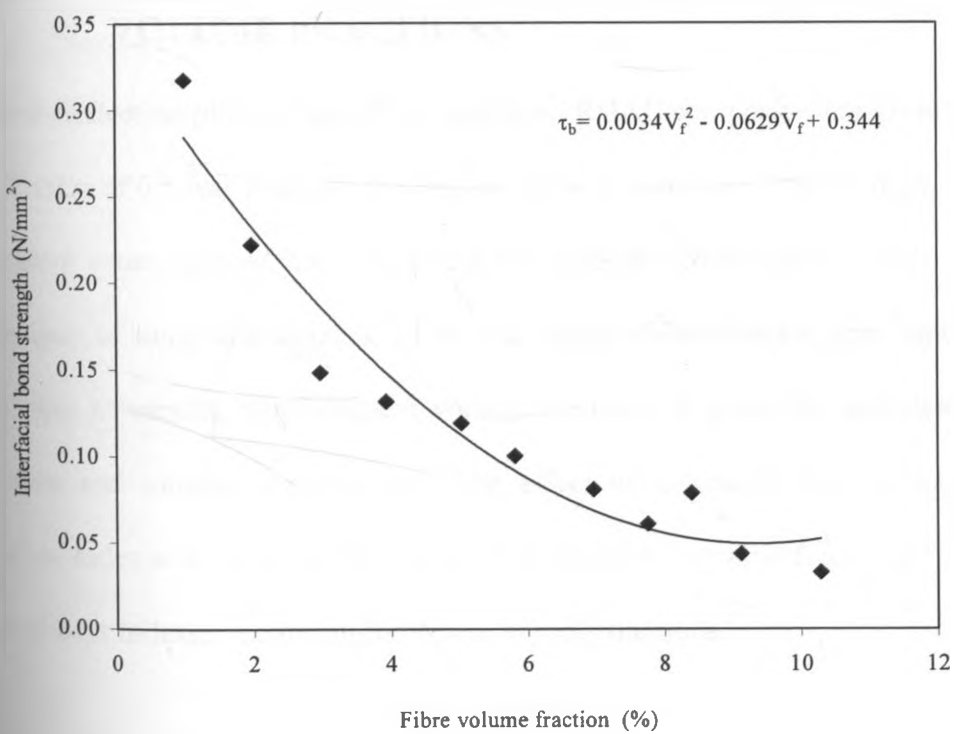


Figure 4.21 Variation of the interfacial bond strength with fibre volume fractions in 30 mm length chopped fibre Sisal/RHAC composites

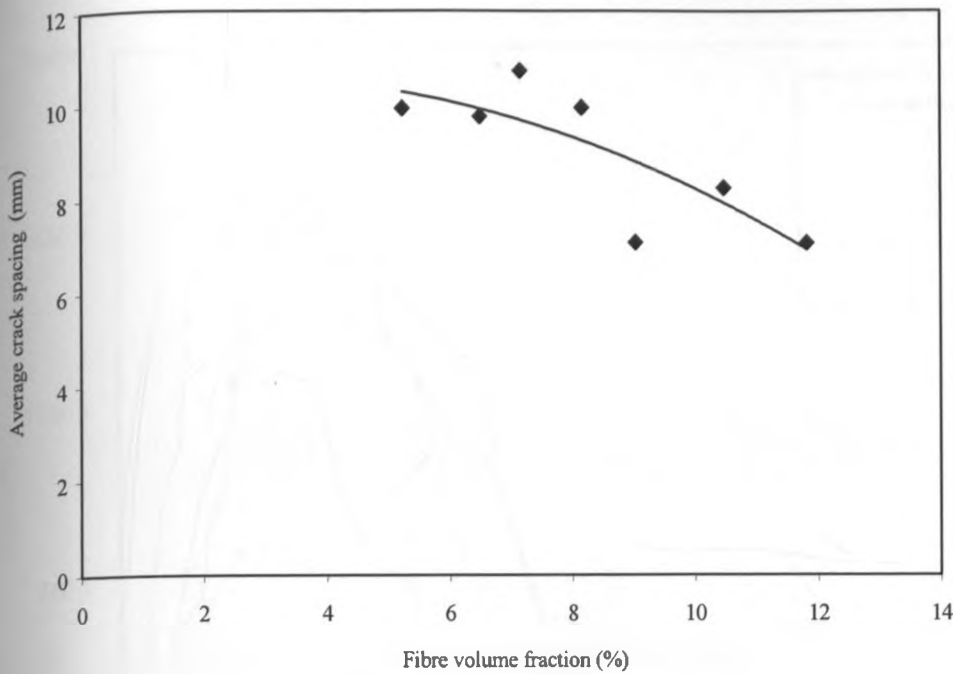


Figure 4.22 Average crack spacing length in continuous fibre Sisal/RHAC composites

4.1.4 FLEXURAL TOUGHNESS

4.1.4.1 VARIATIONS OF FLEXURAL TOUGHNESS WITH FIBRE VOLUME FRACTIONS

The load-deflection plots of sisal-fibre reinforced RHAC composites are given in figure 4.23. A W/C ratio of 0.5 was used and the specimens were cured in air for 28 days. The toughness parameters were obtained after analysing the load-deflection curves. Table 4.3 shows the comparison of toughness indexes, of 30 mm length discontinuous fibre reinforced cement composites at varying reinforcement volume fractions. It gives the peak loads, first crack deflection and toughness parameters. The effect of increased fibre contents on various toughness indexes is shown in the bar chart of figure 4.24, while figure 4.25 gives a plot of the toughness indexes versus reinforcement volume fractions.

It can be seen from table 4.3 that the highest toughness values of sisal fibre reinforced RHAC composites was obtained at 8.34% V_f as 11.57 Nm. This was followed by composites of fibre

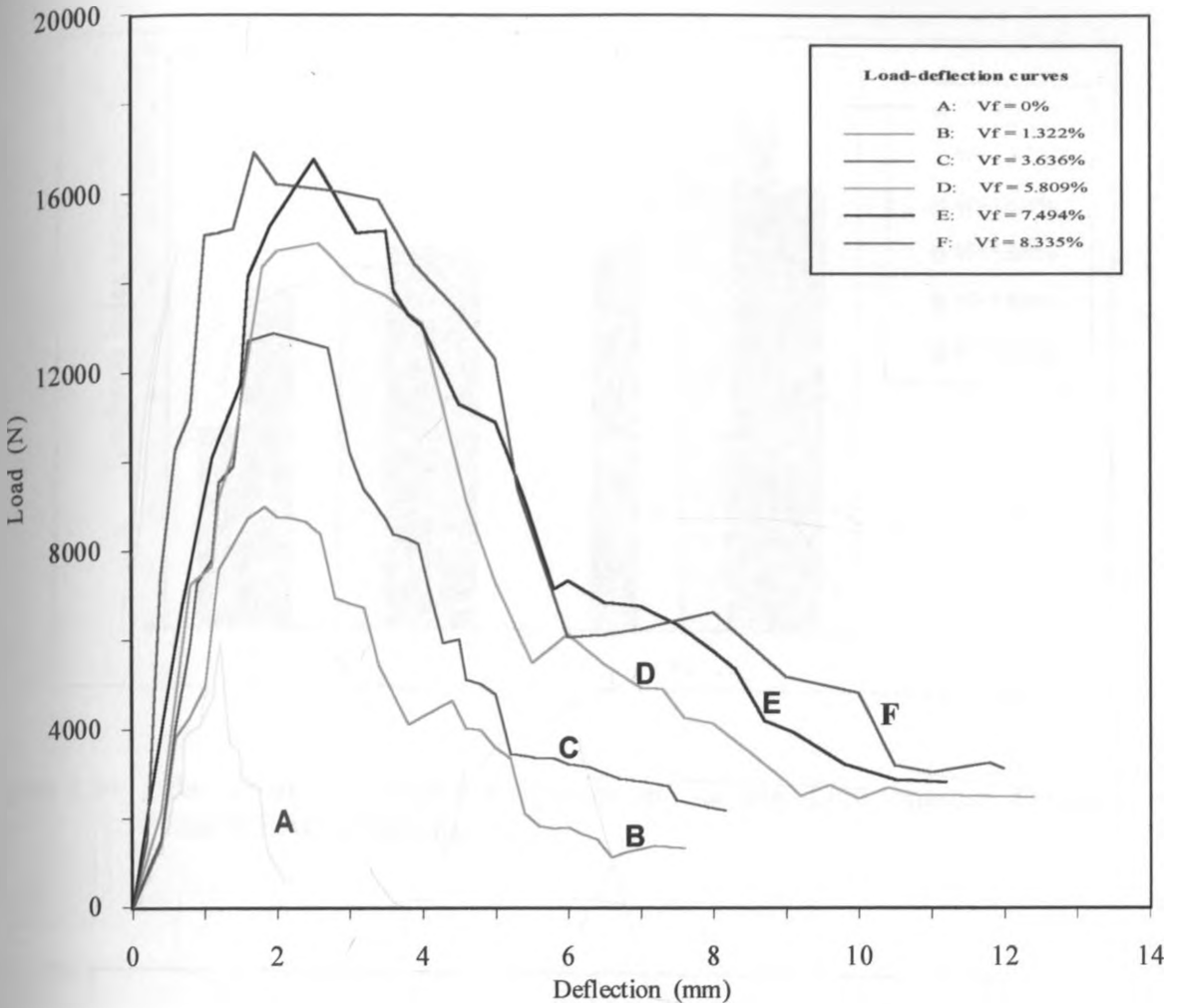


Figure 4.23 Load-deflection curves of Sisal/RHAC composites at varying fibre volume fractions for 30 mm length discontinuous randomly aligned fibres

Fibre content V_f (%)	Peak load (N)	First crack deflection (mm)	First crack energy (Nm)	Toughness indexes	
				I_5	I_{10}
0	5952.18	1.26	1.30	3.44	-
1.3	8992.54	1.34	4.40	5.87	6.53
3.6	12878.00	1.79	6.20	5.91	7.42
5.8	14889.91	1.63	7.50	6.29	8.20
7.5	16746.86	1.65	9.25	6.63	8.96
8.3	16918.27	1.51	11.57	6.51	7.72

Table 4.3 Toughness indexes at varying fibre contents in 30 mm length discontinuous randomly aligned Sisal/RHAC composites

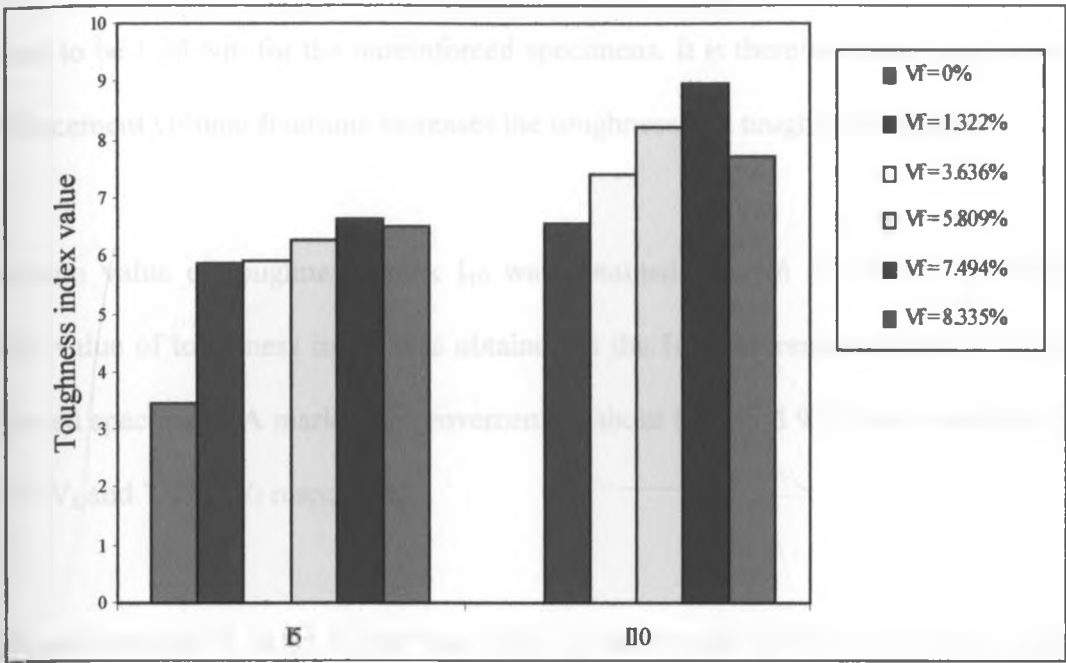


Figure 4.24 Bar chart of toughness indexes at varying fibre volume fractions in Sisal/RHAC composites

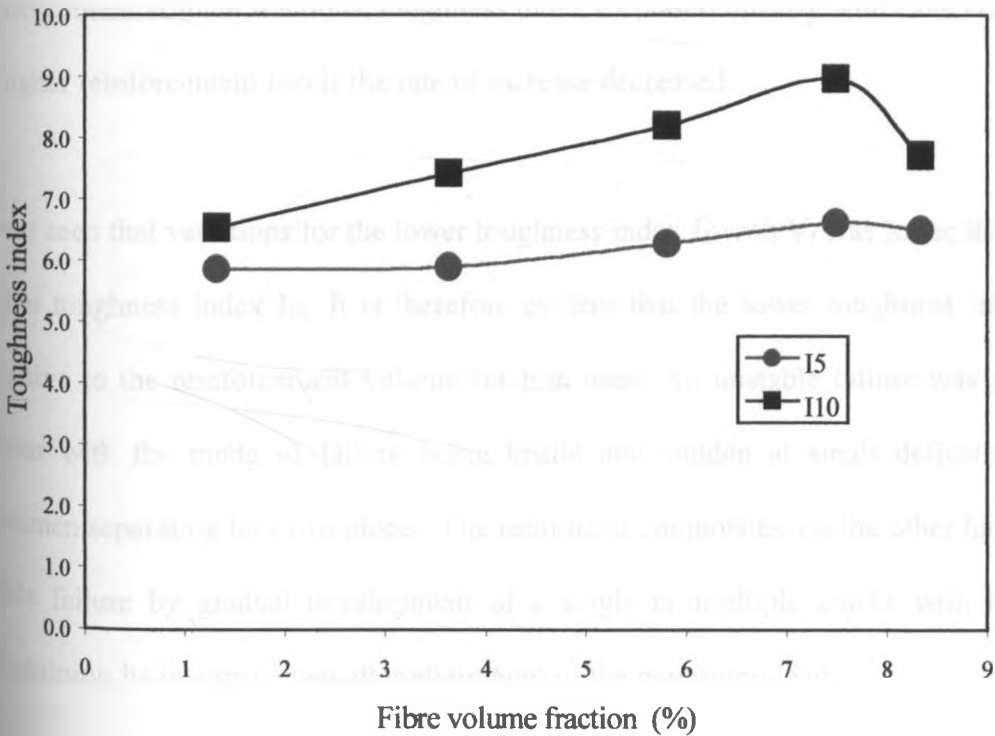


Figure 4.25 Variation of toughness indexes with fibre volume fraction in 30 mm length discontinuous randomly aligned sisal/RHAC composites

contents 7.49%, 5.81% and 3.64 % in descending order. Finally, the lowest toughness value was found to be 1.30 Nm for the unreinforced specimens. It is therefore clear that increasing the reinforcement volume fractions increases the toughness and toughness indexes.

A maximum value of toughness index I_{10} was obtained as 8.96 at 7.49% V_f , while the minimum value of toughness index was obtained in the I_5 measurements to be 3.44 for the unreinforced specimens. A marked improvement of about 82% and 92% were recorded for I_5 at 5.81 % V_f and 7.49% V_f respectively.

For I_{10} measurements a large scatter was seen in the results with the maximum flexural toughness value occurring at about 7.49% fibre content. It is evident from figure 4.25 that the addition of fibres increased the I_{10} toughness index by more than 37% at 7.49% V_f , and that increases were nearly proportional to the values of the fibre volume fractions. At low reinforcement volume fractions, toughness index increased linearly with fibre contents, while at higher reinforcement levels the rate of increase decreased.

It was seen that variations for the lower toughness index I_5 with V_f was lower than that of the higher toughness index I_{10} . It is therefore evident that the lower toughness index I_5 is not sensitive to the reinforcement volume fraction used. An unstable failure was seen in plain mortar with the mode of failure being brittle and sudden at small deflections, and the specimen separating into two pieces. The reinforced composites, on the other hand, exhibited stable failure by gradual development of a single or multiple cracks with the specimen maintaining its integrity even after attainment of the maximum load.

4.1.4.2

VARIATIONS OF FLEXURAL TOUGHNESS WITH W/C RATIOS

The load-deflection curves shown in figure 4.26 are for sisal fibre reinforced RHAC mortar composites at varying W/C ratios. Variations of the W/C ratio with toughness and toughness indexes are given in table 4.4. It can be seen from figure 4.26 and table 4.4 that flexural toughness has an inverse relationship with the W/C ratio. However the proportional relationship between W/C ratio and toughness index is not clear.

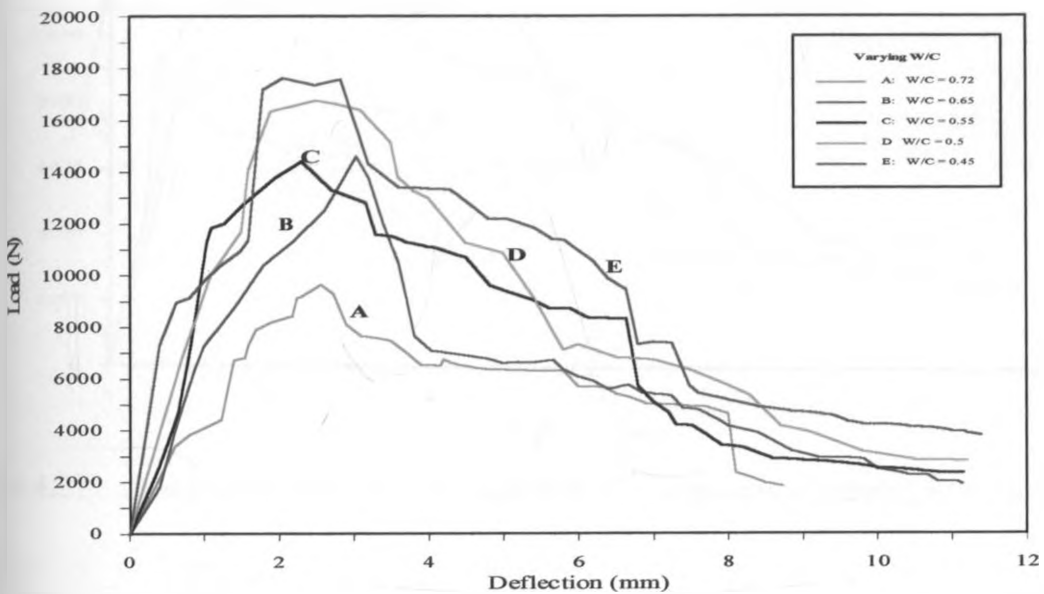


Figure 4.26 Load-deflection curves of sisal/RHAC composites at varying W/C ratios for 30 mm length discontinuous randomly aligned fibres

W/C ratio	Peak load (N)	First crack deflection (mm)	First crack energy (Nm)	Toughness indexes	
				I ₅	I ₁₀
0.45	17591.23	1.73	8.21	5.66	8.04
0.50	16746.86	1.65	9.25	6.73	8.96
0.55	14415.07	1.81	7.75	7.10	9.74
0.65	14629.72	1.72	7.63	5.57	8.61
0.72	9673.15	1.17	3.33	6.65	11.03

Table 4.4 Toughness indexes at various W/C ratios in Sisal/RHAC composites for 30 mm length discontinuous fibre composites

4.1.4.3

VARIATION OF FLEXURAL TOUGHNESS WITH CURING AGE

The relationship between flexural toughness and curing age in 30 mm length chopped sisal fibre reinforced RHAC mortar specimens is shown figure 4.27 and table 4.5.

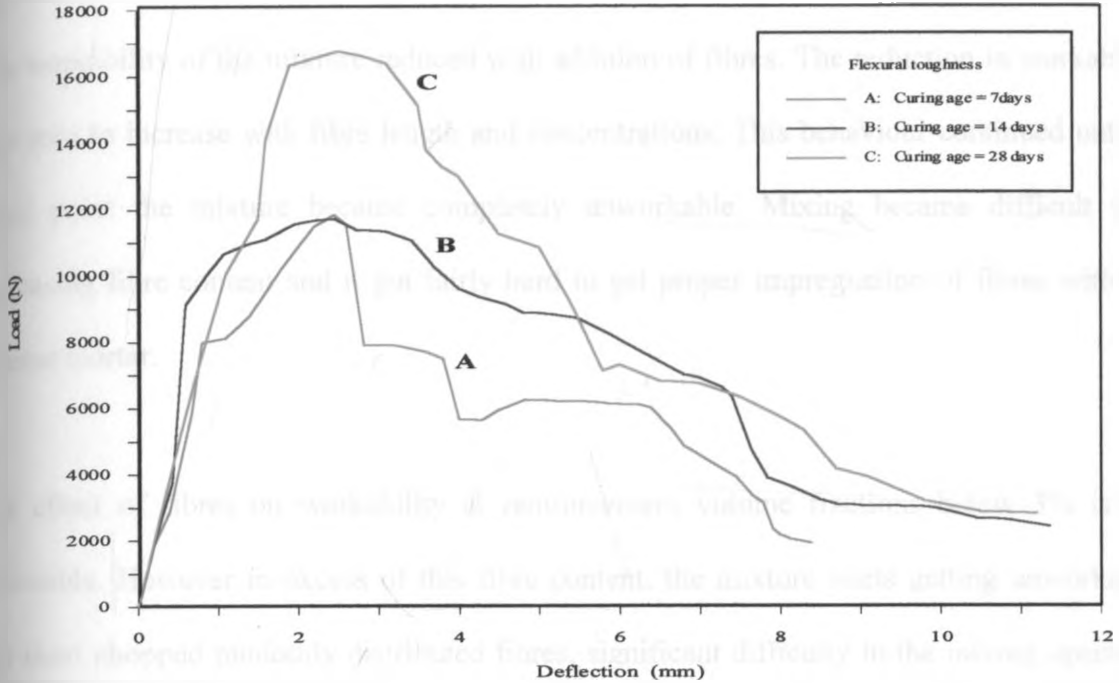


Figure 4.27 Load-deflection curves of sisal/RHAC composites at varying W/C curing ages

Curing age (days)	Peak load (N)	First crack deflection (mm)	First crack energy (Nm)	Toughness indexes	
				I ₅	I ₁₀
7	11850.60	1.49	7.33	5.11	6.95
14	11741.45	1.57	9.21	5.48	7.60
28	16746.86	1.65	9.25	6.73	8.96

Table 4.5 Toughness indexes at varying curing ages in Sisal/RHAC composites

It was found that both toughness and toughness indexes increased with curing age. An I₁₀ toughness index of 8.96 was obtained for specimens cured for 28 days in air, while those cured for 14 and 7 days in air only realised I₁₀ toughness indexes of 7.60 and 6.95 respectively.

4.1.5 WORKABILITY OF PLAIN RHAC MORTAR AND SISAL/RHAC COMPOSITES

The workability of plain RHAC mortar (at W/C = 0.5) was found to be good as it was easily placed into the moulds for casting. It was however observed that inclusion of sisal fibres into the RHAC mortar significantly altered the workability behaviour of the resulting composites. The workability of the mixture reduced with addition of fibres. The reduction in workability was seen to increase with fibre length and concentrations. This behaviour continued until at some point the mixture became completely unworkable. Mixing became difficult with increasing fibre content and it got fairly hard to get proper impregnation of fibres with the cement mortar.

The effect of fibres on workability at reinforcement volume fractions below 3% is not noticeable. However in excess of this fibre content, the mixture starts getting unworkable. For short chopped randomly distributed fibres, significant difficulty in the mixing operation was observed at reinforcement volume fractions beyond 7-8% V_f . This was as a result of bundling and mixing-up of fibres during the mixing operation.

4.1.6 COMPOSITE DENSITY AND VOID VOLUME VARIATION

Figure 4.28 shows the variation of composite density with fibre content in chopped sisal fibre reinforced RHAC composites. A general trend of decreasing density was seen with increasing reinforcement volume fractions. The density decreased from 2.104 g/cm³ in unreinforced specimens to 1.437 g/cm³ at 10.19% V_f . A nearly constant rate of decrease was seen initially, but at higher reinforcement levels the composite showed a sudden rate of decrease.

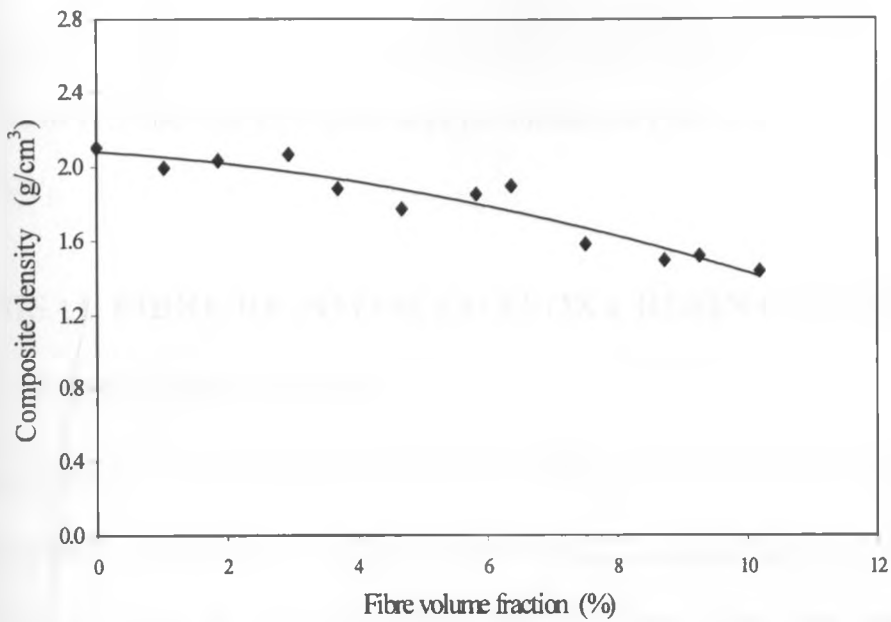


Figure 4.28 Variation of the composite density with fibre volume fraction in chopped fibre Sisal/RHAC composites

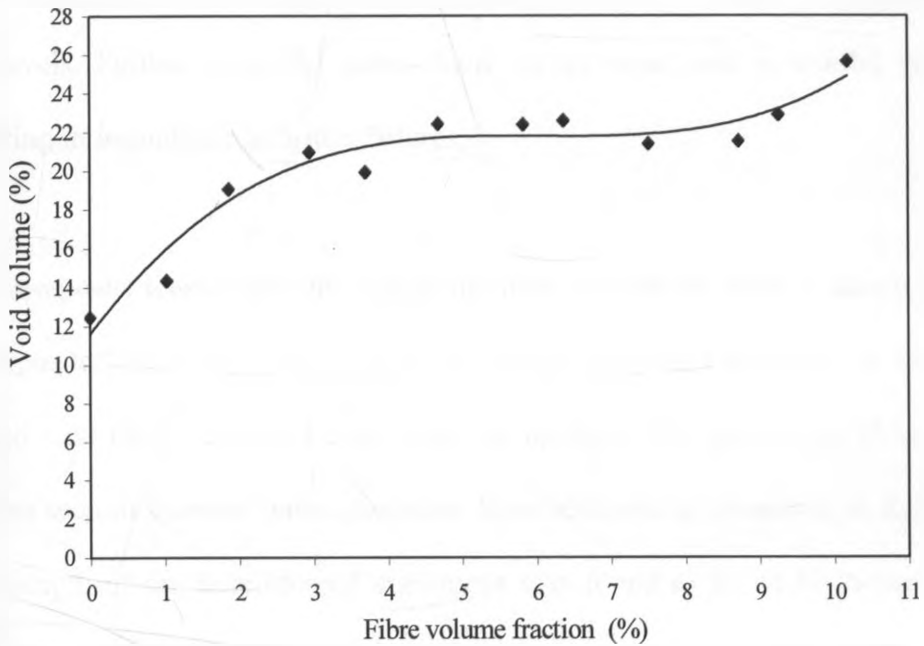


Figure 4.29 Variation of the void volume value with fibre volume fraction in chopped fibre Sisal/RHAC composites

A plot of the void volume value against the reinforcement volume fraction is shown in figure 4.29. The void volume value was seen to increase with increasing fibre contents. Plain RHAC mortar had a void volume fraction of 12.475%. This increased to about 25.648% at a fibre content of 10.19% V_f . A sudden rate of increase in the amount of voids was seen up to

2.95% V_f . This was followed by a region of gentle increase up to about 6.37% V_f . Finally a sudden rate of increase was seen again until the maximum fibre volume fraction was attained at 10.19% V_f .

4.2 SISAL FIBRE REINFORCED EPOXY RESIN COMPOSITES

4.2.1 TENSILE STRENGTH

The tensile stress-strain curves of continuous parallel aligned sisal fibre reinforced epoxy resin composites are shown in figures 4.30 and 4.31. A linear stress-strain curve up to fracture was obtained for the unreinforced and low fibre content specimens. At higher reinforcement volume fractions the stress-strain curves tend to be curved with scatter and deviations becoming apparent. In general the increase of stress with strain reduced at higher deformation levels. Further more the stress-strain curves were seen to exhibit very little ductility resulting in instantaneous brittle failures.

A plot of the composite tensile strength against the fibre volume fractions is shown in figure 4.32. The composite tensile strength was seen to improve with fibre additions in continuous parallel aligned sisal fibre reinforced epoxy resin composites. The percentage elongation to failure was also seen to increase with successive fibre additions as presented in figure 4.34. The tensile strength of the unreinforced specimens was found to be 43.83 N/mm^2 with a standard deviation of 6.057 N/mm^2 . This increased progressively with fibre additions until a maximum of 113.19 N/mm^2 with a standard deviation of 7.93 N/mm^2 was recorded at 44.83% V_f in parallel fibre reinforced composites. An improvement in the composite tensile strength was also seen with increasing the fibre aspect ratio. No effective strength improvement was however observed with discontinuous randomly aligned fibre reinforcement. The test specimens exhibited brittle failure in both continuous parallel and

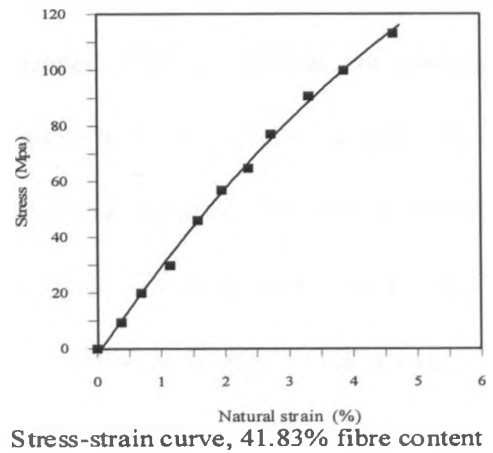
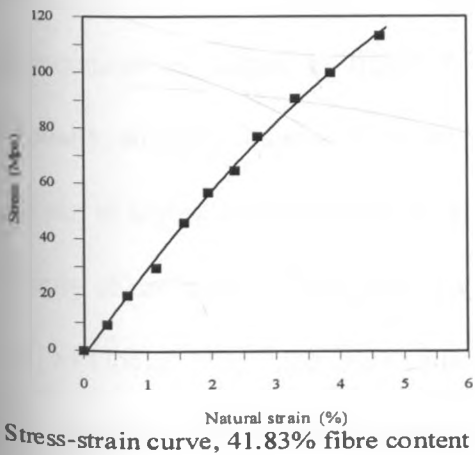
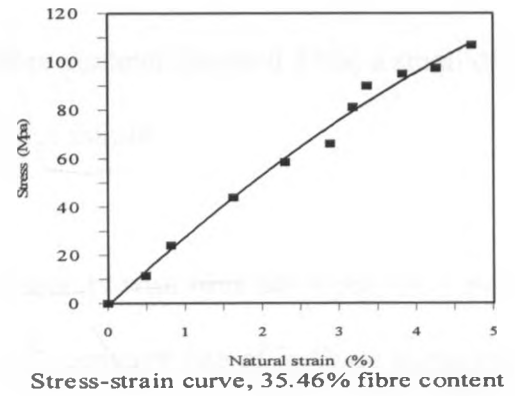
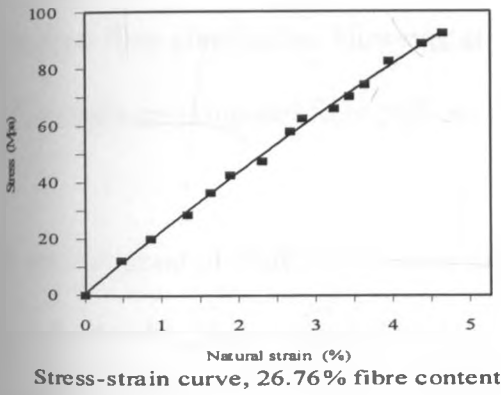
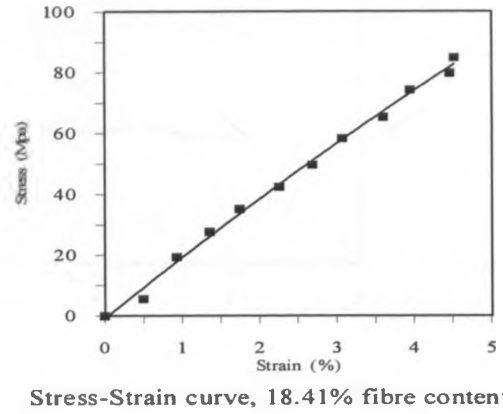
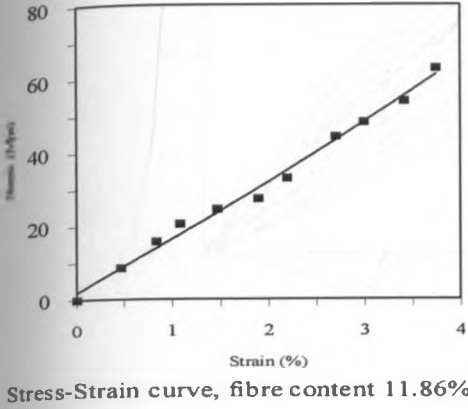
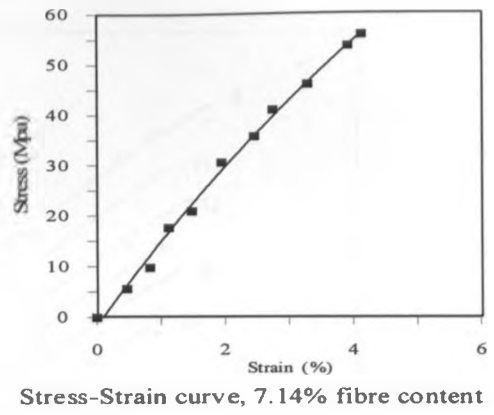
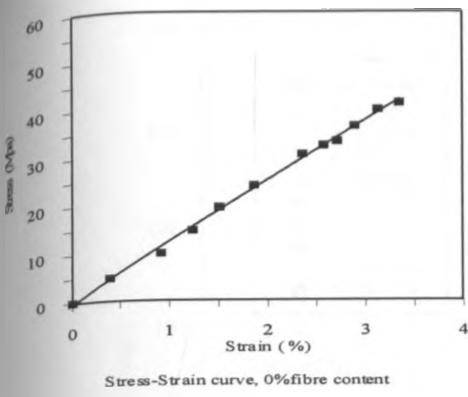


Figure 4.30 Tensile stress-strain curves of sisal fibre reinforced epoxy resin

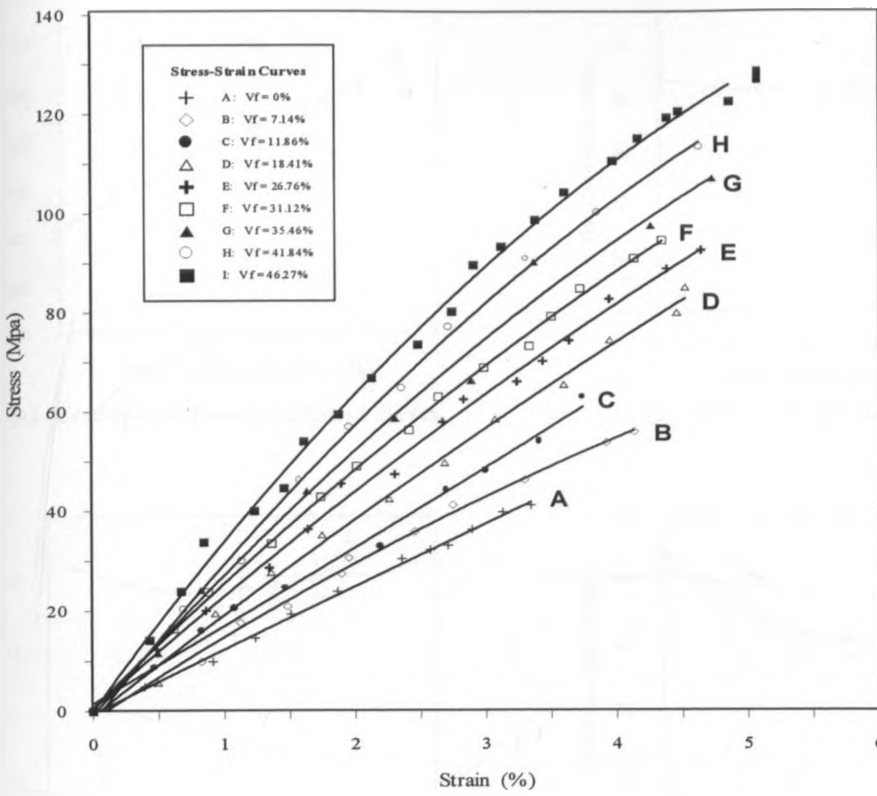
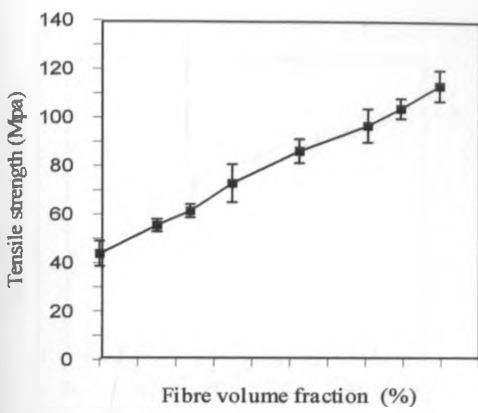


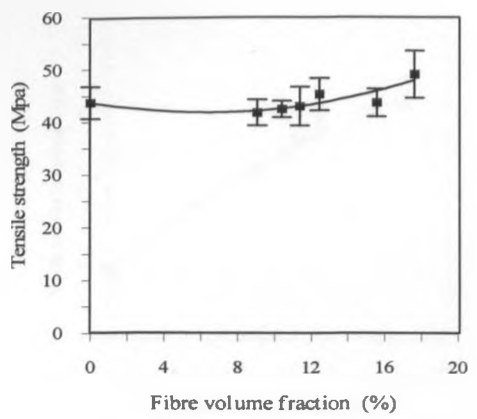
Figure 4.31 Combined tensile stress-strain curves of sisal fibre reinforced epoxy resin

chopped fibre composites. However at very high fibre contents (beyond 35%) a small degree of multiple cracking and fibre pull-out was observed at failure.

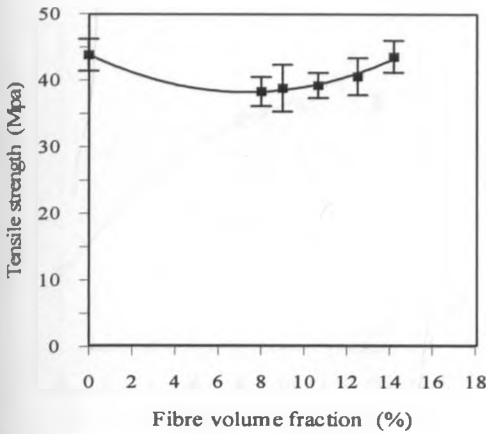
A general trend of increasing tensile Modulus of Elasticity with fibre additions was observed for all fibre lengths as shown in figure 4.33. A nearly constant rate of increase in the tensile modulus of elasticity with fibre volume fraction was realised in continuous parallel fibre reinforcement as shown in figure 4.33 (a). In chopped fibre reinforced composites, the composite stiffness increased rapidly with fibre content at low fibre volume fractions; however, at higher reinforcement levels this rate of increase reduced. The tensile modulus of elasticity of unreinforced test pieces was found to be 0.906 GN/m^2 with a standard deviation of 0.174 GN/m^2 . The maximum value of composite stiffness was obtained at about 44.83% V_f to be 2.427 GN/m^2 with a standard deviation of 0.124 GN/m^2 in parallel fibre reinforced specimens.



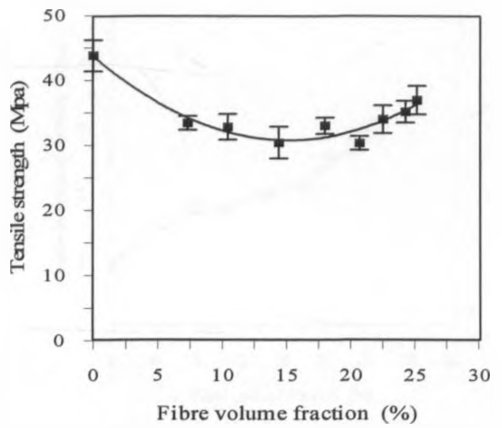
(a) Continuous parallel aligned fibres



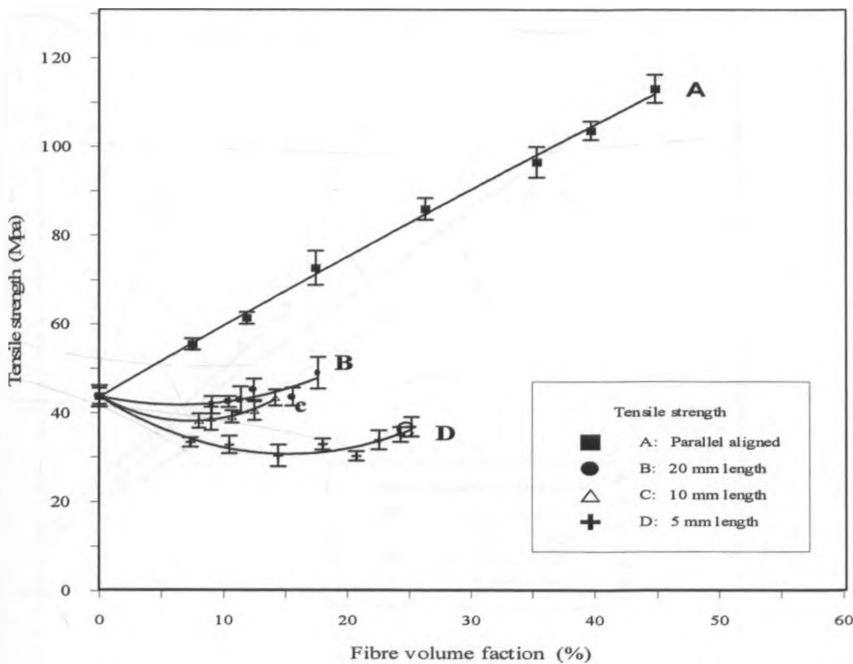
(b) 20 mm length chopped fibres



(c) 10 mm length chopped fibres



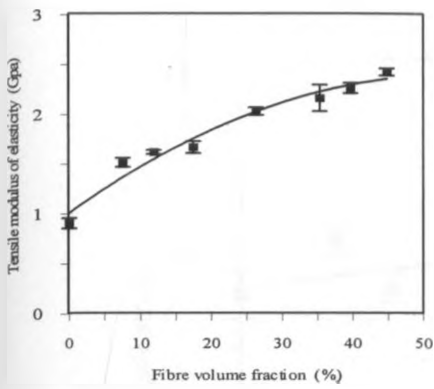
(d) 5 mm length chopped fibres



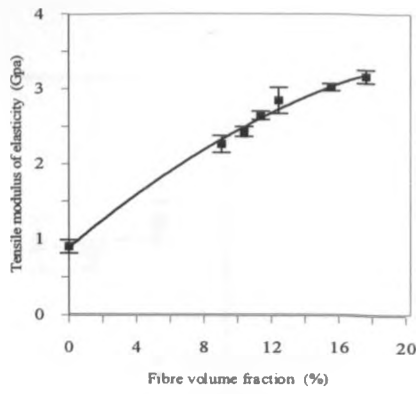
(e) Varying fibre lengths

Figure 4.32

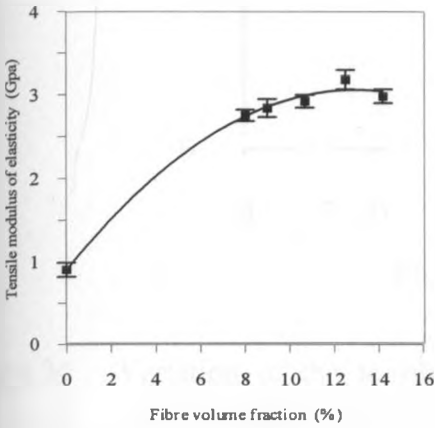
Variation of the tensile strength with fibre volume fractions for varying fibre lengths in sisal fibre reinforced epoxy resin composites



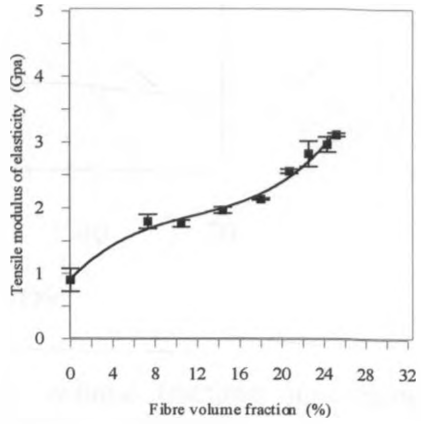
(a) Continuous parallel aligned fibres



(b) 20 mm length chopped fibres



(c) 10 mm length chopped fibres



(d) 5 mm length chopped fibres

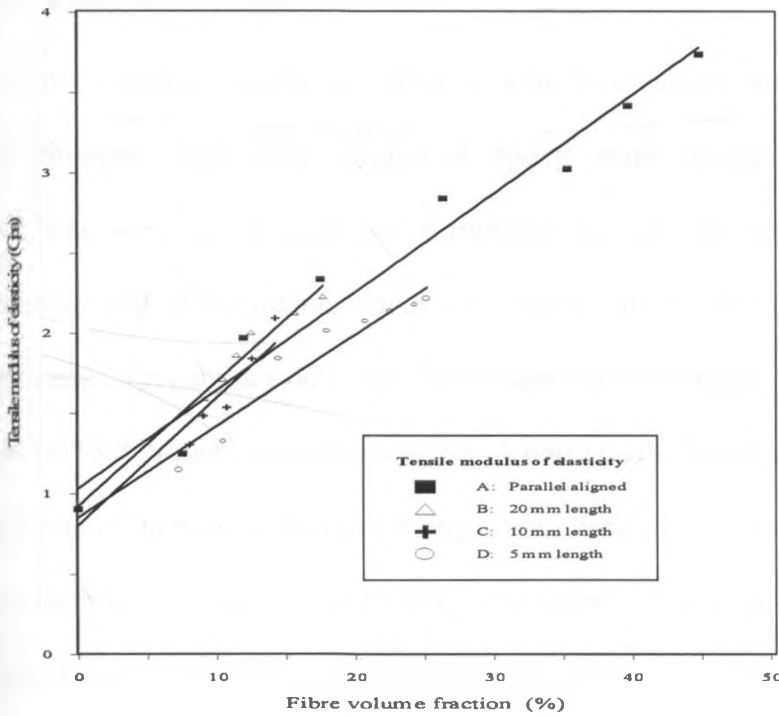


Figure 4.33

Variation of the tensile Modulus of Elasticity with fibre volume fractions in sisal fibre reinforced epoxy resin composites

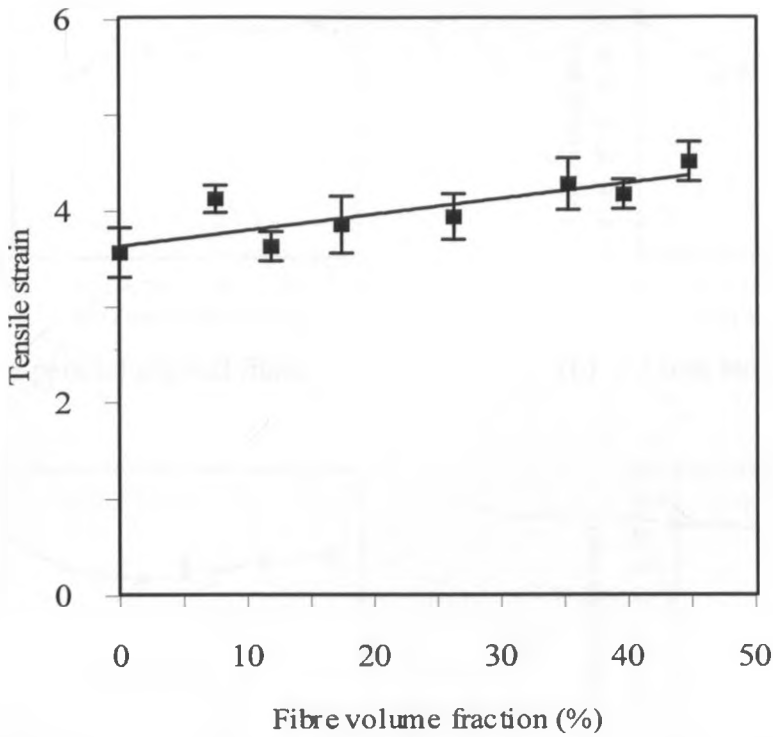
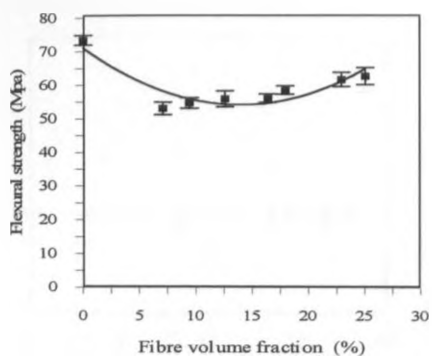
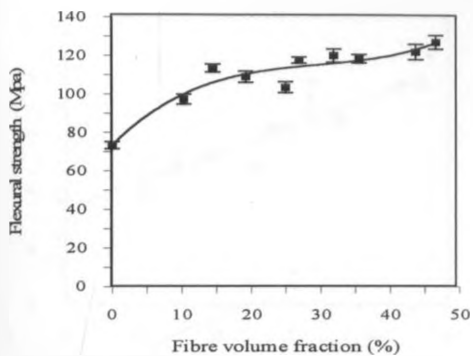


Figure 4.34 Variation of the tensile strain with fibre volume fractions in continuous parallel aligned sisal fibre reinforced epoxy resin composites

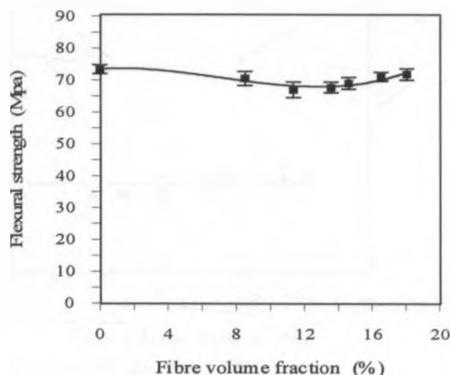
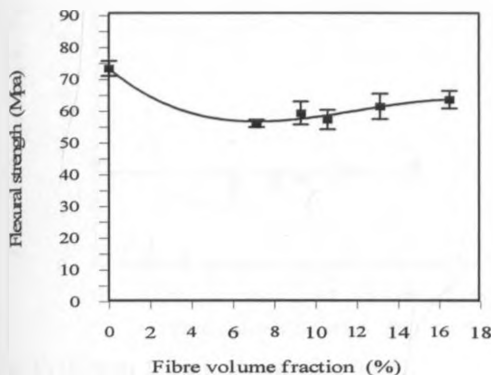
4.2.2 FLEXURAL STRENGTH

Figure 4.35 shows variations in flexural strength with fibre volume fractions in continuous parallel and chopped sisal fibre reinforced epoxy resin composites. Parallel fibre reinforcement was seen to increase the composite flexural strength. It was however interesting to note that discontinuous randomly aligned fibres did not give any flexural strength improvement in comparison to that of the unreinforced matrix. A minimum flexural strength value of 53.2 N/mm^2 was obtained with 5 mm length chopped fibre composites at 7.09% V_f . The rate of increase of flexural strength with fibre additions in continuous parallel aligned fibre reinforced composites was fairly rapid initially but decreased with successive fibre additions. As was seen in the case of tensile strength, an increase in flexural strength with increasing fibre aspect ratio was still evident.



(a) Continuous parallel aligned fibres

(b) 5 mm length chopped fibres



(c) 10 mm length fibres

(d) 20 mm length chopped fibres

(e)

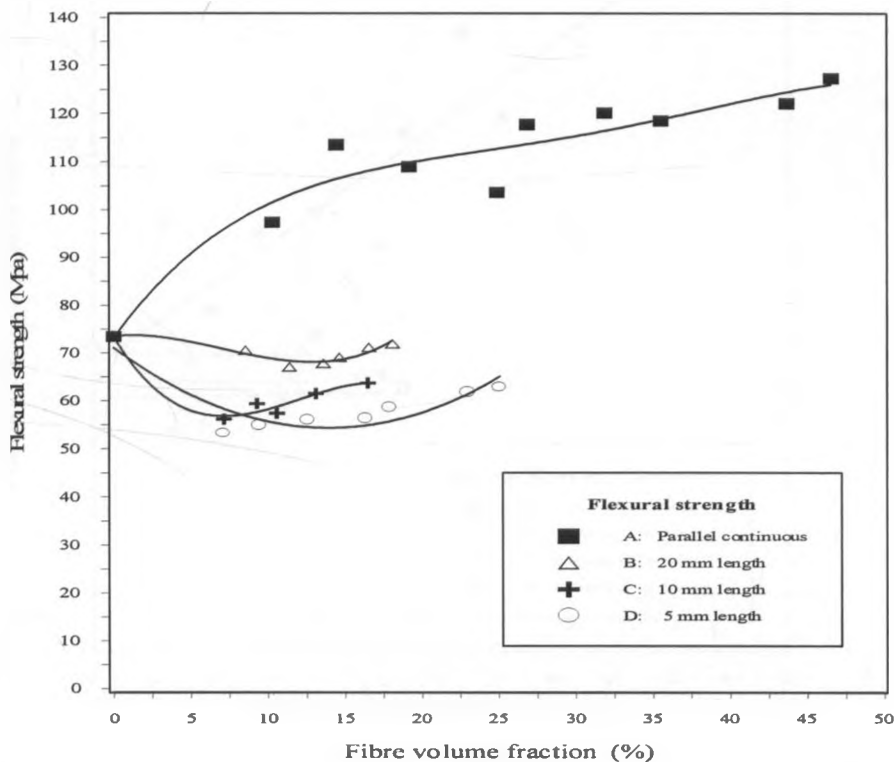
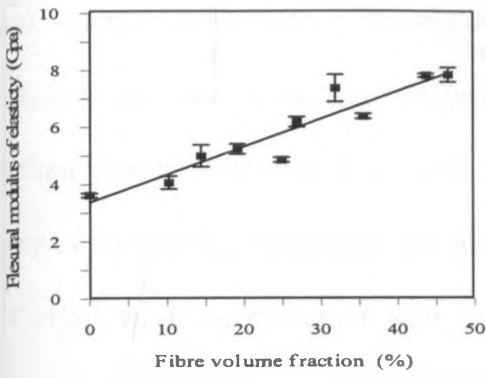
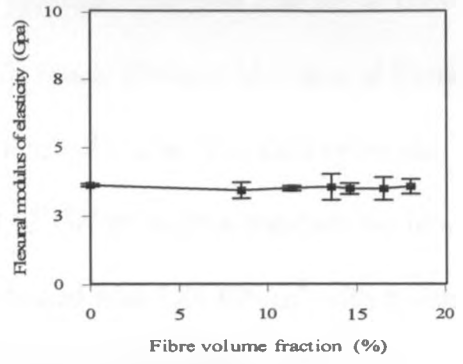


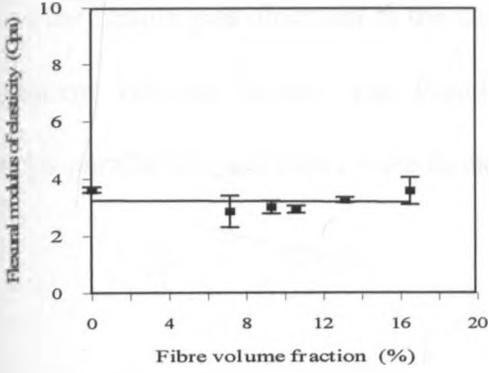
Figure 4.35 Variation of the flexural strength with fibre volume fractions at different fibre lengths in sisal fibre reinforced epoxy resin composites



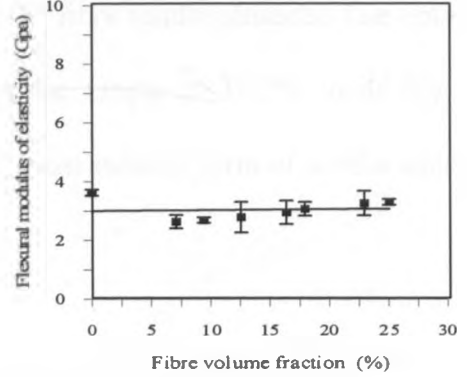
(a) Continuous parallel aligned fibres



(b) 20 mm length fibres



(c) 10 mm length chopped fibres



(d) 5 mm length chopped fibres

(e)

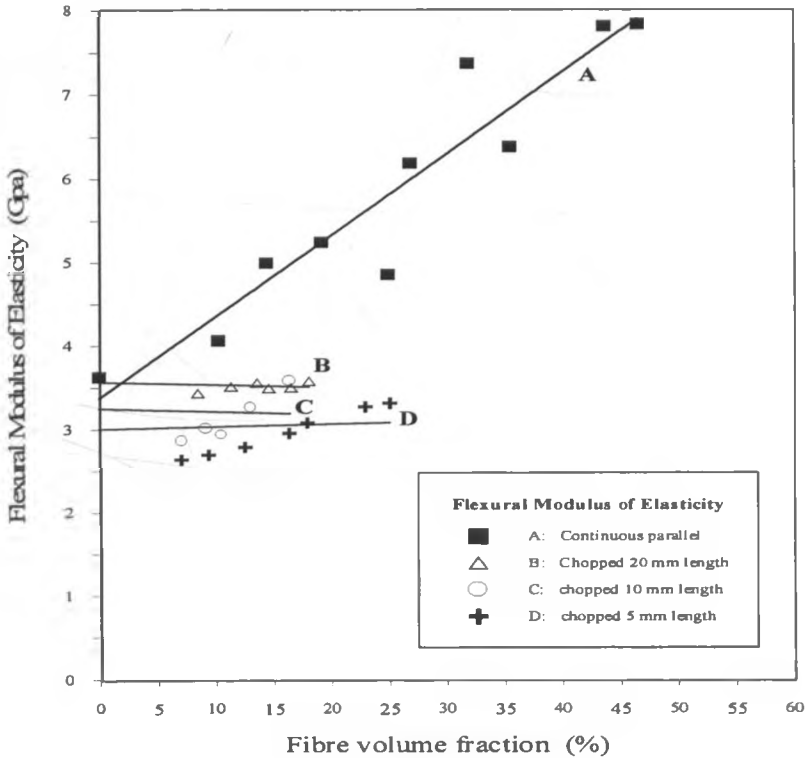


Figure 4.36

Variation of the flexural Modulus of Elasticity with fibre volume fraction at varying fibre lengths in sisal fibre reinforced epoxy resin composites

Flexural Modulus of Elasticity (FMOE) was seen to increase with fibre content as shown in figure 4.36. Long continuous fibre reinforcements gave higher flexural Modulus of Elasticity values than shorter ones at the same reinforcement volume fraction. The flexural modulus of elasticity of unreinforced specimen was obtained as 3.63 GN/m^2 with a standard deviation of 0.074 GN/m^2 , while the maximum value of FMOE obtained was 7.84 GN/m^2 with a standard deviation of 0.256 GN/m^2 at $46.87\% V_f$ in parallel fibre reinforced composites. A large scatter in the results was observed in the case of parallel fibre reinforcements. The optimum reinforcement volume fraction was found to lie in the range of 39.7% to 44.8% , and continuous parallel aligned fibres were found to be the most suitable form of reinforcement.

5. DISCUSSION

5.1 SISAL FIBRE REINFORCED RHAC MORTAR COMPOSITES

5.1.1 FLEXURAL STRENGTH

The addition of sisal fibres as a reinforcement in RHAC mortar resulted in the production of a material with tough and ductile behaviour. Such materials find application in the construction industry where they are used in the manufacture of roofing materials such as flat sheets, corrugated roofing sheets and tiles. They are also suitable in the commercial production of partitioning boards, low pressure water pipes, cladding and shells. In this class of materials the matrix is brittle and fails at a much lower strain than the fibres.

An increase in flexural strength with increasing fibre contents was observed. This agrees well with the predictions of the rule of mixtures stated in Cox [48] and Dieter [20]. The rule of mixtures predicts a linear increase in flexural strength with increasing fibre volume fraction. It also states that long, continuous parallel aligned fibres give higher strength values than those of chopped randomly aligned fibres at the same V_f due to length and orientation efficiency factors discussed in section 2.4.7 of this report. This can be clearly seen in figure 4.7.

When both continuous parallel and short discontinuous randomly aligned fibres were used as reinforcement, it was found that there was a limit beyond which fibre additions did not improve the strength of the composites. This occurred at 9.5% V_f in continuous parallel aligned fibre/cement composites. In the case of chopped fibre reinforcement, after a fibre content of 6% and 8.3% was exceeded in 20 mm and 30 mm length fibres respectively, no

further increase was observed. This apparent loss in strength beyond a certain V_f can be ascribed to a number of factors such as;

- (a) Poor compaction at high fibre volume fractions increases the number of voids in the composites especially as the mixture becomes more and more unworkable. This results in lowering the fibre/matrix bond strength and consequently the composite strength.
- (b) In the case of discontinuous randomly aligned fibres, balling-up and curling of fibres increased with both the fibre contents and fibre lengths. These two phenomenon could have resulted in the formation of more voids and eventually decreased the fibre/matrix bond strength.
- (c) Mutuli et al [63] and Aziz [51] reported that water absorption capacities of sisal fibre is very high, usually in the range of 60-70% by weight. This affects the W/C ratio, which is a fundamental parameter in the strength of cement mortar and concrete. Thus at high fibre volume fractions some water is absorbed by the fibres, reducing the W\C ratio and eventually lowering the composite strengths. It is therefore difficult to determine the correct W/C ratios to be used at high fibre volume fractions.

The increase in strength with increasing V_f points out that fibre lengths used are greater than the critical fibre length ' l_c '. This is deduced from the work of Kelly [50] which explained that if the fibre length is the same or more than the critical fibre length, then complete stress transfer between the fibre and matrix takes place. However for fibres shorter than the critical fibre length, failure is by pull-out and the full potential of fibres as a reinforcement is not realised.

The scatter obtained in flexural strength results could have resulted from a lack of precise control in alignment and dispersal of fibres. In the composite fabrications it was not easy to

obtain a homogenous mixture. The composite properties are altered by the absorption of water, and for this reason a large scatter was observed in the results.

The average values of flexural strength obtained in the present work agrees well with the results of Mutuli [1], Kirima [3], Mutua [64] and Kirima [65] where the strength properties of sisal fibre reinforced cement composites were investigated. In all these cases a reduction in flexural strength becomes apparent with fibre additions beyond a reinforcement volume fraction of approximately 8%.

The initial decrease in flexural strength upon adding a little quantity of short chopped fibres to the RHAC mortar, before any appreciable increase is recorded, can be explained from the concept of critical fibre volume fraction that was put down by Argon and Shack [29]. This concept has also been discussed in section 2.4.9 of this report, where it was pointed out that in order to obtain any benefit from the reinforcing fibres, the critical fibre volume fraction given in equation 2.49 must be exceeded. It is only after this condition has been met that fibre strengthening of the composite can occur. Majumdar [5] established the critical fibre volume fractions of some common fibre/cement composites as shown in table 5.1 below. The critical V_f in most fibre/cement composites were found to be in the range of 0.1 to 1%, with the critical V_f of sisal fibre reinforced OPC being 0.6%. This compares well with the present experimental values, where effective increase in strength was only realised after 1% V_f .

However for continuous parallel aligned fibres, no initial decrease in strength at very low fibre volume fractions was observed. This suggests a stronger fibre/matrix bond strength due

Fibre	Critical V_f (%)
Glass	0.1-0.2
Graphite	0.2-0.3
Chrysotile asbestos	-
Sisal	0.6
Steel	0.2-0.5
Polypropylene	1.0
Polycrystalline alumina	0.8
Kevlar-49	0.2

Table 5.1 Critical fibre volume fraction of some common fibres in cement matrices {after Majumdar [5]}

to greater length of embedment. It was noted that in continuous sisal/RHAC composites, failure was by debonding and fibre pull-out at higher reinforcement volume fractions. This implies that the reinforcing fibres were sufficiently strong and exceeded the critical fibre volume fraction suggested by Aveston et al [52].

It was observed that at the same fibre volume fraction, continuous parallel fibre composites produced higher flexural strengths than discontinuous randomly aligned fibre specimens. This can be attributed to the fact that, longer fibres with higher aspect ratios have a higher value of length efficiency factor as discussed in section 2.4.7 and also predicted by equation 2.34 of the rule of mixtures. The effects of orientation efficiency factors introduced by Krenchel [54] could also have contributed to the lower strengths recorded for chopped randomly oriented fibre composites as given in equation 2.37 of the rule of mixtures.

The present results also agrees well with the predictions of Swift and Smith [37] which pointed out that substantial increase in flexural strengths of sisal fibre reinforced cement composites can only be achieved by suitable choices of fibre length, mix ratio and incorporation techniques. Such increases which had only been predicted theoretically by Swift and Smith [37] have now been confirmed experimentally in the present work.

The fibres bridging the micro-cracks in sisal fibre reinforced RHAC composites inhibit their development. Consequently this lowers the modulus of the tensile zone whilst at the same time increasing the matrix failure strain. The overall result is that low modulus fibres end up increasing the first crack strength of the composites as explained in Swift and Smith [49].

The crack patterns at the flexural failure of fibre reinforced RHAC composites are shown in figure 4.4. One crack traverses the neutral axis in unreinforced and chopped sisal/RHAC composite beams. On the other hand a shear type of failure was seen dominating in parallel fibre reinforced beams. The alignment of fibres in one direction might contribute to this mode of failure coupled with the possibility of the existence of voids between fibre layers in densely packed composites which introduces points of weakness, eventually giving rise to the shear mode of failure along the fibre direction. It was evident that shear strength was not improved by fibre reinforcement as shear failure occurred more easily in composites than in unreinforced beams, probably because shear failure originates at the fibre/cement interface.

Hull [6] explained that two modes of failure are possible in a typical bend test of fibre reinforced composites. When a specimen is loaded in bending a normal tensile (flexural) stress and shear stress exists across the cross-section. A maximum value of the normal stress exists in the middle of the cross-section. In the case of four point bending, the maximum normal stress is given by

$$\sigma_{\max} = \frac{PL}{bd^2} \quad (5.1)$$

and the maximum shear stress

$$\tau_{\max} = \frac{3P}{4bd} \quad (5.2)$$

A comparison of strength results of glass fibre reinforced cements by Majumdar [5] and sisal fibre reinforced RHAC composites obtained in the present work showed a good correlation. Higher values are however obtained for glass fibre reinforced cement because of its associated high fibre strengths. A maximum flexural strength value of 50 N/mm^2 was obtained for glass fibre reinforced cement, while sisal/RHAC composites indicate a maximum value of 9.853 N/mm^2 . A sudden failure at 1.946 N/mm^2 was recorded in the flexural strength test of unreinforced RHAC mortar beams. But the continuous parallel fibre reinforced beams indicated a gradual failure mode reaching the ultimate load with the cracked beam still carrying a certain amount of load. This gives the most important advantage of long continuous parallel fibre reinforced composites, i.e that the composite continues to sustain loads even after the first crack has appeared.

Numerous cracks occur in the specimen during flexure test. The cracks are comparatively small with exception of the failure crack. The deformation at failure is considerable, and this marked deformation is desirable since it provides a visible warning that the material will fail. In general the bending strengths of sisal fibre reinforced RHAC mortar composites were found to be greater than their ultimate tensile strengths. This was explained by Aveston [52], in that the progressive movement of the neutral axis towards the face in compression during flexural tests results in an increase in the bending moment.

5.1.2 TENSILE STRENGTH AND MODULUS OF ELASTICITY

It was observed that continuous parallel aligned fibre/cement composites had approximately 1.3 times higher tensile strength than the chopped randomly aligned fibre composites at the same fibre volume fraction. This can be attributed to a higher adhesion to the cement mortar, due to the larger surface area in the case of longer continuous fibres when compared to the

short chopped ones. The increase in tensile strengths with increasing fibre lengths takes place because, greater fibre lengths have a higher fibre/matrix bond strength due to increased confinement. This observation could also have resulted from the effects of efficiency factors discussed in section 2.4.7.

The reduction in strength at higher reinforcement volume fractions may be attributed to the increased porosity resulting from insufficient compaction due to poor workability at high fibre contents. This increased the number of voids and consequently improper impregnation of fibres into the matrix. The overall effect is to make the composite which is already weak in tension, even weaker when direct tensile load is applied on it.

The general observation for unreinforced RHAC mortar is that tensile stress increases on loading until the first crack stress is reached. Beyond the cracking stress, the matrix cracks and can no longer carry any stress. However in the case of continuous parallel aligned sisal fibre reinforced mortar specimens, the composite continued to carry extra loads even after the matrix had cracked. This shows that the composite has a post-cracking ductility behaviour accompanied by multiple matrix cracking.

The composite tensile strength increased with fibre additions as predicted by the rule of mixtures [48] given in equation 2.4 and discussed in section 2.4.1.2 of this report. It is interesting to note that unlike flexural strength, only a slight increase in the composite tensile strength was recorded with fibre additions. The fibre balling-up phenomenon at fibre volume fractions exceeding 6% enhances the incidence of porosity, which explains why the rate of strength increase is seen to decrease at reinforcement volume fractions above 6%.

The composite failure was by several cracks running perpendicular to the direction of loading followed by fibre fracture at higher fibre volume fractions in continuous fibre composites. This means that the fibre lengths used were greater than the critical fibre length as explained in Hale [14]. The occurrence of multiple fracture points out that the critical fibre volume fraction had also been exceeded by the fibre contents incorporated into the matrix [20,29]. The critical fibre length is defined as twice the length of fibre embedment which would cause failure in a pull-out test [66]. The critical length of sisal fibres in a cement matrix was obtained by Sobrinho [66] as being between 4 and 5 cm.

It can therefore be seen that the use of sisal fibres as a reinforcement provides increased safety due to the post cracking ductile behaviour, enhancing a slow rupture without separation of the damaged parts. However as was observed by Ramirez [24] this too is subject to the effective fibre/matrix bond strength. The large scatter observed in the results can be attributed to some of the problems encountered in the fabrication process employed. It was not easy to eliminate the voids completely even after vibrating the specimens, especially at high fibre contents. A lot of imperfections such as non-uniformity in fibre distributions were also inevitable; this is because evenness of fibre distribution was judged just by looking with the naked eyes.

Cement paste, mortar or concrete contains micro-pores. Nair [13] has noted that the failure of cement mortar is by slow growth and merging of such micro-pores to form macro-scale cracks which then catastrophically propagate through the section. The total effect of all voids, inclusions and micro-cracks is to make the stress-strain relation non-linear. They also act as stress concentrations thus lowering the tensile strength. It was also seen in the present results that the unreinforced RHAC specimens had neither a stable stress-strain curve nor a

well defined tensile strength. It is thus suggested that such unreinforced beams should not be used to bear tensile, bending or even cyclic loads. On the other hand sisal fibre has a well defined tensile strength, modulus of elasticity and its stress-strain curve is linear up to failure [1]. Therefore the inclusion of sisal fibres into the brittle RHAC mortar matrix greatly improves the mechanical properties of the resulting composites. From the present work the important factors affecting the tensile strengths of sisal fibre reinforced RHAC mortar composites have been found to include reinforcement volume fractions, fibre dimensions, incorporation technique and fibre/matrix interfacial bond strength.

Three distinct stages can be seen in the stress-strain curves shown in figure 4.10. In the first stage a linear increase in stress with strain was observed. The onset of cracking accompanied by decreasing stress with increasing strains marks the second region. In the third stage stress stabilises at an almost constant value until composite fracture. A steep slope is seen in stage one, while the slope of the curve in the second stage was found to be gentle indicating a slowly progressing cracking phenomenon as evidenced by the non-linear portion of the curve. This implies a gradual load transfer from the matrix to the fibres.

The stress-strain curves of figures 4.10 and 4.17 shows a marked increase in peak tensile stress and strain with fibre additions. The improvements in peak strains can be attributed to the presence of fibres running across and limiting the micro-cracks thus delaying their propagation in the direction of the principal strain as explained by Jorillo and Shimizu [67]. In general larger strains were recorded at higher reinforcement volume fractions compared to low V_f composites as shown in figure 4.10. This shows the effectiveness of fibres in sharing the tensile load with the main beam. The composite characteristic of increased strains at higher fibre volume fractions shows a higher toughness and ability to undergo more

deformations. All the stress-strain curves of continuous parallel aligned sisal fibre reinforced RHAC mortar composites exhibited a yielding plateau marking a resistance to tensile failure. Greater yielding plateaus were noted at higher fibre volume fractions.

Only minor increases were seen in the composite stiffness with fibre additions in continuous parallel aligned fibre composites. However this is not a serious limitation since the matrix phase is reasonably stiff on its own. Continuous parallel aligned sisal fibre reinforced RHAC composites gave a modulus of elasticity of the order of 43.42 N/mm².

The amount of chopped sisal fibres that can be successfully incorporated into the RHAC mortar matrix is limited by such factors as fibre aspect ratio. Continuous parallel aligned sisal fibre reinforced RHAC mortar composites therefore offer the most effective exploitation of fibre properties. However due to anisotropy such composites are not suited to many applications. Equations 4.8 and 4.9 give the regression correlation between the composite tensile strength and its fibre content in chopped fibre reinforced RHAC composites. These equations agree well with the rule of mixtures, which predicts an increase in composite strength with fibre additions. Equations 4.8 and 4.9 also compare well with the tensile strength law proposed by Fukushima et al [68], which also indicates an improvement in the tensile strength of chopped fibre reinforced cement composites with increased reinforcement volume fractions as given in equation 5.3. It also shows that the composite strength is strongly dependent on the fibre strength.

$$\sigma_t = \alpha \frac{l}{d} V_f \sigma_{fu} \quad (5.3)$$

Where σ_t = tensile strength of chopped fibre reinforced cement composite

α = fibre effective co-efficient

l/d = fibre aspect ratio

σ_{fu} = fibre fracture strength

The experimental stress-strain curves of discontinuous randomly aligned sisal fibre reinforced RHAC composites are given in figure 4.17. The figure shows that both the stress and strain at LOP increases with fibre content. The failure strain of the unreinforced RHAC mortar specimens could not be determined very accurately due to a large scatter in the results. However an average value of 0.073% with a standard deviation of 0.014%, was obtained for a sample size of 6 specimens. Fibre incorporation increases the cracking strain of the unreinforced mortar. The decrease in the Modulus of Elasticity with increasing fibre content and fibre reinforcing index in chopped randomly aligned fibres can be attributed to efficiency factors in the rule of mixtures. Referring to the rule of mixtures in section 2.4.1.2 the composite Modulus of Elasticity is almost entirely dependent on the matrix modulus only, hence fibre additions do not have any appreciable effect.

5.1.3 INTERFACIAL BOND STRENGTH

In order to design a fibre reinforced cement composite with large energy absorption ability, a knowledge of fibre properties and fibre/matrix interfacial bond strength is required. This is because, as has been established by Dyczek and Petri [19], MOR increases proportionately with both the fibre/matrix interfacial bond strength and length of fibres used.

An attempt was made to estimate the value of the interfacial bond strength using the method developed by Aveston et al [52] described in section 2.4.6 and given in equation 2.33. In this approach the bond strength is determined by measuring the inter-crack spacings. The bond strengths were determined for both continuous parallel aligned and discontinuous randomly aligned sisal fibre reinforced RHAC mortar composites.

The strength of the matrix, which is a function of its microstructure and mineral composition, is used in the formula proposed by Aveston et al [52] and therefore affects the fibre/matrix interfacial bond strength. The average value of the interfacial bond strength in continuous parallel aligned fibre composites was found to be 0.139 N/mm^2 while that of chopped randomly aligned sisal fibre reinforced RHAC specimens was obtained as 0.121 N/mm^2 . In general the fibre/matrix bond strength was seen to vary inversely with increasing reinforcement volume fraction. This can be attributed to lack of proper embedment of fibres in the matrix at higher fibre volume fractions because of the increased number of voids in the matrix. Commulative errors could also have resulted from the calculations when equation 2.33 was used due to irregular cross-sectional area of sisal fibres.

Continuous parallel aligned sisal fibre reinforced RHAC mortar composites had higher bond strengths than the chopped randomly aligned fibre/cement composites, probably due to larger surface area of embedment in the matrix. Equation 2.53 in section 2.4.9 gives the expression for critical fibre volume fraction. On substituting the value of the interfacial bond strength obtained in the present work ($\tau_b = 0.121 \text{ N/mm}^2$) to equation 2.53, the critical fibre volume fraction was obtained as 0.2%. This observation compares well with the results in figures 4.15 and 4.16, where increases in tensile strengths were only realised beyond a reinforcement volume fraction of 1%.

The present results compares well with the findings of Ong and Paramasivam [69]. In both cases it has been found that cracks appear much earlier in low fibre volume fraction beams and that the number of cracks per unit length increases with fibre content. The other similarity between the present results and [69] is that the average crack spacing length in the

composites decreases with increased fibre volume fractions. The interfacial bond strength values of other fibre/cement composites are shown in table 5.2 after Majumdar [5].

Fibre	Matrix	Bond strength (N/mm ²)
Asbestos	Cement paste	0.88-3.0
Alkali resistant glass rods	Cement paste	>10
“Cem fil” glass fibre	Cement paste	2-3
Steel wires	Cement paste	6.8-8.3
Polypropylene	Cement paste	0.7-1.2

Table 5.2 Interfacial bond strength values of common fibre/cement composites {after Majumdar [5]}.

The present results however do not compare well with those of Bessel and Mutuli [38] where the interfacial bond strength of sisal fibres reinforcing a cement paste matrix was found to be 0.6 N/mm². Comparatively lower bond strength values were obtained in the present work. This difference might have resulted from the presence of particles in the RHAC mortar inhibiting effective fibre/matrix bonding. In the work of Bessel and Mutuli [38] fine ordinary portland cement paste as opposed to coarse RHAC mortar of the present work was used. The poor workability and compaction at high fibre volume fractions resulting in an increased number of voids and improper impregnation of fibres in the matrix also lowers the fibre/matrix bond strength. The large scatter observed in the results can be attributed to;

- (i) Large variations in fibre cross-sectional area. Despite attempts to select fibres at random, there is a general trend of fibres from the butt end having larger cross-sectional areas than those from the tip [1]. For a given fibre volume fraction this results in a varied interface surface area.

- (ii) Variations in cross-sectional shape. A round cross-sectional shape and a mean fibre diameter were assumed in the calculations. Yet fibres used in the experiments had quite irregular cross-sectional shapes. The variations in cross-sectional shapes and texture also affect the degree of bonding so that rugged surfaces produce stronger bonds.
- (iii) The high water absorptivity of sisal fibres results in voids along the interfacial surface thus weakening the bond strength.
- (iv) The theory of Aveston et al [52] was derived for circular fibres properly embedded in the matrix. This may not be entirely true for sisal fibre reinforced RHAC mortar specimens.

5.1.4 FLEXURAL TOUGHNESS

The first crack toughness in flexure was determined on the basis of ASTM C1018 [74]. Toughness indexes were calculated from the ratios of the areas under the load–deflection curves as described in section 2.4.10. The toughness index I_5 has a maximum value of 1 for an elastic brittle material and a maximum value of 10 for an elastic perfectly plastic material. Fibres bridging across the cracks prevented sudden failure. The area under the load–deflection curves increased due to the presence of fibres, this can be attributed to the energy absorbing mechanisms of fibre pull-out and debonding. The observed toughness gives assurance of safety and integrity of the structural element prior to failure.

Flexural toughness was found to increase with fibre additions. This agrees well with the results of Lin [31], where an increase in toughness with fibre content was obtained in steel fibre reinforced OPC composites. The variation in values between the two results can however be attributed to different curing and testing methods adopted, and to other factors listed on page 121.

The increased area under the load-deflection curve with fibre contents shows an improvement in flexural toughness. This also evidences the presence of post-cracking ductility. The increased area under the load-deflection curve results as energy is progressively absorbed by the composite to crack the matrix and also due to the energy required to debond the fibres when the first crack appears.

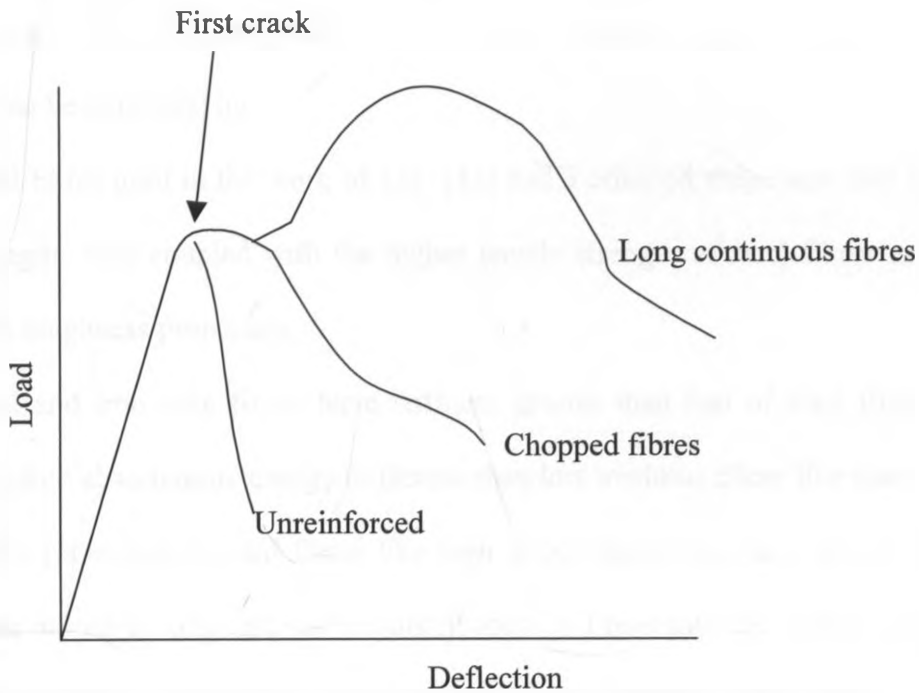


Figure 5.1 Load-deflection behaviour of unreinforced and fibre reinforced cement mortar with chopped and continuous long fibres {after Gram [27]}.

The shape of the flexural load-deflection curves obtained in the present work is similar to that postulated by Gram [27] characterising the behaviour of natural fibre reinforced OPC mortar as shown in figure 5.1. The area under the load-deflection curve for chopped fibre reinforced composites is larger than that of the unreinforced beams signifying an increase in flexural toughness with fibre additions. In the work of Swift and Smith [37] a simplified model which neglected micro-cracking predicted no increase in first crack strength with fibre additions. However the experimental results of the present work showed an increase in first

crack strength with fibre additions. This suggests that fibres inhibit the development of micro-cracks thereby increasing the matrix tensile strain at failure as was suggested in [37].

The experimental results of sisal fibre reinforced RHAC specimens obtained in the present work shows lower toughness and toughness indexes as compared to those of high modulus fibres e.g. steel, iron wire and glass fibre reinforced cements that were investigated by Lin [31]. This can be attributed to;

- (i) Steel fibres used in the work of Lin [31] had a crimped shape and thus higher bond strength. This coupled with the higher tensile strength of steel fibres may result in high toughness properties.
- (ii) Steel and iron wire fibres have stiffness greater than that of sisal fibre. They can therefore absorb more energy in flexure than low modulus fibres like sisal.
- (iii) Some properties of sisal fibres like high water absorption, easy to coil itself into a mass during mixing and uneven distribution of fibres into the mortar could result in lower toughness values compared to other fibres like steel, iron or glass.

Flexural toughness was seen to decrease with increasing the W/C ratio of the composite beams. This is probably because increasing the W/C ratio lowers the fibre/matrix interfacial bond strength and consequently decreases the composite toughness.

The tensile test measurements yielded standard deviations of 18.4% on average of the respective mean for the composites of the same fibre volume fractions, as those tested in flexure to obtain toughness indices. Since in flexure, half of the specimen is in tension and half in compression, it can be assumed that flexure test results will yield less scatter in data than the tensile tests. Thus the toughness index values displayed in tables 4.3 and 4.4, though

measured for a single specimen at each fibre volume fraction, can be reasonably expected to display less scatter than that in the tensile test data.

5.1.5 WORKABILITY

The loss in workability with increasing fibre lengths and volume fractions observed in the present work agrees with the predictions of Jorillo [67], which discussed the loss of workability in fresh concrete in the context of increasing fibre content and aspect ratio. This loss can be attributed to; (i) curling of fibres, (ii) proportions of constituents, (iii) inclusion of sisal fibres as a foreign material in the RHAC mortar results in particle interference between fibres and the coarse aggregates, (iv) and lastly the reduction in W/C ratio of the mortar because of fibres absorptive characteristics could also have resulted in poor workability occurring at high reinforcement levels.

5.1.6 DENSITY AND VOID VOLUME FRACTION

The density and void volume (porosity) in a material are inter-related because both depend on the number of voids in the material. Fibre content in the material was found to influence the composite unit weight. Unit weight varies at every V_f with the composite becoming lighter as fibre content increases. The composite density was therefore seen to decrease with fibre additions as shown in figure 4.28. This can be attributed to an increase in the number of voids due to poor workability at high reinforcement levels.

The present results agree well with the conclusions of Coutts [70] in which an increase in composite porosity with V_f was observed in air cured wood pulp fibre reinforced cement composites as shown in figure 5.2. In the work of Coutts [70] an increase in the number of

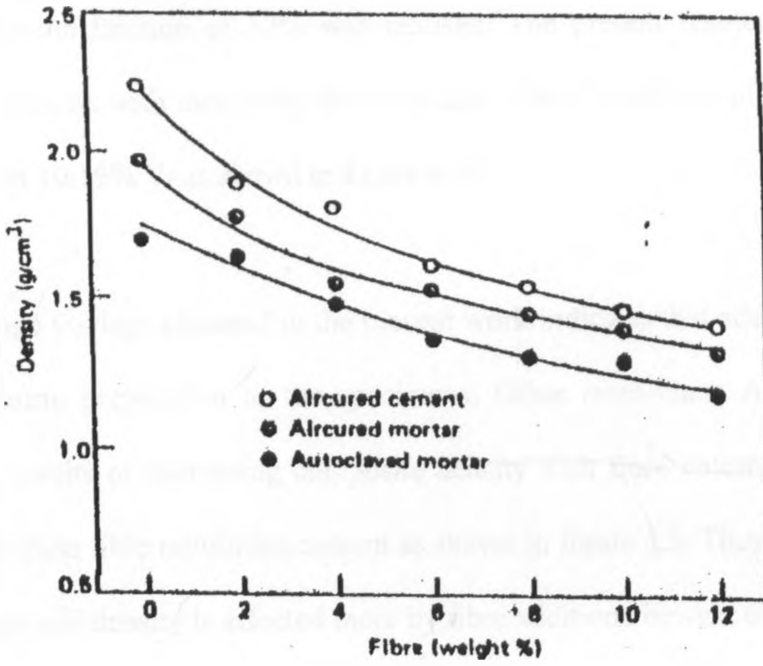


Figure 5.2 Variation of the density of wood pulp reinforced cement mortar with the reinforcement volume fraction {after Coutts [70]}

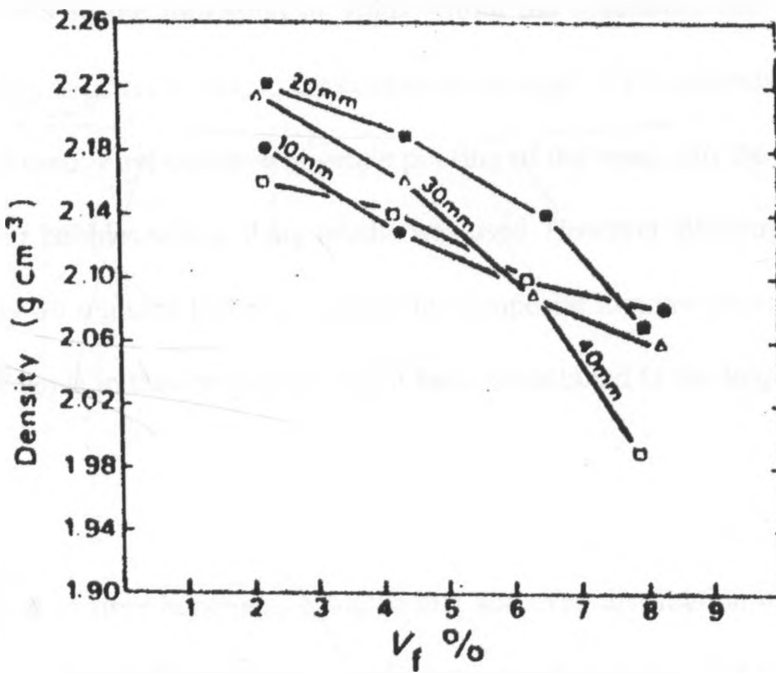


Figure 5.3 Variation of the density of glass fibre reinforced cement with fibre volume fractions at different fibre lengths {after Ali et al [71]}

voids from 24.4% in unreinforced cement mortar cured for 27 days in air, to 38% at a reinforcement volume fraction of 12% was realised. The present results also showed an increase in void volume with increasing fibre contents, from 12.48% in plain RHAC mortar to about 25.65% at 10.19% V_f as shown in figure 4.29.

The low percentage voidage obtained in the present work indicates that adequate compaction was achieved during preparation of the specimens. Other researchers Ali et al [71] also obtained similar results of decreasing composite density with fibre volume fraction in their investigations on glass fibre reinforced cement as shown in figure 5.3. They observed that the value of the composite density is affected more by fibre additions beyond 6% V_f .

5.2 SISAL FIBRE REINFORCED EPOXY RESIN COMPOSITES

The casting method employed in the fabrication of sisal fibre reinforced epoxy resin composites resulted in the formation of voids within the specimens due to entrapped air. These voids have a negative effect on the composite strength. Two methods of elimination of air bubbles were used. First continuous gentle pouring of the resin into the moulds, followed by pinching of air bubbles with a sharp needle was used. However allowing a breathing time of approximately 30 minutes before covering the composite mixture proved more effective. The presence of voids in the composites might have contributed to the large scatter observed in the results.

Complete removal of fibre bunching, straightening and even distribution of fibres within the matrix was not achieved. These factors could have resulted in the variations in composite properties, even for test pieces cut from the same specimen. A mean value was therefore

always computed for all the properties investigated. Since fibre bunching was not completely eliminated, they could have resulted in an increased void volume fraction and consequently lowering the composite strength. The present results however compare well with those of [1,2,72,73] in that, the composite strength and modulus of elasticity values were seen to increase with fibre additions in continuous parallel aligned fibre reinforced epoxy resin. Mutuli [1] obtained a maximum tensile strength of 148.2 N/mm^2 at $64.23\% V_f$. In the work of Maringa [2] a maximum tensile strength of 67.92 N/mm^2 at $29.9\% V_f$ was realised. The present results indicates a maximum tensile strength of 113.19 N/mm^2 at $44.27\% V_f$. The slight variations could have resulted from fibre bunching, uneven fibre distribution, presence of voids and the fact that different commercial forms of epoxy resin exist in the market.

Unreinforced and low fibre content composites exhibited a smooth composite fracture surface without protruding fibres. However at higher reinforcement levels, multiple matrix fracture followed by fibre pull-out mode of failure was observed. This resulted in an irregular fracture surface. It was also noted that the maximum fibre content incorporated into the matrix varied from one researcher to the next when the present results were compared to [1,2,72,73]. This as well can be attributed to different forms of commercial epoxy resin available in the market.

Variations of tensile strength, flexural strength and stiffness with fibre volume fractions are useful considerations in the design of low strength structural members, while the reinforcement volume fraction at which composite properties are a maximum are important in the design of liquid containers. It was observed that long continuous parallel aligned fibres produced higher strength values than chopped randomly aligned ones. The higher strengths obtained in high fibre aspect ratio composites could also be as a result of stronger

fibre/matrix bond strength due to large interfacial surface area for composite impregnation and embedment.

Chopped fibre reinforced composites however did not result in any strength improvements. This points out that fibres incorporated into the matrix probably had lengths less than the critical fibre length ' l_c ' [14,19] thus pull-out occurred and full potential of fibres not realised. Figure 4.31 shows that provided the fibre critical length has been exceeded, the longitudinal tensile stress will increase linearly with the V_f . Some experimental results in support of this conclusion are also given in [1] and [2]. From the present results it was seen that an optimum fibre volume fraction of about 45% with continuous parallel aligned fibre reinforcement is recommended for composite design.

The stress-strain curves of sisal fibre reinforced epoxy resin composites from the present work are similar to those obtained by Hull [6] for glass fibre reinforced epoxy resin. A small amount of non-linearity was noticed at higher strain values indicating that some plastic flow occurred. The strain at failure of the composite was much higher than that of the unreinforced matrix. The epoxy resin used had a failure strain of 3.35%, while the composite system had a maximum failure strain of 4.87% at 46.27% V_f in parallel aligned fibre reinforced test pieces. Failure is progressive but three stages can be identified in the stress-strain curves namely the initial linear portion up to the onset of debonding, a small middle portion with reduced slope signifying cracking and finally the last stage with a small amount of non-linearity up to failure.

Finally it can be noted that by incorporating sisal fibres into an epoxy resin matrix, a composite material is produced with strength and stiffness close to that of the fibres and

obviously having the chemical resistance property of the plastic matrix. The high flexural modulus of elasticity values obtained offers some resistance to crack propagation in any of the existing flaws and thus increasing the composite first crack strength. In addition it provides the composite with an ability to absorb energy during deformation. Thus it was seen that the primary variables affecting the composite strength in addition to matrix properties are fibre volume fraction, fibre length, fibre/matrix interface strength and fibre orientation. The fibres used in the present work were however not given a chemical treatment to improve the fibre/matrix bond strength as suggested by Bisanda [39]. This means that the experimental strength values obtained could be slightly less than those of treated fibre composite systems.

6. CONCLUSIONS

1. The flexural and tensile strength of RHA cement mortar matrix reinforced with sisal fibre was greater than that of the unreinforced matrix.
2. The flexural strength of continuous parallel aligned sisal fibre reinforced RHAC mortar composites depicted a linear increase with fibre additions.
3. The increases in flexural and tensile strength of discontinuous randomly aligned sisal fibre reinforced RHAC mortar composites was of a lesser magnitude in comparison to parallel aligned fibre reinforcement.
4. The strength of short discontinuous randomly aligned fibre composites increased with increasing fibre aspect ratios.
5. The flexural failure of continuous parallel aligned sisal fibre reinforced RHAC mortar composites was accompanied by multiple matrix fracture and fibre pull-out at high reinforcement levels, while a single crack mode of failure with fibre pull-out was realised in the case of chopped fibre reinforcement.
6. The failure of the unreinforced RHAC mortar was sudden with a brittle fracture, fibre reinforced composites on the other hand showed a gradual mode of failure with fractured specimens still capable of sustaining a certain amount of load.
7. Increasing the fibre content and aspect ratios in the RHAC mortar matrix reduced the workability of the mix.
8. Flexural and tensile strength properties of sisal fibre reinforced RHAC mortar composites were correlated with fibre volume fractions and presented in the form of equations.
9. The effectiveness of sisal fibres in controlling the occurrence of multiple matrix cracking phenomena depend on the reinforcement volume fraction.

10. The flexural toughness of sisal fibre reinforced RHAC composites increases with fibre content and curing age, but decreases with the W/C ratio. The toughness index also increases with increasing the fibre volume fractions and curing age, however the relationship between the toughness index and curing age is not clear.
11. Only the higher toughness index I_{10} is sensitive to the reinforcement volume fraction of the composite. Lower toughness index I_5 shows very little variations with the fibre volume fraction.
12. The short discontinuous randomly aligned sisal fibre reinforced RHAC composites tested in flexure failed by a single crack, with fibre pull-out accompanied by a drastic and sudden decrease in load. The continuous parallel aligned fibre reinforced specimens on the other hand failed by multiple cracks, with the failed specimen able to carry higher loads than at first crack. The resulting multiple cracks appeared parallel to each other and perpendicular to the direction of the applied load.
13. The inclusion of sisal fibres in RHAC mortar matrix increased the tensile and flexural strengths of the resulting composites with fibre additions until the maximum strengths were attained at an optimum fibre volume fraction of about 8%. Beyond this fibre content, composite strength decreased with further fibre additions.
14. Only minor increases were realised in the Modulus of Elasticity with increasing fibre volume fraction in parallel aligned sisal fibre reinforced RHAC mortar composites. This shows that the reinforcement volume fraction has no marked effect on stiffness of the composites.
15. The Modulus of Elasticity of short discontinuous randomly aligned sisal fibre reinforced RHAC mortar composites showed a linear decrease with increasing fibre contents.
16. Continuous parallel aligned fibres leads to the development of a stronger fibre/matrix interfacial bond strength, than in chopped randomly aligned sisal fibre reinforced

RHAC mortar composites. In both cases the interfacial bond strength decreases with the reinforcement volume fraction.

17. The density of fibre reinforced RHAC mortar composites is lowered by fibre additions.
18. Inclusion of fibres in the RHAC mortar matrix introduces voids in the composite. The volume fraction of the voids in the composite increases with increasing fibre contents.
19. The significant increase in flexural strength, tensile strength, flexural toughness and the observed post cracking ductility with fibre reinforcement in sisal fibre reinforced RHAC mortar composites are good material properties. It is therefore suggested that this material will be of a considerable potential in such areas as housing construction in developing countries. It can find effective use in roofing materials in the form of flat and corrugated roofing sheets and tiles. Other applications may include areas such as partitioning panels and wall claddings.
20. Both the tensile and flexural strength increased with the reinforcement volume fraction in continuous parallel aligned sisal fibre reinforced epoxy resin composites.
21. Sisal fibre reinforced epoxy resin composites gave higher flexural strength values than tensile strength at the same fibre content.
22. No effective reinforcement was realised in the case of discontinuous fibre reinforced epoxy resin composites.

7. RECOMMENDATIONS FOR FURTHER WORK

1. In the context of this research, durability is defined as the degree of retention of mechanical properties of the hardened cement composite over long periods and ages. Since building materials are expected to last for 50 years or more under severe environmental conditions, it is therefore important that information on the long-term properties of this fibre/cement composite be available, if they are to be widely used. It is therefore suggested that future researchers should conduct tests to establish the sustainability and durability of the sisal/RHAC composites over long periods of time. Emphasis should be laid on determining the long-term strength properties in relation to weather and bacterial decay. Furthermore since sisal/RHAC composite is a relatively new material in the in building industry, it is suggested that accelerated testing procedures should be developed to predict the composite mechanical properties over a long period of time without having to wait for long term field results.
2. The work of Majumdar [5] established that cement paste and mortar expands if allowed to set and harden in water. It was also found out that during drying they undergo shrinkage. The effects of fibre additions on shrinkage and moisture movements have not been examined thoroughly in most cases. This should therefore be investigated in the case of sisal fibre reinforced RHAC mortar composites by future researchers.
3. The fibre/matrix interfacial bond strength influences the strength properties of most fibre reinforced composites. Oakley and Proctor [16] described the nature of the interfacial bond between glass fibres and a cement matrix as being purely frictional. This argument can be extended to sisal/cement composites, even though sisal fibres on the other hand have a number of unusual characteristics such as irregular cross-sectional area and high water absorption characteristics [1]. The method applied in the assessment of the interfacial bond strength in the present work assumed existence of a frictional bond between sisal fibres and the RHAC mortar matrix. In order to develop a more specific method of measuring the bond strength, further work needs to be done to establish the nature and magnitude of the sisal/cement interfacial bond strength.

4. The effect of span to depth ratio on the modulus of rupture of sisal fibre reinforced RHAC mortar composites was not studied in the present work. It should therefore be pursued by future researchers with the objective of coming up with optimum dimensions for standard test pieces.
5. The strength of the bond between sisal fibres and the RHAC mortar matrix should be determined after curing for more than one year to ascertain the effect of curing age on bond strength. Further work should also be done to investigate the effects of varying W/C ratios and the sand to cement ratios on the interfacial bond strength of these composites.
6. No quantitative measurement of workability was made, since the resulting sisal/cement material at higher reinforcement volume fractions proved to be quite different from the conventional cement base materials. A need therefore exists to develop a method of measuring the workability of the resulting sisal/cement composite material.
7. The flexural and tensile strengths of continuous parallel aligned fibre reinforced composites were found to be higher than those of chopped randomly aligned fibre reinforced composites. This can probably be attributed to the length and orientation efficiency factors [54-56]. In practice however, short randomly oriented fibres finds extensive use in fibre/cement products due to the ease in mix and composite fabrication. There is therefore need for future researchers to try and come up with alternative methods of product fabrication that will ensure chopped fibres are uniaxially aligned in the matrix.
8. The resulting sisal/epoxy-resin composite has been found to have attractive properties in regard to the tensile and flexural strengths. Furthermore the water-proofing characteristics of the embedding matrix assures fibre protection from water. As a result the material promises potential application in areas requiring low strength-to-weight ratios and in the making of bodies of domestic appliances. However the current market price of epoxy resin is prohibitive and may create a big hindrance in most of these potential applications. Further research therefore needs to be done on the use of cheap filler materials in the composite. This should be done with the aim of reducing the price

of the resulting material, while also striking a balance on the acceptable strength properties.

9. There is need for future researchers to repeat the toughness index measurements for a statistically valid sample size at each fibre volume fraction.

8. REFERENCES

1. Mutuli, S. M., The properties of sisal fibres and sisal fibre reinforced composite materials, M.Sc. thesis, University of Nairobi (1979).
2. Maringa, M., The mechanical properties of sisal and loofah fibres and their composites resulting from the reinforcement of epoxy resin, M.Sc. thesis, University of Nairobi (1993).
3. Kirima, C. C. M., An investigation into the mechanical properties of composite materials reinforced with locally obtained natural fibres, M.Sc. thesis, University of Nairobi (1993).
4. Leslie, N. Philips (editor), Design with advanced composite materials, The Design Council – London (1989).
5. Majumdar, A. J., Properties of fibre cement composites, Rilem symposium on fibre reinforced cement and concrete (1975) PP 279-314.
6. Hull, D., An introduction to composite materials, Cambridge University Press (1990).
7. Holister, G. S. and Thomas, C., Fibre reinforced composite materials, Elsevier Publishing Co. Ltd (1966).
8. Hancox, N. I. (editor), Fibre composite hybrid materials, Applied Science Publishers Ltd London (1981).
9. Harald, G. Kloss, "Properties and testing of asbestos fibre cement", Rilem symposium on fibre reinforced cement and concrete, U.K (1975) PP 259-267.
10. Parameswaran, V. S. and Rajagopalan, K., "Strength of concrete beams with aligned or random steel fibre micro-reinforcement", Rilem symposium on fibre reinforced cement and concrete, U.K (1975) PP 95-103.
11. Luong, M. P. and Liu, H., "Tensile properties of steel fibre reinforced concrete", Proceedings of the fourth Rilem symposium on fibre reinforced cement and concrete, U.K (1992) PP 343-353.
12. Ahmed, H. I. and Pama, R. P., "Ultimate flexural strength of reinforced concrete beams with large volumes of short randomly oriented steel fibres", Proceedings of the fourth Rilem symposium on fibre reinforced cement and concrete, U.K (1992) PP 467-485.
13. Nair, N. G., "Mechanics of glass fibre reinforced cement", Rilem symposium on fibre reinforced cement and concrete, U.K (1975) PP 81-93.
14. Hale, D. K., "Fibre pull-out in multiply cracked discontinuous fibre composites", Rilem symposium on fibre reinforced cement and concrete, U.K (1975) PP 55-69.

15. Laws, V. and Ali, M. A., "The tensile stress-strain curve of a brittle matrix reinforced with glass fibre", *Fibre reinforced materials: Design and engineering applications* (1977) Paper 13, PP 115-124, Institution of civil engineers, London.
16. Oakley, D. R. and Proctor, B. A., "Tensile stress-strain behaviour of glass fibre reinforced cement composites", *Rilem symposium on fibre reinforced cement and concrete U.K* (1975) PP 347-358.
17. Hannant, D. J., Zonsveld, J. J. and Hughes, D. C., "Polypropylene film in cement based materials", 'Composites', Vol. 9 (April 1978) PP 83-88.
18. Zonsveld, J. J., "Properties and testing of concrete containing fibres other than steel", *Rilem symposium on fibre reinforced cement and concrete U.K* (1975) PP 217-226.
19. Dyczek, J. R. L. and Petri, M. A., "Polypropylene FRC: Fibre/matrix bond strength", *Proceedings of the fourth Rilem symposium on fibre reinforced cement and concrete, U.K* (1992) PP 324-342.
20. Dieter, G. E., *Mechanical Metallurgy*, McGraw-Hill Publishing Company (1986).
21. FAO Study group on hard fibres, *Kenya Sisal Board Bulletin*, November 1966.
22. Burgwin, W. A., *Progress with sisal in Kenya*, *Kenya Sisal Board bulletin* (May 1971) PP 15-20.
23. Jones-Rigby E., *Sisal production in East Africa*, *Kenya Sisal Board Bulletin* (February 1968) PP 15-18.
24. Ramirez-Coretti, A., "Physical-mechanical properties of fibre cement elements made of rice straw, sugar cane bagasse, banana racquis and coconut husk fibres; *Proceedings of the fourth Rilem symposium on fibre reinforced cement and concrete, U.K* (1992) PP 1203-1214.
25. Gram, Hans-Erik, "Durability of natural fibres in concrete", *Natural fibre reinforced cement and concrete, Concrete Technology and Design Vol. 5*, edited by Swamy, R. N., Published by Blackie and Son Ltd (1988) PP 157-160.
26. Lola, C. R., "Fibre reinforced roofing sheets", *Technology Appraisal Report -AT International, Washington DC, USA* (1985).
27. Gram, Hans-Erik, "Natural fibre concrete roofing", *Natural fibre reinforced cement and concrete, Concrete Technology and Design Vol. 5*, edited by Swamy R. N., Published by Blackie and Son Ltd (1988) PP 257-262.
28. Forsyth, P. J. E., *Composite Materials*, Publication for the Institution of Mechanical Engineers -London (1966).
29. Argon, A. S. and Shack, W. J., "Theories of fibre cement and fibre concrete", *Rilem symposium on fibre reinforced cement and concrete, U.K* (1975) PP 39-52.

30. Lankard, D. R., "Fibre concrete applications", Rilem symposium on fibre reinforced cement and concrete (1975) PP 3-17.
31. Lin, Wei-Ling, "Toughness behaviour of fibre reinforced concrete" Proceedings of the fourth Rilem symposium on fibre reinforced cement and concrete, U.K (1992) PP 299-315.
32. Lock G. W., *Sisal: Thirty years of sisal research in Tanzania*, 2nd edition, Longmans (1969).
33. Osborn, J. F., The prospects for and limitations of long fibre agave hybrids, Kenya Sisal Board Bulletin (November 1967) PP 16-21.
34. Wilson Paul, A study of the plant and its leaf fibre (F.A.O) of the United Nations, Hard fibres research series No. 8, April 1971.
35. Agopyan, V., "Vegetable fibre reinforced building materials –developments in Brazil and other Latin American countries", Natural fibre reinforced cement and concrete -Concrete Technology and Design Vol. 5, edited by Swamy, R. N., Published by Blackie and Son Ltd (1988) PP 208-240.
36. Rehsi, S. S., "Use of natural fibre concrete in India", Natural fibre reinforced cement and concrete -Concrete Technology and Design Vol. 5, edited by Swamy, R. N., Published by Blackie and Son Ltd (1988) PP 243-253.
37. Swift, D. G. and Smith, R. B. L., "The flexural strength of cement based composites using low modulus (sisal) fibres", 'Composites', July 1979, PP 145-148.
38. Bessel, T. J. and Mutuli, S. M., "The interfacial bond strength of sisal cement composites using a tensile test", Journal of Material Science Letters 1 (1982) PP 244-246.
39. Bisanda, E. T. N. (ENG), "The prospects of sisal fibre reinforced composite materials and their impact on the Tanzanian economy", The Tanzania Engineer Journal (September 1988) PP 36-42.
40. Hammond, A. A., "Research on rice husk ash binders for low cost housing technology", Housing Research and Development Unit, University of Nairobi, December 1990.
41. Smith, R. G., "Alternatives to ordinary portland cement", Overseas Building Note, UK Building Research Establishment – International Division, March 1993.
42. Waswa, B. S., "Rice husk ash production process", Housing and Building Research Institute, University of Nairobi, Paper presented at a seminar on 'The development of rice husk ash and burnt clay as a supplementary pozzolana in the Kenyan building industry – Nairobi, Kenya (July 1998).

43. Mbindyo, J. K. N., Kamau, G. N. and Tuts, R. J., "Recycling of rice husk wastes for use as a cement replacement material in Kenya", Paper presented at 'Environment and Development' Session of the World Conference of Philosophy at KICC – Nairobi Kenya, July 1991.
44. Tuts, R. J., "Potentialities and constraints for using Pozzolanas as alternative binders in Kenya", 1st International seminar on lime and other alternative cements, 9-11th December 1991, Nairobi Kenya.
45. Dulo, S. O., "Engineering properties of rice husk ash cement", Department of Civil Engineering, University of Nairobi, Paper presented at a seminar on 'The development of rice husk ash and burnt clay as a supplementary pozzolana in the Kenyan building industry –Nairobi, Kenya (July 1998).
46. Potter, W. G., Uses of epoxy resins, London Newness – Butter worth (1975).
47. Skeist, I., Epoxy Resins, Reinhold Publishing Corporation New York (1958).
48. Cox, H. L., Br. Journal of Applied Physics, Vol. 3, (1952) PP 72-79.
49. Swift, D. G. and Smith, R. B. L., "The physical significance of flexure test on fibre cement composites", Rilem symposium on testing and test methods of fibre cement composites, U. K (April 1979).
50. Kelly, A. and Zweben, C., Journal of Material Science, Vol. 11 (1976) PP 582.
51. Aziz, M. A., Paramasivan, P. and Lee, S. L., "Concrete reinforced with natural fibres, - New reinforced concrete" Concrete Technology and Design Vol. 2 (1984) PP 107-140.
52. Aveston, J., Cooper, G. A. and Kelly, A., "Single and multiple fracture", Proceedings of a conference on the properties of fibre composites -National physical laboratory (November 1971) Published by IPC Science and Technology Press Ltd, PP 15-26.
53. Broutman, J. L. and Krock, R. H., Composite Materials -Mechanics of composite materials, PP 47-48.
54. Krenchel, H., "Fibre spacing and specific fibre surface", Rilem Symposium on fibre reinforced cement and concrete, U.K (1975) Construction Press Ltd, Vol. 1 PP 69-79 and Vol. 2 PP 511-513.
55. Allen, H. G., Journal of Physics D: Applied Physics, Vol. 5 (1972) PP 331-343.
56. Laws, V., "The efficiency of fibrous reinforcement of brittle matrices", Journal of Physics, D. Applied Physics, Vol.4 (1971) PP 1737-1746.
57. Tsai, S. W., Fundamental aspects of fibre reinforced composites, Inter-Science Ltd New York (1968) PP 3-11.
58. Nielson, L. E., Mechanical properties of polymers and composites, Vol. 2 (1974).

59. Hannant, D. J., "Fibre cements and fibre concrete", John Wiley and Sons (1978) PP 8-31.
60. Bantia, N., Trottier, J. F., Wood, D. and Beaupre, D., "Steel fibre reinforced dry-mix shot crete; effect of fibre geometry on fibre rebound and mechanical properties", Proceedings of the fourth Rilem symposium on fibre reinforced cement and concrete, U.K (1992) PP 277-295.
61. Ambroise, J. and Pera, J., "Pressing of premixed GRC: Influence of fibre length on toughness", Proceedings of the fourth Rilem symposium on fibre reinforced cement and concrete, U.K (1992) PP 316-323.
62. Arnout, S., Parlovic, M. N. and Dogill, J. W., A new method for measurement of tensile properties of curved beam specimen materials and structures (1990) PP 23, 296-304.
63. Mutuli, S. M., Bessel, T. J. and Talitwala, E. S. J., "The properties of sisal as a reinforcing fibre in cement base materials", African Journal of Science and Technology (ANSTI) Vol. 1, No. 1. (April 1982) PP 5-16.
64. Mutua, J. M., "Mechanical properties of sisal fibre reinforced concrete" M.Sc. thesis (1993) University of Nairobi.
65. Kirima, C. C. M. and Mutuli, S. M., "The mechanical properties of sisal fibre reinforced mortar", Paper presented at the second symposium on Science and Technology in Harare, Zimbambwe (September 11-13, 1990).
66. Sobrinho, Pires de C. W., "Coconut and sisal fibre reinforced cement and gypsum matrices", Proceedings of the fourth Rilem symposium on fibre reinforced cement and concrete, U.K (1992) PP 1193-1202.
67. Jorillo, P. Jr. and Shimizu, G., "Coir fibre reinforced cement composites", Proceedings of the fourth Rilem symposium on fibre reinforced cement and concrete, U.K (1992) Part 1 - Microstructure and properties of fibre mortar PP 1080-1095, Part 2 -Fresh and mechanical properties of fibre concrete 1096-1109.
68. Fukushima, T., Shirayama, K., Hitotsuya, K. and Maruyama, T., "Mechanical characteristics of chopped fibre composites mainly using carbon fibre", Proceedings of the fourth Rilem symposium on fibre reinforced cement and concrete, U.K (1992) PP 965-979.
69. Ong, K. C. G. and Paramasivam, P., "Cracking of steel fibre reinforced mortar due to restrained shrinkage", Paper presented at the International Conference on recent developments in fibre reinforced cements and concrete, held at the University of Wales, College of Cardiff, U.K (September 18-20, 1989), edited by Swamy, R. N. and Barr, B., Published by Elsevier Science publishing Co. Ltd Inc., PP 179-187.
70. Coutts, R. S. P., "Air cured wood pulp fibre/cement mortars", 'Composites' Vol. 18, No.4 (September 1987) Butterworth and Co. Publishers Ltd.

71. Ali, M. A., Majumdar, A. J. and Singh, B., "Properties of glass fibre cement -the effect of fibre length and content", Building Research Establishment, CP 94/75 (October 1975).
72. Ng'ang'a, S. P. and Waweru, L. M. N., "Mechanical properties of sisal fibre reinforced epoxy resin", Final year undergraduate Project, B.Sc. Mechanical Engineering, University of Nairobi (1980).
73. Otieno, F. J. and Ogango, I., "Literature survey on loofah and its potential as a reinforcement material in plastics -epoxy resin", Final year undergraduate Project, B.Sc. Mechanical Engineering, University of Nairobi (1991).
74. ASTM C 1018; Standard test method for
Flexural toughness and first crack strength of fibre reinforced concrete (using beam with third point loading).
75. ASTM C 78; Standard test method for
Flexural strength of concrete (using simple beam with third point loading).
76. BS 1881: Part 109: 1983
Method for making test beams from fresh concrete.
77. ASTM C 496, Standard test method for;
Splitting tensile strength of cylindrical concrete specimens.
78. BS EN-12390: Part 5: 2000
Method for the determination of flexural strength of test beams.
79. ASTM C 220-75, Standard test method for;
Standard test method for determination of water absorption and void volume values in concrete.
80. BS 2782: Part 3: Method 320E: 1996
Plastics, mechanical properties, Tensile strength, elongation and elastic modulus.
81. BS 2782: Part 3: Method 335A: 1993
Plastics, mechanical properties, Determination of flexural properties.

APPENDIX

EXPERIMENTAL DATA

SISAL/RHAC SPECIMENS FLEXURAL STRENGTH RESULTS

Flexural strength results of continuous parallel aligned (100X100X500) mm Sisal/RHAC mortar composite

mmens

Mass of fibres added (g)	Fibre volume fraction Vf (%)	Mean fibre volume fraction (%)	Ultimate flexural load (N)	Ultimate flexural strength (N/mm ²)	Mean flexural strength (N/mm ²)	Max. Flexural strength (N/mm ²)	Min. Flexural strength (N/mm ²)	Standard deviation (N/mm ²)
0	-		5952.18	1.786				
0	-		6880.56	2.064				
0	-		5124.67	1.537				
0	-	0	5853.57	1.756	1.946	2.368	1.537	0.251
0	-		7892.03	2.368				
0	-		6749.30	2.025				
0	-		6852.93	2.056				
0	-		6582.84	1.975				
40	1.64		13239.00	3.972				
40	1.656		14634.11	4.390				
40	1.672	1.6724	13946.97	4.184	3.924	4.390	3.190	0.455
40	1.697		10633.14	3.190				
40	1.697		12945.73	3.884				
80	2.676		14925.72	4.478				
80	2.669		17218.35	5.166				
80	2.736	2.6914	18189.46	5.457	4.962	5.457	4.279	0.549
80	2.662		18103.90	5.431				
80	2.714		14262.84	4.279				
120	3.274		17487.06	5.246				
120	3.377		17399.76	5.220				
120	3.327	3.3548	17277.54	5.183	5.346	6.250	4.832	0.532
120	3.403		20832.86	6.250				
120	3.393		16107.72	4.832				
160	4.775		20045.33	6.014				
160	4.704		19709.26	5.913				
160	4.681	4.711	24005.30	7.202	6.444	7.202	5.913	0.613
160	4.714		20257.74	6.077				
160	4.681		23387.68	7.016				
190	5.741		24362.81	7.309				
190	5.768		26483.20	7.945				
190	5.712	5.754	22530.46	6.759	7.189	7.945	6.635	0.522
190	5.763		24319.16	7.296				
190	5.786		22116.73	6.635				
220	6.82		23235.77	6.971				
220	6.787		24265.91	7.280				
220	6.72	6.7496	23816.31	7.145	7.524	8.175	6.971	0.550
220	6.654		27248.95	8.175				
220	6.767		26831.64	8.049				
250	7.844		30747.83	9.224				
250	7.805		26926.81	8.078				
250	7.766	7.7834	26823.76	8.047	8.285	9.224	8.034	0.525
250	7.728		26779.01	8.034				
250	7.774		26812.93	8.044				
280	8.484		26975.50	8.093				
280	8.568		26828.17	8.048				
280	8.441	8.5162	32327.04	9.698	8.494	9.698	8.029	0.714
280	8.563		26764.43	8.029				
280	8.525		28667.92	8.600				
310	9.501		27541.40	8.262				
310	9.5124		24580.19	7.374				
310	9.548	9.50548	27369.42	8.211	8.610	9.853	7.374	0.988
310	9.492		31173.96	9.352				
310	9.474		32842.26	9.853				
330	11.198		26103.57	7.831				
330	11.186		27588.86	8.277				
330	11.22	11.2	28020.27	8.406	7.810	8.406	7.202	0.540
330	11.253		24453.84	7.336				
330	11.143		24006.39	7.202				

Flexural strength results of 30 mm length discontinuous randomly aligned (100X100X500) mm specimen,
FRHAC mortar composite beams

Specimen	Mass of fibres added (g)	Fibre volume fraction ' Vf' (%)	Mean fibre volume fraction (%)	Ultimate flexural load (N)	Ultimate flexural strength (N/MM ²)	Standard deviation (N/MM ²)	Mean flexural strength (N/MM ²)	Max. Flexural strength	Min. Flexural strength
1	0	-		5952.18	1.786				
2	0	-		6880.56	2.064				
3	0	-		5124.67	1.537				
4	0	-		5853.57	1.756				
5	0	-	0	7892.03	2.368	0.251	1.946	2.368	1.537
6	0	-		6749.30	2.025				
7	0	-		6852.93	2.056				
8	0	-		6582.84	1.975				
9	20	0.914		7782.88	2.335				
10	20	1.286		7751.42	2.325				
11	20	0.623	0.855	9428.18	2.828	0.242	2.510	2.828	2.325
12	20	0.516		7820.78	2.346				
13	20	0.937		9041.95	2.713				
14	40	1.277		9829.70	2.949				
15	40	1.205		10732.35	3.220				
16	40	1.322	1.378	8992.54	2.698	0.247	2.939	3.220	2.683
17	40	1.632		10482.82	3.145				
18	40	1.454		8944.28	2.683				
19	60	2.152		11825.22	3.548				
20	60	1.977		11532.78	3.460				
21	60	1.785	1.981	9820.83	2.946	0.292	3.201	3.548	2.909
22	60	2.067		10468.39	3.141				
23	60	1.923		9696.12	2.909				
24	80	2.778		11462.32	3.439				
25	80	2.309		10784.06	3.235				
26	80	2.643	2.540	12819.85	3.846	0.260	3.464	3.846	3.222
27	80	2.560		11927.95	3.578				
28	80	2.410		10741.45	3.222				
29	100	2.936		-	-				
30	100	3.333		12327.39	3.698				
31	100	3.011	3.147	12840.16	3.852	0.141	3.849	4.038	3.698
32	100	3.542		13458.59	4.038				
33	100	2.912		12695.32	3.809				
34	120	3.878		14128.59	4.239				
35	120	3.636		12878.00	3.863				
36	120	3.240	3.647	12782.04	3.835	0.212	4.079	4.265	3.835
37	120	3.955		14216.14	4.265				
38	120	3.528		13974.53	4.192				
39	140	4.659		14373.83	4.312				
40	140	4.121		13737.16	4.121				
41	140	3.905	4.374	14195.05	4.259	0.190	4.317	4.575	4.121
42	140	4.541		15248.94	4.575				
43	140	4.843		-	-				
44	160	5.314		15639.28	4.692				
45	160	4.930		15381.93	4.615				
46	160	5.187	4.945	14544.93	4.363	0.212	4.431	4.692	4.216
47	160	4.813		14223.08	4.267				
48	160	4.483		14052.63	4.216				
49	180	5.600		15399.58	4.620				
50	180	5.940		16458.99	4.938				
51	180	6.087	5.815	14409.42	4.323	0.232	4.568	4.938	4.323
52	180	5.641		14976.86	4.493				
53	180	5.809		14889.91	4.467				
54	200	6.567		16704.52	5.011				
55	200	6.394		15010.95	4.503				
56	200	6.931	6.450	16239.70	4.872	0.222	4.825	5.011	4.503
57	200	5.909		16374.67	4.912				

Mass of fibres added (g)	Fibre volume fraction ' Vf' (%)	Mean fibre volume fraction (%)	Ultimate flexural load (N)	Ultimate flexural strength (N/MM ²)	Standard deviation (N/MM ²)	Mean flexural strength (N/MM ²)	Max. Flexural strength	Min. Flexural strength
200	6.832		15032.67	4.510				
220	7.938		15774.28	4.732				
220	7.538		17090.85	5.127				
220	7.494	7.423	16746.86	5.024	0.210	4.898	5.127	4.709
220	7.217		-	-				
220	6.926		15695.1	4.709				
240	8.722		15602.59	4.681				
240	8.37		16220.59	4.866				
240	7.936	8.377	16629.99	4.989	0.155	4.923	5.075	4.681
240	8.335		16918.27	5.075				
240	8.52		16670.39	5.001				
260	9.425		14427.68	4.328				
260	9.931		15749.92	4.725				
260	8.944	9.406	15770.62	4.731	0.197	4.534	4.731	4.328
260	9.078		14462.55	4.339				
260	9.654		15164.01	4.549				
280	9.907		13118.8	3.936				
280	10.234		14368.25	4.310				
280	9.839	9.797	14689.53	4.407	0.225	4.156	4.407	3.907
280	9.488		14066.77	4.220				
280	9.516		13022.2	3.907				
300	10.649		13192.03	3.958				
300	9.971		11478.39	3.444				
300	10.352	10.284	11946.55	3.584	0.241	3.572	3.958	3.313
300	10.061		11041.89	3.313				
300	10.387		11875.76	3.563				

SISAL/RHAC SPECIMENS TENSILE STRENGTH RESULTS

Strength results of continuous parallel aligned (50X50X350) mm specimens, Sisal RHAC composite beams

Specimen	Mass of fibres added (g)	Fibre volume fraction (V_f) (%)	Mean Fibre volume fraction (%)	Ultimate tensile load (N)	Ultimate tensile strength (N/MM ²)	Mean tensile strength (N/MM ²)	Standard deviation (N/MM ²)	Max. Tensile strength (N/MM ²)	Min. Tensile strength (N/MM ²)
0	0	-		2274.01	0.910				
0	0	-		2881.00	1.152				
0	0	-		2191.35	0.877				
0	0	-	0	2029.43	0.812	0.922	0.107	1.152	0.812
0	0	-		2309.72	0.924				
0	0	-		2261.99	0.905				
0	0	-		2052.08	0.821				
0	0	-		2433.57	0.973				
4	4	0.965		3449.74	1.380				
4	4	0.961		3886.95	1.555				
4	4	1.003	0.982	3584.83	1.434	1.280	0.255	1.555	0.944
4	4	0.983		2716.75	1.087				
4	4	0.998		2360.37	0.944				
9	9	2.305		3486.01	1.394				
9	9	2.397		4873.15	1.949				
9	9	2.351	2.359	4351.03	1.740	1.815	0.266	2.090	1.394
9	9	2.406		4747.65	1.899				
9	9	2.336		5225.40	2.090				
14	14	3.202		6301.04	2.520				
14	14	3.416		4603.98	1.842				
14	14	3.265	3.310	5999.39	2.400	2.279	0.287	2.520	1.842
14	14	3.278		5350.86	2.140				
14	14	3.390		6238.44	2.495				
19	19	4.327		6244.38	2.498				
19	19	4.226		6880.42	2.859				
19	19	4.145	4.238	5850.94	2.340	2.618	0.202	2.859	2.340
19	19	4.309		6782.24	2.713				
19	19	4.185		6701.29	2.681				
24	24	5.087		6900.87	2.974				
24	24	5.316		7219.07	2.888				
24	24	5.136	5.238	7008.81	2.694	2.956	0.262	3.388	2.694
24	24	5.258		7090.41	2.836				
24	24	5.394		7400.24	3.388				
29	29	6.528		8128.40	3.251				
29	29	6.426		8273.11	3.309				
29	29	6.618	6.502	8891.21	3.556	3.359	0.224	3.610	3.068
29	29	6.513		9024.85	3.610				
29	29	6.426		7670.35	3.068				
34	34	6.966		7971.48	3.189				
34	34	6.970		9170.37	3.668				
34	34	7.361	7.158	8852.52	3.541	3.469	0.243	3.712	3.189
34	34	7.218		9278.95	3.712				
34	34	7.275		8089.60	3.236				
39	39	7.988		8832.30	3.390				
39	39	8.178		9074.24	3.630				
39	39	8.051	8.164	9243.16	3.697	3.621	0.162	3.827	3.390
39	39	8.290		9566.43	3.827				
39	39	8.312		8907.64	3.563				
44	44	8.855		8880.28	3.413				
44	44	9.082		9115.14	3.646				
44	44	8.939	9.040	8940.88	3.576	3.642	0.164	3.853	3.413
44	44	9.114		9632.46	3.853				
44	44	9.208		9298.23	3.719				

Specimen No.	Mass of fibres added (g)	Fibre volume fraction (V _f) (%)	Mean Fibre volume fraction (%)	Ultimate tensile load (N)	Ultimate tensile strength (N/MM ²)	Mean tensile strength (N/MM ²)	Standard deviation (N/MM ²)	Max. Tensile strength (N/MM ²)	Min. Tensile strength (N/MM ²)
54	49	10.462		8711.46	3.485				
55	49	10.502		7759.06	3.211				
56	49	10.462	10.478	8719.11	3.488	3.466	0.162	3.663	3.211
57	49	10.401		9158.42	3.663				
58	49	10.564		8709.88	3.484				
59	54	11.826		8328.60	3.331				
60	54	12.037		7315.50	3.033				
61	54	11.524	11.825	8512.80	3.405	3.263	0.140	3.405	3.033
62	54	11.801		8189.53	3.276				
63	54	11.936		8171.11	3.268				

ile strength results of 30 mm length discontinuous randomly aligned (50X50X350) mm specimen,
 /RHAC mortar composite beams

Specimen No.	Mass of fibres added (g)	Fibre volume fraction (V_f) (%)	Mean fibre volume fraction (%)	Ultimate tensile load (N)	Ultimate tensile strength (N/mm^2)	Mean tensile strength (N/mm^2)	Standard deviation (N/mm^2)	Max. Tensile strength (N/mm^2)	Min. Tensile strength (N/mm^2)
1	0	0		2274.01	0.910				
2	0	0		2881.00	1.152				
3	0	0		2191.35	0.877				
4	0	0		2029.43	0.812				
5	0	0	0	2309.72	0.924	0.922	0.107	1.152	0.812
6	0	0		2261.99	0.905				
7	0	0		2052.08	0.821				
8	0	0		2433.57	0.973				
9	4	1.014		2225.84	0.890				
10	4	0.993		2049.55	0.820				
11	4	1.002	0.999	2847.12	1.139	0.928	0.168	1.139	0.820
12	4	0.997		2236.99	0.895				
13	4	0.987		2243.35	0.897				
14	9	1.966		3241.17	1.296				
15	9	2.026		2519.72	1.008				
16	9	2.038	1.974	2322.61	0.929	1.085	0.206	1.296	0.929
17	9	1.902		2762.46	1.105				
18	9	1.939		2715.43	1.086				
19	14	3.088		3685.71	1.474				
20	14	2.979		3862.73	1.545				
21	14	2.882	2.975	2933.60	1.173	1.343	0.176	1.545	1.173
22	14	2.949		2957.25	1.183				
23	14	2.979		3351.09	1.340				
24	19	4.011		3535.88	1.414				
25	19	3.932		4705.32	1.882				
26	19	3.995	3.935	3833.79	1.534	1.592	0.372	1.882	1.414
27	19	3.856		3555.33	1.422				
28	19	3.879		4264.24	1.706				
29	24	4.710		5879.25	2.352				
30	24	4.835		5680.35	2.272				
31	24	4.867	5.031	5680.35	2.272	2.171	0.358	2.352	1.939
32	24	4.916		5052.18	2.021				
33	24	5.829		4846.31	1.939				
34	29	5.829		6196.43	2.479				
35	29	5.717		6346.35	2.539				
36	29	5.695	5.818	5534.52	2.214	2.395	0.230	2.539	2.214
37	29	5.878		6290.85	2.516				
38	29	5.969		5573.55	2.229				
39	34	7.089		4264.24	2.423				
40	34	6.950		5879.25	2.531				
41	34	7.005	6.966	5680.35	2.380	2.552	0.169	2.792	2.380
42	34	7.131		5680.35	2.792				
43	34	6.657		5052.18	2.633				
44	39	7.426		6104.53	2.442				
45	39	7.935		7077.98	2.831				
46	39	7.679	7.758	7281.55	2.913	2.672	0.165	2.913	2.442
47	39	8.114		6301.55	2.521				
48	39	7.637		6628.51	2.651				
49	44	8.644		7054.30	2.822				
50	44	8.339		6938.05	2.775				

Specimen No.	Mass of fibres added (g)	Fibre volume fraction (V_f) (%)	Mean fibre volume fraction (%)	Ultimate tensile load (N)	Ultimate tensile strength (N/mm^2)	Mean tensile strength (N/mm^2)	Standard deviation (N/mm^2)	Max. Tensile strength (N/mm^2)	Min. Tensile strength (N/mm^2)
51	44	8.258	8.340	6559.44	2.624	2.708	0.185	2.965	2.535
52	44	8.373		6338.53	2.535				
53	44	8.390		7413.18	2.965				
54	49	9.324		6759.83	2.704				
55	49	9.435		6706.70	2.683				
56	49	8.135	9.124	6910.08	2.764	2.727	0.279	3.023	2.462
57	49	8.964		7558.02	3.023				
58	49	9.762		6155.99	2.462				
59	54	10.514		5399.33	2.160				
60	54	9.965		6326.28	2.531				
61	54	10.467	10.285	5733.79	2.294	2.268	0.317	2.531	2.065
62	54	9.978		5163.29	2.065				
63	54	10.500		5723.86	2.290				

1.3 SISAL/RHAC SPECIMENS INTERFACIAL BOND STRENGTH RESULTS

Interfacial bond strength results of continuous parallel aligned (50X50X350) mm sisal fibre reinforced RHAC mortar composites

Specimen No.	Mass of fibres added (g)	Fibre volume fraction (V_f) (%)	Mean Fibre volume fraction (%)	Average crack spacing (mm)	Average crack spacings for mean fibre Vf	Interfacial bond strength N/mm^2	Standard deviation N/mm^2	Average interfacial bond strength N/mm^2
9	4	0.965		14.73		0.397		
10	4	0.961		14.87		0.395		
11	4	1.003	0.982	13.19	12.93	0.426	0.0675	0.453
12	4	0.983		10.46		0.549		
13	4	0.998		11.38		0.497		
14	9	2.305		10.09		0.239		
15	9	2.397		8.73		0.266		
16	9	2.351	2.359	10.72	9.92	0.221	0.0172	0.239
17	9	2.406		9.61		0.241		
18	9	2.336		10.47		0.228		
19	14	3.202		8.19		0.210		
20	14	3.416		11.74		0.137		
21	14	3.265	3.310	9.18	9.69	0.184	0.0291	0.175
22	14	3.278		8.84		0.190		
23	14	3.390		10.50		0.155		
24	19	4.327		9.21		0.137		
25	19	4.226		13.27		0.097		
26	19	4.145	4.238	8.39	10.06	0.157	0.0220	0.131
27	19	4.309		10.05		0.126		
28	19	4.185		9.37		0.139		
29	24	5.087		10.28		0.103		
30	24	5.316		8.05		0.126		
31	24	5.136	5.238	10.98	9.92	0.096	0.0164	0.106
32	24	5.258		8.67		0.118		
33	24	5.394		11.63		0.086		
34	29	6.528		8.20		0.100		
35	29	6.426		9.63		0.086		
36	29	6.618	6.502	11.44	9.75	0.070	0.0106	0.085
37	29	6.513		9.31		0.088		
38	29	6.426		10.18		0.082		
39	34	6.966		12.86		0.059		
40	34	6.970		10.49		0.073		
41	34	7.361	7.158	9.43	10.72	0.076	0.0101	0.070
42	34	7.218		8.87		0.083		
43	34	7.275		11.96		0.061		
44	39	7.988		13.11		0.050		
45	39	8.178		10.96		0.058		
46	39	8.051	8.164	9.65	9.93	0.067	0.0147	0.067
47	39	8.290		8.84		0.071		
48	39	8.312		7.07		0.089		
49	44	8.855		6.39		0.092		
50	44	9.082		5.13		0.111		
51	44	8.939	9.040	7.45	7.06	0.078	0.0180	0.084
52	44	9.114		8.61		0.066		
53	44	9.208		7.73		0.073		
54	49	10.462		10.16		0.048		
55	49	10.502		9.07		0.054		
56	49	10.462	10.478	5.63	8.21	0.087	0.0149	0.062
57	49	10.401		7.95		0.062		
58	49	10.564		8.23		0.059		
59	54	11.826		6.69		0.064		
60	54	12.037		5.60		0.074		
61	54	11.524	11.825	8.78	7.05	0.050	0.0091	0.061
62	54	11.801		6.75		0.063		
63	54	11.936		7.44		0.057		

Interfacial bond strength of 30 mm length discontinuous randomly aligned (50X50X350) mm specimens, sisal fibre reinforced RHAC mortar composites

Specimen No.	Mass of fibres added (g)	Fibre volume fraction (V_f) (%)	Mean fibre volume fraction (%)	Average crack spacing (mm)	Interfacial bond strength (N/mm^2)	Average interfacial bond strength (N/mm^2)	Standard deviation (N/mm^2)
9	4	1.014		23.6	0.236		
10	4	0.993		18.53	0.307		
11	4	1.002	0.999	17.34	0.325	0.317	0.058
12	4	0.997		14.23	0.398		
13	4	0.987		17.8	0.321		
14	9	1.966		15.3	0.186		
15	9	2.026		11.4	0.242		
16	9	2.038	1.974	12.07	0.227	0.222	0.023
17	9	1.902		13.8	0.213		
18	9	1.939		11.93	0.242		
19	14	3.088		10.43	0.172		
20	14	2.979		13.56	0.137		
21	14	2.882	2.975	12.81	0.150	0.148	0.019
22	14	2.949		11.77	0.159		
23	14	2.979		14.93	0.124		
24	19	4.011		9.36	0.146		
25	19	3.932		12.78	0.109		
26	19	3.995	3.935	11.73	0.117	0.132	0.019
27	19	3.856		9.32	0.152		
28	19	3.879		10.51	0.134		
29	24	4.710		8.13	0.142		
30	24	4.835		10.47	0.107		
31	24	4.867	5.031	11.93	0.093	0.119	0.021
32	24	4.916		9.508	0.116		
33	24	5.829		6.642	0.139		
34	29	5.829		11.43	0.081		
35	29	5.717		8.02	0.117		
36	29	5.695	5.818	9.93	0.095	0.100	0.017
37	29	5.878		10.14	0.090		
38	29	5.969		7.58	0.118		
39	34	7.089		8.56	0.087		
40	34	6.950		9.34	0.082		
41	34	7.005	6.966	10.37	0.073	0.081	0.013
42	34	7.131		11.42	0.065		
43	34	6.657		8.21	0.097		
44	39	7.426		10.46	0.068		
45	39	7.935		12.39	0.053		
46	39	7.679	7.76	10.409	0.066	0.061	0.006
47	39	8.114		11.62	0.056		
48	39	7.637		11.021	0.063		
49	44	8.644		9.42	0.064		
50	44	8.339		8.45	0.074		
51	44	8.258	8.414	7.05	0.090	0.076	0.013

Specimen No.	Mass of fibres added (g)	Fibre volume fraction (V_f) (%)	Mean fibre volume fraction (%)	Average crack spacing (mm)	Interfacial bond strength (N/mm^2)	Average interfacial bond strength (N/mm^2)	Standard deviation (N/mm^2)
52	44	8.373		9.03	0.069		
53	44	8.390		6.385	0.097		
54	49	9.324		10.74	0.052		
55	49	9.435		14.39	0.038		
56	49	8.135	9.124	13.2907	0.048	0.044	0.007
57	49	8.964		12.8	0.045		
58	49	9.762		14.77	0.036		
59	54	10.514		14.13	0.034		
60	54	9.965		15.73	0.033		
61	54	10.467	10.285	15.48	0.031	0.033	0.002
62	54	9.978		14.75	0.035		
63	54	10.500		15.41	0.032		

1.4 SISAL/RHAC SPECIMENS FLEXURAL TOUGHNESS RESULTS

Flexural toughness data of continuous parallel aligned sisal fibre reinforced RHAC mortar specimens for varying fibre volume fractions

Deflection (mm)	Vf = 0% load (N)	Deflection (mm)	Vf = 1.322% load (N)	Deflection (mm)	Vf = 3.636% load (N)	Deflection (mm)	Vf = 5.809% load (N)	Deflection (mm)	Vf = 7.494% load (N)	Deflection (mm)	Vf = 8.335% load (N)
0	0	0	0	0	0	0	0	0	0	0	0
0.11	124.90	0.40	1429.36	0.40	1528.67	0.40	2142.81	0.40	3948.15	0.20	1528.92
0.14	427.52	0.60	3833.94	0.60	4069.19	0.80	7240.12	0.70	6823.97	0.40	7469.36
0.23	629.08	0.80	4297.81	0.80	5947.64	1.10	7668.43	1.10	10094.62	0.60	10267.33
0.28	1172.41	1.00	4972.43	0.90	7286.90	1.20	9175.30	1.50	11725.31	0.80	11074.47
0.42	1228.65	1.20	7586.54	1.10	7810.51	1.40	10214.02	1.60	14118.49	1.00	15050.21
0.43	1633.47	1.40	8163.51	1.20	9544.68	1.80	14358.67	1.90	15257.83	1.20	15112.84
0.50	1797.64	1.60	8738.82	1.40	9897.03	2.00	14717.49	2.51	16746.86	1.40	15197.15
0.57	2462.49	1.83	8992.54	1.60	12709.47	2.57	14889.91	2.80	15949.42	1.69	16918.59
0.69	2651.80	2.00	8769.90	1.96	12878.00	3.10	14013.42	3.10	15107.00	2.00	16210.36
0.71	3796.97	2.20	8742.44	2.30	12728.52	3.50	13729.71	3.50	15162.97	2.80	16050.08
0.78	3927.50	2.40	8656.71	2.70	12546.89	4.00	13085.29	3.60	13824.18	3.40	15849.24
0.88	4046.80	2.60	8378.49	3.00	10205.71	4.60	9147.35	3.80	13295.40	3.90	14412.73
0.92	4081.19	2.80	6940.52	3.20	9387.64	5.00	7294.61	4.00	13013.61	4.50	13366.07
0.99	4345.63	3.00	6834.90	3.30	9164.93	5.50	5486.57	4.50	11281.93	5.00	12309.68
1.12	4718.35	3.20	6722.45	3.50	8710.05	6.00	6139.30	5.00	10872.45	5.30	9420.89
1.13	5126.16	3.40	5435.21	3.60	8372.56	6.50	5460.35	5.40	9169.85	6.00	6072.55
1.21	5952.18	3.80	4116.98	3.80	8270.49	7.00	4936.12	5.80	7139.54	6.50	6124.68
1.31	4135.71	4.20	4475.13	3.95	8162.73	7.30	4902.55	6.00	7328.07	7.00	6257.41
1.35	3670.15	4.40	4647.93	4.10	7050.91	7.60	4257.31	6.50	6841.71	8.00	6631.47
1.47	3548.67	4.60	4023.75	4.28	5934.65	8.00	4128.67	7.00	6753.88	9.00	5172.29
1.51	2919.03	4.80	3976.11	4.50	6018.70	8.50	3479.28	7.50	6346.59	10.00	4813.72
1.56	2866.52	5.00	3584.60	4.60	5116.83	9.00	2823.75	8.00	5750.30	10.50	3198.51
1.64	2749.18	5.20	3346.85	4.80	5023.76	9.20	2508.49	8.30	5349.02	11.00	3043.67
1.75	2658.34	5.40	2111.73	5.00	4782.91	9.60	2747.39	8.70	4183.09	11.80	3245.01
1.83	1507.49	5.60	1829.67	5.20	3459.84	10.00	2453.81	9.10	3934.71	12.00	3119.43
1.87	1233.61	5.80	1764.42	5.50	3381.20	10.40	2692.36	9.80	3205.87		
1.94	1029.05	6.00	1797.29	5.56	3359.76	10.80	2538.06	10.50	2867.46		
1.99	937.28	6.20	1635.86	5.80	3347.56	12.40	2484.82	11.20	2813.65		
2.11	567.52	6.40	1517.60	6.00	3215.90						
		6.60	1118.91	6.30	3148.61						
		6.80	1237.82	6.40	3076.44						
		7.00	1311.79	6.7	2891.09						
		7.20	1376.43	6.9	2846.75						
		7.40	1347.80	7.1	2803.48						
		7.60	1328.54	7.38	2720.36						
				7.5	2398.13						
				7.94	2247.92						
				8.17	2165.25						

Flexural toughness data of 30 mm length discontinuous randomly aligned sisal fibre reinforced RHAC mortar composites, cured for 28 days, Vf = 7.494%, varying the water cement ratio.

Deflection (mm)	W/C = 0.72 load (N)	Deflection (mm)	W/C = 0.65 load (N)	Deflection (mm)	W/C = 0.55 load (N)	Deflection (mm)	W/C = 0.50 load (N)	Deflection (mm)	W/C = 0.45 load (N)
0.00	0.00	0.00	0.00	0.00	0.00	0.00	0.00	0.00	0.00
0.40	2182.19	0.40	1836.86	0.40	2683.00	0.40	3948.15	0.20	3427.81
0.60	3396.70	0.60	3941.49	0.65	4720.69	0.70	6823.97	0.40	7305.00
0.81	3857.71	0.88	6425.15	0.80	6935.37	1.10	10094.62	0.63	8963.41
1.00	4117.36	1.00	7284.71	1.04	11296.15	1.50	11725.31	0.80	9147.50
1.23	4430.87	1.42	8834.34	1.10	11850.24	1.60	14118.49	1.00	9781.52
1.40	6738.30	1.80	10401.27	1.27	12017.42	1.90	16357.83	1.21	10376.63
1.55	6843.27	2.20	11363.36	1.50	12683.67	2.51	16793.37	1.49	10959.65
1.60	7368.19	2.62	12552.30	1.94	13765.20	2.80	16649.42	1.60	11404.31
1.70	7930.43	3.04	14629.72	2.31	14415.57	3.10	16407.00	1.80	17215.82
1.90	8211.16	3.21	13782.83	2.71	13313.54	3.50	15162.97	2.06	17655.09
2.11	8460.02	3.40	12019.52	3.17	12819.16	3.60	13824.18	2.49	17382.51
2.34	9147.84	3.60	10561.70	3.30	11614.94	3.80	13295.40	2.83	17591.23
2.50	9188.69	3.81	7691.42	3.55	11495.40	4.00	13013.61	3.20	14347.17
2.57	9673.15	4.04	7106.96	3.70	11293.27	4.50	11281.93	3.61	13428.59
2.73	9312.38	4.80	6781.83	3.98	11125.71	5.00	10872.45	4.00	13377.00
2.80	8130.60	4.97	6642.15	4.10	11094.89	5.40	9169.85	4.29	13348.41
3.10	7693.49	5.00	6611.92	4.38	10807.91	5.80	7139.54	4.40	13146.27
3.39	7565.83	5.20	6656.73	4.50	10705.32	6.00	7328.07	4.80	12227.41
3.50	7489.25	5.40	6639.42	4.83	9615.74	6.50	6841.71	5.07	12201.93
3.70	7042.30	5.67	6746.01	5.07	9364.21	7.00	6753.88	5.42	11854.81
3.80	6578.93	5.80	6367.48	5.20	9142.58	7.50	6346.59	5.65	11421.47
3.86	6523.07	6.00	6104.35	5.40	9050.17	8.00	5750.30	5.82	11380.21
3.90	6772.48	6.20	5913.76	5.60	8753.17	8.30	5349.02	6.20	10563.66
4.00	6652.12	6.40	5602.41	5.89	8721.41	8.70	4183.09	6.40	9902.73
4.02	6564.24	6.67	5763.82	6.08	8420.31	9.10	3934.71	6.64	9474.65
4.02	6438.19	6.85	5475.83	6.13	8372.56	9.80	3205.87	6.80	7342.28
4.02	6372.06	7.01	5436.41	6.40	8361.44	10.50	2867.46	7.00	7432.47
4.04	6358.73	7.24	5344.92	6.64	8319.37	11.20	2813.65	7.25	7397.94

Deflection (mm)	W/C = 0.72 load (N)
5.40	6329.26
5.80	6314.58
6.00	5726.71
6.37	5683.41
6.50	5664.59
6.37	5661.80
6.50	5439.42
6.70	5272.73
6.90	5049.66
7.10	5021.19
7.38	4987.52
7.50	4942.87
7.70	4938.05
7.91	4728.27
8.00	4664.31
8.10	2378.56
8.34	2141.28
8.50	1983.35
8.73	1843.11

Deflection (mm)	W/C = 0.65 load (N)
7.40	4892.10
7.61	4811.25
7.89	4392.80
8.00	4176.58
8.40	3900.78
8.85	3217.36
9.20	2976.91
9.64	2941.06
9.82	2903.16
10.00	2524.38
10.26	2410.41
10.40	2314.20
10.67	2276.42
10.80	2057.39
11.07	2023.81
11.14	1927.48

Deflection (mm)	W/C = 0.55 load (N)
6.80	5718.92
7.01	5079.48
7.20	4708.73
7.31	4246.18
7.52	4184.52
7.70	3871.32
7.90	3452.61
8.20	3340.07
8.58	2918.28
9.00	2837.51
9.40	2762.94
9.80	2648.20
10.00	2561.82
10.22	2533.04
10.60	2439.38
10.86	2347.76
11.15	2360.93

Deflection (mm)	W/C = 0.45 load (N)
7.48	5745.28
7.60	5458.39
8.02	5173.11
8.40	4925.41
8.84	4761.55
9.00	4723.00
9.29	4639.06
9.41	4590.32
9.60	4371.79
9.80	4255.63
10.00	4231.76
10.20	4226.94
10.43	4170.13
10.60	4127.93
10.80	4094.32
11.00	3981.47
11.17	3969.82
11.20	3911.51
11.39	3815.27

Flexural toughness data of 30 mm length discontinuous randomly aligned sisal fibre reinforced RHAC mortar composites, $V_f = 7.494\%$, $W/C = 0.5$, Varying the curing age

Deflection (mm)	7 days cured load (N)	Deflection (mm)	14 days cured load (N)	Deflection (mm)	28 days cured load (N)
0.00	0.00	0.00	0.00	0.00	0.00
0.20	1856.83	0.20	1914.15	0.40	3948.15
0.40	2941.85	0.43	3803.46	0.70	6823.97
0.67	5860.17	0.60	9152.14	1.10	10094.62
0.80	7987.90	0.89	10141.08	1.50	11725.31
1.09	8135.46	1.07	10676.43	1.60	14118.49
1.40	8823.14	1.34	10941.05	1.90	16357.83
1.80	10249.39	1.60	11132.91	2.51	16793.37
2.20	11483.56	1.95	11567.44	2.80	16649.42
2.45	11850.60	2.19	11683.18	3.10	16407.00
2.60	11562.60	2.46	11741.45	3.50	15162.97
2.82	7947.00	2.72	11409.92	3.60	13824.18
3.20	7918.61	3.10	11347.41	3.80	13295.40
3.61	7711.53	3.42	11081.78	4.00	13013.61
3.80	7508.74	3.70	10279.26	4.50	11281.93
4.00	5690.18	4.00	9629.35	5.00	10872.45
4.28	5648.37	4.26	9381.01	5.40	9169.85
4.47	5916.43	4.60	9152.43	5.80	7139.54
4.60	6054.96	4.80	8911.20	6.00	7328.07
4.83	6271.15	5.08	8867.42	6.50	6841.71
5.20	6234.50	5.48	8741.76	7.00	6753.88
5.60	6218.35	5.85	8293.11	7.50	6346.59
5.85	6149.72	6.20	7826.54	8.00	5750.30
6.00	6133.81	6.67	7204.39	8.30	5349.02
6.25	6120.43	6.80	7027.17	8.70	4183.09
6.40	6015.09	7.00	6922.92	9.10	3934.71
6.64	5418.44	7.28	6638.56	9.80	3205.87
6.80	4870.05	7.40	6373.87	10.50	2867.46
7.23	4253.86	7.64	4755.38	11.20	2813.65
7.46	3924.18	7.84	3906.37		
7.66	3359.73	8.00	3769.20		
7.78	3176.50	8.16	3613.43		
7.80	3043.24	8.34	3424.60		
7.91	2377.69	8.50	3253.74		
8.00	2181.47	8.70	3118.15		
8.12	2047.73	9.00	3076.45		
8.20	2025.15	9.41	3051.14		
8.39	1913.45	9.50	3043.53		
		9.79	3029.78		
		10.00	2957.26		
		10.45	2685.40		
		10.81	2653.02		
		11.36	2417.82		

1.5 SISAL/EPOXY SPECIMENS TENSILE STRENGTH RESULTS

Tensile strength data for continuous parallel aligned sisal fibre reinforced epoxy resin composites

Unreinforced specimens, $V_f = 0\%$

Specimen no.	Fibre volume fraction (%)	Mean fibre vol. fraction (%)	Ultimate tensile load (N)	Tensile strength (N/mm^2)	Tensile strain (%)	Tensile Modulus of Elasticity (GN/mm^2)	Mean tensile strength (N/mm^2)	Stdev. (N/mm^2)	Mean tensile strain (%)	Stdev. (%)	Mean tensile Mod. of Elasticity (GN/mm^2)	Stdev. (GN/mm^2)
1	0		4703.10	37.625	3.025	0.741						
2	0		4297.00	34.376	2.945	0.602						
3	0		5138.75	41.110	3.346	0.864						
4	0		5510.22	44.082	3.588	0.926						
5	0	0	6634.59	53.077	4.113	1.166	43.825	6.057	3.571	0.429	0.906	0.174
6	0		5916.31	47.330	3.916	0.995						
7	0		5540.91	44.327	3.894	0.932						
8	0		6083.83	48.671	3.741	1.023						

Average fibre volume fraction, $V_f = 7.503\%$

Specimen no.	Fibre volume fraction (%)	Mean fibre vol. fraction (%)	Ultimate tensile load (N)	Ultimate tensile strength (N/mm^2)	Tensile strain (%)	Tensile Modulus of Elasticity (GN/mm^2)	Mean tensile strength (N/mm^2)	Stdev. (N/mm^2)	Mean tensile strain (%)	Stdev. (%)	Mean tensile Mod. of Elasticity (GN/mm^2)	Stdev. (GN/mm^2)
9	7.955		7268.69	58.150	4.409	1.654						
10	7.140		6983.08	55.865	4.137	1.387						
11	7.346		7109.59	56.877	4.212	1.625						
12	6.894		6262.35	50.099	3.974	1.378						
13	8.526	7.503	7312.62	58.501	4.312	1.663	55.532	3.210	4.131	0.239	1.517	0.147
14	8.125		7345.21	58.762	4.352	1.669						
15	7.445		6743.19	53.946	3.713	1.339						
16	6.595		6507.35	52.059	3.941	1.420						

Mean value of fibre volume fraction $V_f = 11.89\%$

Specimen no.	Fibre volume fraction (%)	Mean fibre vol. fraction (%)	Ultimate tensile load (N)	Tensile strength (N/mm^2)	Tensile strain (%)	Tensile Modulus of Elasticity (GN/mm^2)	Mean tensile strength (N/mm^2)	Stdev. (N/mm^2)	Mean tensile strain (%)	Stdev. (%)	Mean tensile Mod. of Elasticity (GN/mm^2)	Stdev. (GN/mm^2)
17	11.044		7475.99	59.808	3.327	1.613						
18	11.627		7554.77	60.438	3.595	1.639						
19	12.564		7881.62	63.053	3.812	1.691						
20	10.975	11.890	7231.32	57.851	3.282	1.525	61.460	3.385	3.635	0.255	1.621	0.069
21	10.122		7296.44	58.372	3.633	1.542						
22	14.223		8556.57	68.453	4.071	1.725						
23	11.858		7860.01	62.880	3.740	1.585						
24	12.706		7602.97	60.824	3.618	1.648						

Mean value of fibre volume fraction $V_f = 17.45\%$

Specimen no.	Fibre volume fraction (%)	Mean fibre vol. fraction (%)	Ultimate tensile load (N)	Tensile strength (N/mm^2)	Tensile strain (%)	Tensile Modulus of Elasticity (GN/mm^2)	Mean tensile strength (N/mm^2)	Stdev. (N/mm^2)	Mean tensile strain (%)	Stdev. (%)	Mean tensile Mod. of Elasticity (GN/mm^2)	Stdev. (GN/mm^2)
25	19.755		10809.32	86.475	4.504	1.987						
26	19.901		9357.01	74.856	3.853	1.762						
27	18.413		10616.25	84.930	4.527	1.838						
28	16.311		8507.38	68.059	3.628	1.547						
29	14.136	17.448	8179.16	65.433	3.618	1.542	72.772	9.698	3.859	0.494	1.670	0.203
30	17.433		8852.38	70.819	3.775	1.653						
31	18.048		9276.62	74.213	3.956	1.706						
32	15.589		7174.28	57.394	3.012	1.324						

e) Mean value of fibre volume fraction $V_f = 26.31\%$

specimen no.	Fibre volume fraction (%)	Mean fibre vol. fraction (%)	Ultimate tensile load (N)	Tensile strength (N/mm^2)	Tensile strain (%)	Tensile Modulus of Elasticity (GN/mm^2)	Mean tensile strength (N/mm^2)	Stdev. (N/mm^2)	Mean tensile strain (%)	Stdev. (%)	Mean tensile Modulus of Elasticity (GN/mm^2)	Stdev. (GN/mm^2)
33	23.032		10038.05	80.304	3.543	2.082						
34	32.785		11843.04	93.144	4.137	2.108						
35	24.445		10119.16	80.953	3.732	2.083						
36	26.756	26.313	11551.46	92.412	4.653	1.978	86.072	6.174	3.941	0.396	2.033	0.133
37	31.119		11798.44	94.388	4.351	2.138						
38	22.797		10043.37	80.347	3.704	1.818						
39	25.543		10566.87	84.535	3.788	2.191						
40	24.048		10311.29	82.490	3.623	1.887						

f) Mean fibre volume fraction $V_f = 35.32\%$

specimen no.	Fibre volume fraction (%)	Mean fibre vol. fraction (%)	Ultimate tensile load (N)	Tensile strength (N/mm^2)	Tensile strain (%)	Tensile Modulus of Elasticity (GN/mm^2)	Mean tensile strength (N/mm^2)	Stdev. (N/mm^2)	Mean tensile strain (%)	Stdev. (%)	Mean tensile Modulus of Elasticity (GN/mm^2)	Stdev. (GN/mm^2)
41	43.716		13613.44	108.908	4.722	2.966						
42	41.721		12705.01	101.640	4.824	2.702						
43	29.629		11246.60	89.973	3.774	1.892						
44	38.957	35.325	12202.50	97.620	4.499	1.908	96.627	8.622	4.285	0.451	2.164	0.443
45	35.462		13363.63	106.909	4.735	2.277						
46	33.014		11642.71	93.142	3.911	1.898						
47	28.543		11226.96	89.816	3.977	1.891						
48	31.555		10626.24	85.010	3.837	1.781						

g) Mean fibre volume fraction $V_f = 39.70\%$

specimen no.	Fibre volume fraction (%)	Mean fibre vol. fraction (%)	Ultimate tensile load (N)	Tensile strength (N/mm^2)	Tensile strain (%)	Tensile Modulus of Elasticity (GN/mm^2)	Mean tensile strength (N/mm^2)	Stdev. (N/mm^2)	Mean tensile strain (%)	Stdev. (%)	Mean tensile Modulus of elasticity (GN/mm^2)	Stdev. (GN/mm^2)
49	44.176		13471.84	107.775	4.209	2.241						
50	37.808		12650.45	101.204	3.714	2.066						
51	41.826		14144.00	113.152	4.635	2.533						
52	40.580	39.699	13034.11	104.273	4.341	2.334	103.755	5.177	4.179	0.259	2.267	0.173
53	38.857		12567.64	100.541	4.082	2.251						
54	34.638		12055.53	96.444	4.105	2.016						
55	37.649		12606.51	100.852	4.131	2.258						
56	42.058		13225.09	105.801	4.212	2.437						

h) Mean fibre volume fraction $V_f = 44.83\%$

specimen no.	Fibre volume fraction (%)	Mean fibre vol. fraction (%)	Ultimate tensile load (N)	Tensile strength (N/mm^2)	Tensile strain (%)	Tensile Modulus of Elasticity (GN/mm^2)	Mean tensile strength (N/mm^2)	Stdev. (N/mm^2)	Mean tensile strain (%)	Stdev. (%)	Mean tensile Modulus of Elasticity (GN/mm^2)	Stdev. (GN/mm^2)
57	46.832		14348.94	114.791	4.417	2.406						
58	47.040		14616.51	116.932	4.508	2.451						
59	41.926		13817.18	110.537	4.553	2.432						
60	51.070	44.829	15492.04	123.936	5.124	2.598	113.190	7.927	4.520	0.344	2.427	0.124
61	42.614		13293.89	106.351	4.318	2.323						
62	43.974		13746.10	109.969	4.372	2.431						
63	38.907		12574.16	100.593	4.000	2.209						
64	46.271		15300.71	122.406	4.867	2.566						

9.1.6 SISAL/EPOXY SPECIMENS FLEXURAL STRENGTH RESULTS

Flexural strength results of sisal fibre reinforced epoxy resin composites

Vol. Fract.	Parallel Flex. Strength	Stdev.	Vol. Frac.	20 mm length disc. Flex. Strength	Stdev.
(%)	(N/mm ²)	(N/mm ²)	(%)	(N/mm ²)	(N/mm ²)
0	73.463071	4.678	0	73.463071	4.678
10.2648	97.43731	6.3716	8.5197	70.622	7.2735
14.42615	113.5809516	5.2657	11.3684	67.08172	8.273
19.173904	109.04911	7.23	13.59701	67.8409	5.6738
24.90732	103.65842	7.12906	14.6341	69.1041	6.1147
26.872336	117.743119	4.02471	16.5419	71.217	4.5961
31.86724	120.146241	8.469	18.0762	71.9352	5.8814
35.518137	118.5379	5.4273			
43.67952	122.1583	10.08117			
46.5611	127.35621	8.9345			

Vol. Frac.	10 mm length disc. Flex. Strength	Stdev.	Vol. Frac.	5 mm length disc. Flex. Strength	Stdev.
(%)	(N/mm ²)	(N/mm ²)	(%)	(N/mm ²)	(N/mm ²)
0	73.463071	4.678	0	73.46307	4.678
7.1268	56.1783	2.3569	7.086	53.197	6.381
9.27107	59.4132	7.1863	9.421	54.83	5.359
10.5638	57.3815	6.1385	12.576	56.025	7.784
13.1052	61.5421	8.0431	16.382	56.334	4.172
16.4819	63.7024	5.4972	17.948	58.672	4.086
			22.946	61.829	6.931
			25.075	62.814	8.427

Flexural Modulus of Elasticity of sisal fibre reinforced epoxy resin composites

Vol. fract.-1 (%)	Parallel FMOE (GN/mm ²)	Stdev. (N/mm ²)	Vol. Frac.-2 (%)	20 mm disc. FMOE (GN/mm ²)	Stdev. (N/mm ²)
0	3.6274	0.0742	0	3.6274	0.0742
10.2648	4.06792	0.2238	8.5197	3.4365	0.416
14.42615	5.00106	0.37925	11.3684	3.5164	0.1245
19.173904	5.24949	0.17534	13.59701	3.5618	0.6814
24.90732	4.862053	0.08629	14.6341	3.49582	0.2904
26.872336	6.19371	0.1742	16.5419	3.50279	0.5931
31.86724	7.376694	0.4775	18.0762	3.5816	0.3875
35.518137	6.388071	0.09235			
43.67952	7.821679	0.0638			
46.5611	7.84731	0.2564			

Vol. Frac.-3 (%)	10 mm disc. FMOE (GN/mm ²)	Stdev. (N/mm ²)	Vol. Frac.-4 (%)	5 mm disc. FMOE (GN/mm ²)	Stdev. (N/mm ²)
0	3.6274	0.0742	0	3.6274	0.0742
7.1268	2.8703	0.4258	7.086	2.6459	0.158
9.27107	3.0158	0.1729	9.421	2.703	0.069
10.5638	2.9407	0.09311	12.576	2.795	0.374
13.1052	3.2719	0.0713	16.382	2.961	0.283
16.4819	3.5862	0.3678	17.948	3.084	0.164
			22.964	3.275	0.297
			25.075	3.317	0.073